Thesis submitted for the degree of

Doctor of Philosophy

at the University of Leicester

By

Clare Helen Wright B.Sc. (Hons) (Leicester)

Department of Cell Physiology and Pharmacology,

University of Leicester

October 2006

ProQuest LLC
789 East Eisenhower Parkway
P.O. Box 1346
Ann Arbor, MI 48106-1346

Studies of cellular correlates of ischaemia cardioprotection and K_{ATP} channel function in rat isolated ventricular cells

Thesis submitted for the degree of

Doctor of Philosophy

at the University of Leicester

By

Clare Helen Wright B.Sc. (Hons) (Leicester)

Department of Cell Physiology and Pharmacology,

University of Leicester

October 2006

"Who taught you all this Doctor?"
The reply came promptly:
"Suffering"

-Albert Camus, The Plague

I would like to thank so many people. Firstly thanks to Nick-your patience appears to be as vast as your knowledge! Noel, thanks for helping me with all the single channel analysis and the bounty bars-I won't forget it! Glenn, thanks for all your help. Diane, thanks for letting me gossip with you.

There are also other people whom made my time during my PhD special and supported me through the difficult times-Paul, Sam, Kym, Louise and Liz.

I would also like to thank my family-Mum, Dad, Louise and Mama especially.

During my Ph.D I also gained a fantastic nephew, Blandy and equally cute niece-Brooke. If either of you ever irritate me, I might just read you this for a bed time story!

I would also like to dedicate this to a few very special people who didn't manage to see me finish this. Granny and Grandpa-I know you would have loved to have seen this. Dada-I really would have wanted you to have been here to see me finish this, but I know you couldn't.

Lastly, Dr. R.T.A Glover-thanks for everything in the last few months-your support and kindness are very special to me.

Abstract

Clare Helen Wright

Studies of cellular correlates of ischaemic cardioprotection and K_{ATP} channel function in rat isolated ventricular cells

Hearts from female animals have been reported to be more resistant to ischaemia than those from males. Using rat isolated cardiac myocytes, I investigated gender differences in ischaemic resistance and whether it could be correlated with increased ATP-sensitive K^+ (K_{ATP}) current density. Cells from female animals showed greater resistance to simulated ischaemia and reperfusion measured by an increase in the proportion of cells that recovered contractile function in response to stimulation and a reduction the number of hypercontracted cells. Female cells also had a greater ability to maintain calcium homeostasis in response to ischaemic challenge.

To measure K_{ATP} current density, whole-cell K_{ATP} currents were measured using patch clamp and normalised to cell capacitance. The K_{ATP} openers pinacidil or P-1075 elicited a higher K_{ATP} current density in female myocytes. However currents elicited by metabolic inhibition (NaCN + iodoacetate) were much larger than those produced by openers, and did not differ between genders. Similarly in cell-attached patch experiments there was no difference in the number of channels observed or their time to activation. Experiments using quantitative PCR experiments showed no significant difference between male and female rats in the transcript levels of genes encoding the subunits, Kir6.2 and SUR2A, that comprise the sarcolemmal K_{ATP} channel.

I also investigated the possibility, proposed recently, that protein kinase C may lead to internalisation of the K_{ATP} channel. In response to metabolic inhibition, whole-cell K_{ATP} currents are activated and then decline with time. Pre-incubation of myocytes with phorbol myristate acetate (PMA) did not affect the time course of the decline in contrast to the PKC inhibitor chelerythrine. Further, in cell attached patches, the single-channel open probability declined in the same way as did whole cell current, suggesting that the decline of whole-cell current reflects a fall in open probability rather than channel internalisation.

Table of abbreviations

ATP-sensitive potassium channel	K_{ATP}
Ca^{2+}-dependent potassium channel	Kca/ BKCa
Muscarinic acetylcholine activated potassium channel	$K_{(Ach)}$
Voltage gated potassium channel	K_V
Two-pore-domain potassium channels	TWIK
Slow afterhyperpolarization	sAHP
Intermediate conductance Ca^{2+}-activated channel	IK
Action potential duration	APD
K^+ equilibrium potential	E_K
Inwardly rectifying potassium channel super family	Kir
Sulphonylurea receptors	SUR
ATP-binding cassette super family	ABC
Endoplasmic reticulum retention signal	RKR
Nucleotide binding site 1	NBF-1
Nucleotide binding site 2	NBF-2
Potassium channel opener	KCO
Transmembrane domain	TMD
Magnesium ADP	MgADP
Protein kinase A	PKA
Phosphatidylinositol 4,5-bisphosphate	PIP_2
Phosphatidylinositol 4,5-trisphosphate	PIP_3
Phospholipase C	PLC
Ischaemic preconditioning	IPC
Reduced nicotinamide adenine dinucleotide	NADH
Reduced flavin adenine dinucleotide	$FADH_2$
Dinitrophenol	DNP
Mitochondrial permeability transition pore	MPTP
Deoxyglucose	[^{3}H]-DOG
Inositol 1,3,4-triphosphate	IP_3
Diacylglycerol	DAG
Protein kinase C	PKC
Extracellular receptor kinase	ERK
Mitogen-activated protein kinase	MAPK
Phosphatidylinositol 3-OH kinase	PI 3-K
Reactive oxygen species	ROS
Glycogen synthase kinase 3 beta	GSK-3β
Voltage dependent anion channel 1	VDAC1
Second window of protection	SWOP
Mitochondrial K_{ATP} channel	mK_{ATP} or $mitoK_{ATP}$

Inducible nitric oxide synthase	iNOS
Nitric oxide synthase	NOS
5-hydroxydecanoic acid	5-HD
Phorbol 12-myristate 13-acetate	PMA
Oestrogen receptor knockout	ERKO
Alpha oestrogen receptor knock out	Alpha ERKO
Beta oestrogen receptor knock out	Beta ERKO
Ultrarapid delayed rectifier K^+ current	I_{KUR}
Coronary heart disease	CHD
High-density lipoprotein	HDL
Metabolic Inhibition	MI
Sodium cyanide	NaCN
Iodoacetic acid	IAA
pA/pF	picoampes/picofarads
Reverse transcription polymerase chain reaction	RT-PCR
Quantitative polymerase chain reaction	QPCR
Threshold cycle	Ct
Extracellular-regulated kinase	ERK

CHAPTER 1

GENERAL INTRODUCTION

Chapter 1 Introduction

This investigation focuses on studying various aspects of ATP-sensitive potassium (K_{ATP}) channels in sarcolemmal membrane of Adult Wistar rat cardiac myocytes by electrophysiological and molecular biological techniques. The K_{ATP} channel is part of the potassium channel family and is classified as an inward rectifier. These channels are thought to couple the metabolic state of the cell to membrane potential by sensing the changes in adenine nucleotide concentration within the cell (Seino & Miki, 2003).

1.1 The diversity of potassium channels

In recent years, electrophysiological techniques have made it possible to investigate the properties of macromolecular pores in cell membranes, known as ion channels. Ion channels are protein molecules that contain an aqueous pore that allows the flow of ions across cell membranes (Aidley and Stanfield, 1996). Important discoveries from Sidney Ringer (1881 to 1887) qualified the roles of Na^+, K^+ and Ca^{2+} in the ability to make a heart beat. Both Nernst (1888) and Bernstein (1902, 1912) produced theories leading to the idea that cells are excitable entities that have an electrical potential dependent upon the movement of ions across the cell membrane. The Na^+, K^+, Ca^{2+} and Cl^- ions are responsible for almost all excitation and electrical signaling (Hille., 2001). Each channel is regarded as an excitable molecule, as it responds to a specific stimulus such as membrane potential change, or a neurotransmitter or other chemical stimulus.

Ion channels are found in the membrane of all cells, both prokaryotic and eukaryotic (Hille, 2001). Their functions are diverse, ranging from involvement in the action

potential to controlling cell volume (Hille, 2001). The differences in channel function reflect the type of ions that move across the membrane, which depends on the molecular structure of the channel itself.

More than 80 related mammalian genes for subunits of K^+-selective channels have been identified from cloning techniques and genome projects (Hille, 2001) (figure 1.1). Although the structural diversity of the potassium channel family encompasses five main types categorized upon the basis of their transmembrane topology possessing either 2, 4, 6, 7 or 8 transmembrane domains, they all share common features. Figure 1.2 shows the structures of the potassium channels that have 2, 4 and 6 transmembrane domains. All potassium channels have a pore-lining P-loop containing an amino acid sequence, which is either –GYG- (thr-X-X-thr-X-gly-tyr-gly-glu) –GFG- (thr-X-X-thr-X-gly-phe-gly-glu-) making them highly selective for the potassium ion (Hille, 2001). Four repeats of the subunit line the selectivity filter, are identical, while flanking the P-region is a minimum of two transmembrane segments, crucial for the pore-forming core (Hille, 2001).

The potassium channel family is truly diverse, the variation arises from the numerous ways in which potassium channels are gated open (MacKinnon, 2003). Some potassium channels are ligand-gated and therefore open due to binding of a chemical ligand such as the Ca^{2+}-dependent potassium channel (K_{Ca} channel), while others, the muscarinic acetylcholine activated potassium channel $K_{(Ach)}$, are G-protein coupled. Other potassium channels are voltage gated (K_v) and contain a voltage sensor (Mackinnon, 2003).

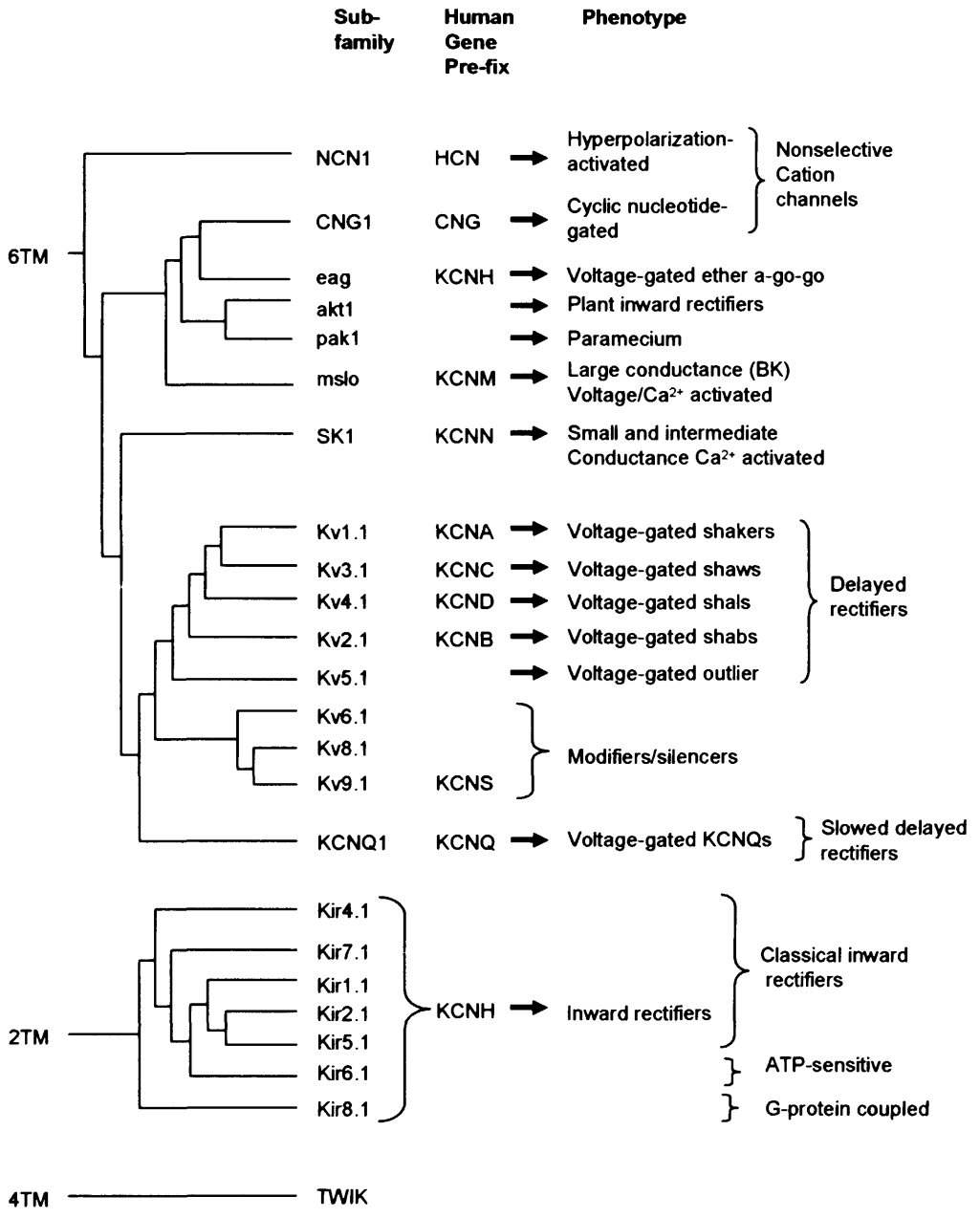

Figure 1.1 Ramification of K^+ channels in Higher Animals

Potassium channel genes are grouped according to similarity of amino acid sequence. Three groupings can be identified by membrane topology (2TM, 4TM, 6TM). This diagram was made by aligning 89 channel sequences, mostly from mammals, using just 47-49 amino acids including their P-regions and extending into the subsequent hydrophobic domains.

Taken from Hille (2001) Ion channels of excitable membranes, 3rd edition, Sinauer Associates, Inc. U.S.A. pg. 135.

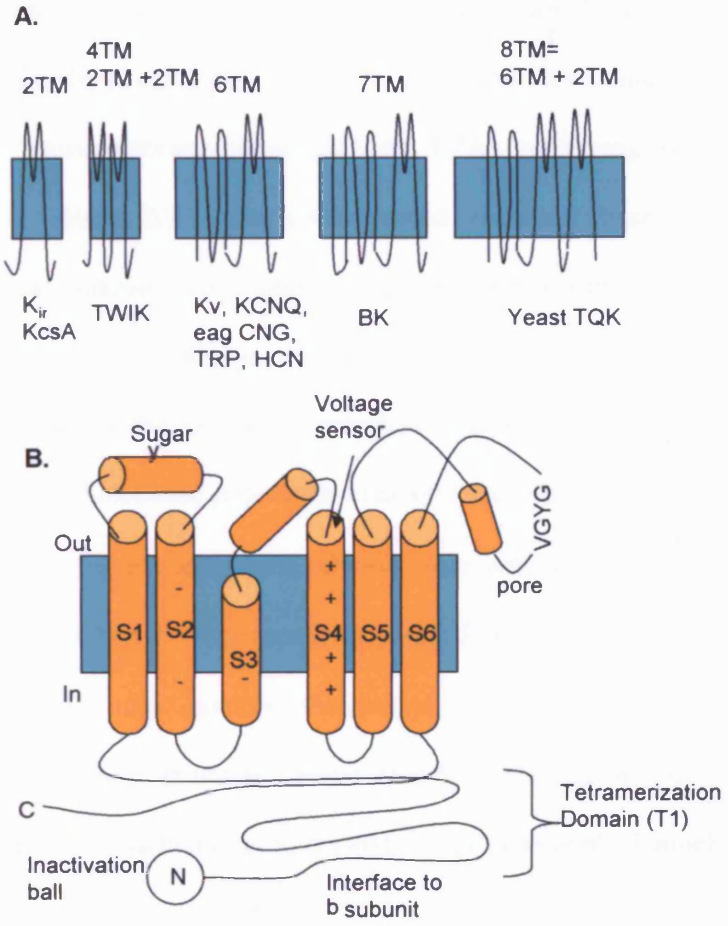

Figure 1.2 Structure of potassium channels

A, Shows the different transmembrane topologies of K-channel subunits. 2TM, 4TM, 6TM, 7TM and 8TM are abbreviations for proteins with 2, 4, 6, 7 and 8 transmembrane regions. Each potassium channel must have enough subunits for four P-loops to line the pore.

B, Shows functional regions of the α-subunit of a voltage-gated K channel.

Adapted from Hille (2001) Ion channels of excitable membranes, 3rd edition, Sinauer Associates, Inc. U.S.A. pg. 133.

The simplest of the potassium channel structures is the two transmembrane (2TM) K-channel as represented by the bacterial K channel, KcsA, which has been revealed at atomic resolution (Doyle et al., 1998). There are also other K-channel subunits, which have four, or eight transmembrane domains (figure 1.2A), containing two P-regions for each subunit (TWIK) (Hille, 2001). The voltage gated potassium channels are composed of six transmembrane domains. They sense a depolarization via the S4 segment (figure 1.2B). The S4 segment responds to a depolarization by moving and producing a movement of charge across the membrane, which somehow opens the pore, possibly via a twisting mechanism. Functional potassium channels are either tetramers or dimers of homo- or heteromeric arrangements of the subunits often with the addition of auxiliary β-subunits (Hille, 2001). When the four repeats embedded in the membrane come together, the four P-loops form the outer mouth of the channel and selectivity filter (Hille, 2001). The voltage-gated potassium channels can be broadly classified into three categories; Fast delayed rectifiers, slow delayed rectifiers and A-type (transient) channels.

Initially, diversity among the voltage sensitive potassium channel family was found to be due to variations of the Shaker gene; originally discovered in Drosophila but later identified in mice, rat and humans. The Shaker gene possesses at least 23 exons, alternative splicing of these leads to 10 different channel variants. There are also five different N-terminal regions and two different C termini. The existence of sister genes, Shab, Shaw and Shal, respectively named KCNBx, KCNCx and KCNDx in mammals, where x is the isoform number, further increases the variety of voltage-gated potassium channels. Mice do not possess introns, consequently there is a minimum of 12 varieties of

Shaker, named Kv1.1 to Kv1.12. Almost identical sequences have been identified for rat (rKv1.1 etc) and human (hKv1.1 etc) potassium channels. The rat possesses exons and alternative splicing in the Kv3 family.

As previously mentioned, two other potassium channels that share similar features to the voltage gated potassium channels, are the Ca^{2+}-activated potassium channels and the two-pore-domain potassium channels (TWIK). The Ca^{2+}-activated potassium channels are similar architecturally to the voltage-gated potassium channels but possess an extra transmembrane segment near the amino acid terminus (Miller, 1999). The two-pore-domain potassium channel have 4 transmembrane domains but novelly have a tandem pair of two potassium channel sequences (Miller, 1999; Lesage and Lazdunski, 2000). Large conductance Ca^{2+}-activated potassium (BK) channels are so called due to their unitary conductance values of between 100-250 pS (Hille, 2001). These channels are fundamental to neuronal excitability, being activated by both membrane depolarization and increases in intracellular calcium (Toro et al., 1998). The Ca^{2+}-activated potassium (BK) channel family can be divided into three subfamilies: BK, SK and IK channels (Vergara et al., 1998). BK channels are found to coexist with voltage-dependent calcium channels, where they are thought to act as their feedback modulators in both neurons and smooth muscle cells (Robitaille et al., 1993; Yazejian et al., 1997). Structurally, BK channels consist of a pore-forming α subunit and a regulatory β subunit (Garcia-Calvo et al., 1994). Functional diversity of the BK channel is achieved through the splice variations of the α subunit (Adelman et al., 1992; Tseng-Crank et al., 1994). Small conductance calcium-activated potassium (SK) channels have unitary conductances

between 4-20 pS (Hille, 2001) and are activated by an increase in intracellular calcium, for instance as occurs during an action potential. Upon activation these channels produce membrane hyperpolarization, which inhibits firing (Vergara et al., 1998). These channels are important in the prevention of tetanic firing in all excitable cells, as the increase and associated slow decrease in intracellular calcium that occurs during the action potential enables the SK channels to produce a long-lasting hyperpolarization, known as the slow afterhyperpolarization (sAHP) (Vergara et al., 1998). There are two classifications of slow sAHP, those sensitive to the bee venom toxin apamin and those that are not (Sah et al., 1996). The general consensus is that apamin-sensitive sAHPs are activated rapidly following a single action potential and decay with time constant of approximately 150 ms (Pennefather et al., 1985; Sah et al., 1991). By contrast, apamin-insensitive sAHPs exhibit slow rise times and decay with a time constant of approximately 1.5 s (Lancaster et al., 1986; Constanti et al., 1987; Sah et al., 1995). The final classification of Ca^{2+}-activated potassium channels is the intermediate conductance Ca^{2+}-activated (IK) channel. These channels are unique in having a conductance value of between 20-80 pS and are insensitive to apamin (Latorre et al., 1989).

The two-pore-domain potassium channels (TWIK) are unique in being the only potassium channel family to possess 2P domains rather than the one. They are distinguished by the presence of four transmembrane segments (M1-M4), the 2P domains, a short NH_2-terminal and long COOH cytosolic section. In addition they have an extensive extracellular loop between M1 and P1. Currently eight different types of the TWIK channels have been cloned in rodents and humans, which can be divided into four

different classes: TWIK1 and TWIK-2 are weak inward rectifiers; TREK-1 and TRAAK are polyunsaturated fatty acid and stretch-activated K+ channels; TASK-1 and TASK-2 are acid insensitive and KCNK6 and KCNK7 are silent subunits that are thought to require the association of other molecules to become activated (Lesage and Lazdunski, 2000).

Inward rectifier potassium channels are characterized by a greater inward flow of K^+ ions compared to the outward movement for the opposite driving force (Nichols and Lopatin, 1997). Different inward rectifier potassium channels were united under a standard classification scheme, similar to that for voltage-gated potassium channels. For example the ROMK group is included in the Kir1 subfamily, of which there are splice variants; ROMK1 (Kir1.1a) and ROMK2 (Kir1.1b). Subsequent to the isolation by expression cloning of the first members of the Kir channel family Kir1.1a (ROMK1) (Higgins, 1992), Kir2.1 (IRK1) (Kubo, Baldwin & Jan. 1993), and Kir3.1 (GIRK1) (Dascal et al., 1995), at least seven subfamilies (Kir1.0-Kir7.0) have been identified, sharing approximately 40% amino acid residues, while there is an estimated 60% homology with respect to amino acid sequence within the same subfamily (Nichols and Lopatin, 1997; Seino, 1999). These channels are composed of two transmembrane domains within each subunit, differing from the Kv channels which are composed of six transmembrane domains, while being similar by conserving the H5-loop that is responsible for K^+ selectivity in Kv channels (Heginbotham et al., 1992). Investigations of mutants which express channels with altered rectification properties suggest that these channels form as tetramers (Yang et al., 1995) similar to Kv channels (Mackinnon. 1991).

Other types of potassium current have been identified but at present their gene counterparts are not known, for example a current activated by high intracellular sodium ions has been found in the heart as well as in vertebrate and invertebrate neurons (Martin and Dryer, 1989). This channel appears to contribute towards the repolarization phase, being activated by an action potential although its gating shows little voltage dependence (Koh et al., 1994).

1.2 The role and function of the ATP-sensitive potassium channel

Adenosine 5'-triphosphate-sensitive potassium (K_{ATP}) channels are inward rectifiers, they are found in a variety of tissues and cell types where they couple the metabolic state of the cell to the membrane potential. Noma (1983) discovered the K_{ATP} channel using patches excised from cardiac myocytes. He suggested that K_{ATP} channels in the heart contribute to the cardiac action potential but mainly under ischaemic conditions. The primary regulator of the channel is ATP, therefore under normal myocardial conditions and even strong exercise the K_{ATP} channel is inhibited (Gogelein et al., 1999). Therefore the cardiac K_{ATP} channel is activated when ATP levels are critically reduced under ischaemia or hypoxic conditions, resulting in a large outward $I_{K\ (ATP)}$ current and consequently a shortening of the cardiac action potential duration (APD) and associated decrease in the refractory period (Sperelakis, 2001). This results in a decrease in Ca^{2+} influx and contraction and therefore ATP is conserved (Yokoshiki et al., 1998).

The role of the K_{ATP} channel differs depending upon where the channel resides in the body (Rodrigo and Standen, 2005). In vascular smooth muscle, opening of K_{ATP} channels are suggested to lead to hyperpolarization and smooth muscle relaxation. Activation of K_{ATP} channels in non-vascular smooth muscle like those found in the urinary bladder are also thought to cause relaxation, consequently they are implicated in having a central role in bladder electrical excitability and contraction (Petkov et al., 2001; Shieh et al., 2001). Noma (1983) suggested that the role of cardiac K_{ATP} channels was to prevent cellular calcium overload under stress, such as hypoxia, through shortening of the action potential. Opening of the K_{ATP} channel is thought to lead to an efflux of potassium from the cell, clamping the cell membrane potential towards the E_K for potassium, therefore opposing depolarization (figure 1.3). K_{ATP} channels are also involved in the regulation and release of insulin in pancreatic beta cells. K_{ATP} channels prevent the release of insulin when levels of nutrients within the bloodstream are low (Cook and Hales, 1984). The K_{ATP} channels in pancreatic β-cells are usually active when blood glucose levels are low (2-3 mM), thereby setting the membrane potential close to the K^+ equilibrium potential (E_K), resulting in a decrease in cell excitability and consequently a reduction in insulin secretion. A rise in the blood glucose level (5-7 mM) following a meal increases $[ATP]_i$, which closes the K_{ATP} channels, depolarising the plasma membrane of the β-cells. The depolarisation activates the voltage-gated calcium channels resulting in an increase in the intracellular calcium concentration. The associated rise in calcium triggers exocytosis of insulin granules and the release of insulin.

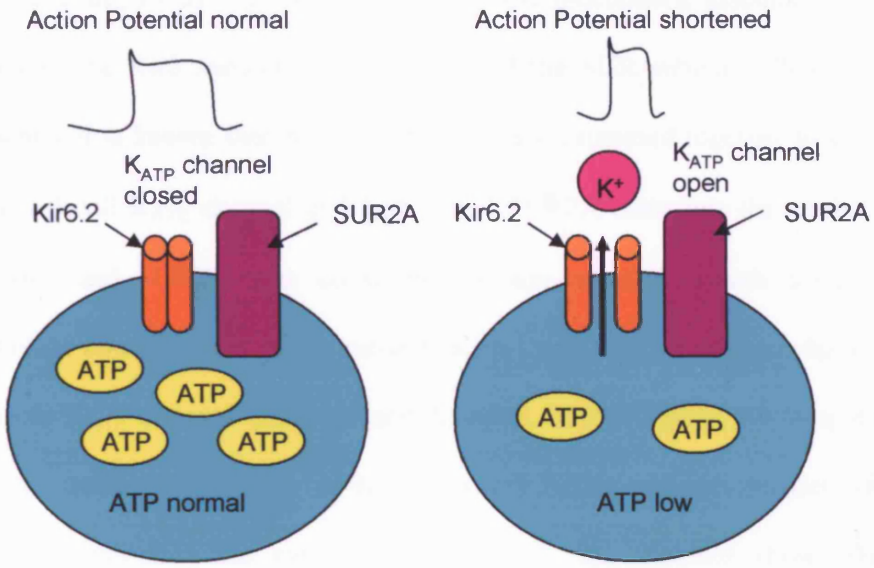

Figure 1.3 A schematic representation for the opening of K_{ATP} channels and subsequent shortening of the action potential due to the low intracellular ATP levels.

Adapted from Gogelein, H., Hartung, J. and Englert, H. (1999) Cardiac Ion Channels. Ed. Andreas E. Busch, Frankfurt am Main: Karger. pp. 229.

1.3 The molecular structure and subtypes of the ATP-sensitive potassium channel

Studies have shown that K_{ATP} channels are composed from pore-forming subunits of the Kir6 family (Kir6.1 and Kir6.2) and sulphonylurea receptors (SUR), regulatory proteins (Aguilar-Bryan et al., 1998). Together they form a hetero-octameric assembly composed of a tetramer of the Kir6 subunit and a tetramer of the SUR subunit (Clement et al., 1997). Presently it is known that Kir6.2 and SUR1 are expressed together to constitute the pancreatic β-cell K_{ATP} channel and Kir6.2 and SUR2A constitute the cardiac K_{ATP} channel. Kir6.2 and SUR2B may constitute the non-vascular smooth muscle K_{ATP} channel, whereas co-expression of the subunits Kir6.1 and SUR2B produce the vascular smooth muscle K_{ATP} channel (Rodrigo and Standen, 2005). Figure 1.4 is a diagram illustrating the membrane topology of Kir6.2, which forms a hetero-octamer with the SUR subunits constituting the cardiac K_{ATP} channel. The diagram shows the two transmembrane segments (M1 and M2) as well as the K^+ ion pore forming H5 region (Seino, 1999).

The large SUR subunit binds sulphonylureas and ATP, and is a member of the ATP-binding cassette (ABC) super family (Aguilar-Bryan et al., 1998) (figure 1.4Ai). The pore-forming Kir6 subunit is part of the inwardly rectifying potassium channel super family (Kir) (figure 1.4Aii). K_{ATP} channels were the first example of a heteromultimeric combination between an ion channel and a receptor that are not related to each other. For active K_{ATP} channels, both these subunits must be present (Seino, 1999). Investigations have found there to be two genes for the SUR subunits; SUR1 and SUR2. The SUR1 subunit is a high-affinity sulphonylurea receptor, whereas SUR2 is a low-affinity

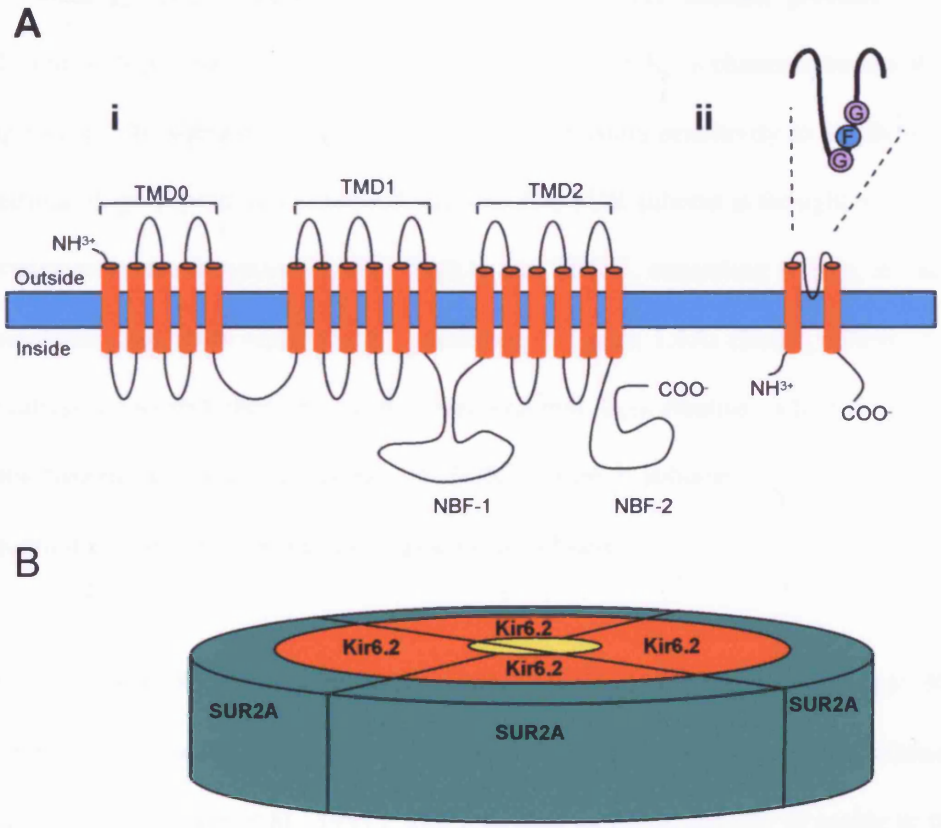

Figure 1.4 A diagram depicting the general structure of the cardiac K_{ATP} potassium channel.

A, i, Diagrammatic representation of the SUR2A subunit, which is found occurring with Kir6.2, which constitute the cardiac K_{ATP} channel. NBF-1 and NBF-2 (nucleotide binding folds) are located in the intracellular loop between TMD1 and TMD2 and in the C-terminal region, respectively. NH^{3+} and COO^- indicate the N^- and C terminus respectively. ii, shows the structural representation of the K_{ir} subunit that occurs with the SUR subunit to constitute the K_{ATP} channel. Also shown are the three residues located in the pore of the K_{ir} subunit that confer potassium selectivity; glycine and phenyalanine.

Adapted from Seino (1999) ATP-SENSITIVE POTASSIUM CHANNELS: A model of Heteromultimeric Potassium Channel/Receptor Assemblies. Annu. Rev. Physiol. 61:337-62.

B, The cardiac K_{ATP} channel is thought to be composed of four Kir6.2 subunits (tetramer) and four SUR2A subunits (tetramer) to produce a hetero-octamer arrangement.Green indicates the SUR2A subunit, orange indicates the Kir6.2 subunit and yellow indicates the pore of the channel.

sulphonylurea receptor. Alternative splicing of the SUR2 subunit produce SUR2A, SUR2B and SUR2C (Seino, 1999). The ATP inhibition of K_{ATP} channels occurs through binding to the Kir6 subunit, while the SUR subunit confers sensitivity to sulphonylureas and pharmacological potassium channel openers.The SUR subunit is thought to consist of three transmembrane domains, TMDO, TMD1 and TMD3, consisting of five, six and six transmembrane segments respectively, as shown in figure 1.4Ai (Seino, 1999). As this investigation is focused upon the cardiac sarcolemmal K_{ATP} channel, which consists of a heteromultimeric structure consisting of SUR2A/Kir6.2 subunits (figure 1.4B), most subsequent discussion will be focused upon these subunits.

Both Kir6.2 and SUR1 possess an endoplasmic reticulum (ER) retention signal (RKR), which prevents the trafficking of either subunit to the plasma membrane in the absence of the other subunit (Tucker et al., 1997). The retention signal is thought to reside in the C-terminus of the Kir6.2 subunit and in an intracellular loop between TM11 and nucleotide binding site 1 (NBF-1) in SUR1 and the C-terminus. (Tucker et al., 1997) Co-expression of these two subunits together masks the signals, thereby resulting in the trafficking of the subunits to the plasma membrane. The C-terminus of the SUR1 subunit has been suggested to contain an anterograde signal containing part of a dileucine motif and downstream phenylalanine, which is important for K_{ATP} channels to exit the ER/cis-Golgi organelles and be trafficked to the cell membrane (Sharma et al., 1999). Deletion of up to seven amino acids, including the phenylalanine significantly reduces cell surface expression of the K_{ATP} channels (Babenko et al., 1998a). Paradoxically, deletion of more

residues from the C-terminus results in expression of the K_{ATP} channel (Sakura et al., 1999).

1.4 The Regulation and Pharmacology of the ATP-sensitive potassium channel

Channel inhibitors and activators have been central to studying K^+ channel function. They have been used to identify and investigate the large number of different channel types and the information has been used to develop drugs for treating medical conditions; for example, sulphonylureas are used to treat non-insulin-dependent diabetes.

The main targets for potassium channel openers (KCOs) of K_{ATP} channels are the SUR subunits. Generally, activators of the K_{ATP} channel cause the membrane potential of the cell to hyperpolarize toward E_K, the consequences of which are dependent upon the tissue in which this occurs. There are three main classes of KCOs; the first generation include benzopyrans, cyanoguanidines, thioformamides, thiadiazines and pyridyl nitrates. Second generation KCOs contain cyclobuteediones, dihydropyridine-related compounds and tertiary carbinols (Edwards et al., 1990; Mannfold et al., 2004). Currently, four KCOs are in clinical use: nicorandil (a pyridine derivative), minoxidil (a pyrimidine), pinacidil (a cyanoguanidine) and diazoxide (a benzothiadiazine) (Rodrigo and Standen, 2005; Quayle et al., 1997). All four of the aforementioned KCOs are used for their vasorelaxant quailities in angina or hypertension, minoxidil is also used to treat male pattern baldness, while diazoxide is used to treat some hypoglycaemic conditions due to its hyperglycaemic action.

K_{ATP} channels can be blocked by many of the agents that block other types of potassium channel, such as tetraethylamonium ions, Ba^{2+} and aminopyridines (Quayle et al., 1997). Currently, the main interest centres around the hypoglycaemic drugs as used to treat type 2 diabetes, such as the sulphonylureas and glinides (Rodrigo and Standen, 2005). The best known inhibitors of the K_{ATP} channel are the sulphonylureas, which have a sulphonylurea group, causing membrane depolarization when they block the channel. Sulphonylureas can be classified as either first or second generation inhibitors, the latter being the most potent. Tolbutamide belongs to the first generation of sulphonylurea inhibitors and is therefore less effective as a hypoglycaemic treatment compared to glibenclamide, which is a second generation sulphonylurea. There are also newer sulphonylureas such as gliclazide and glimepiride (Rodrigo and Standen, 2005). A second group of inhibitors known as the glinides, are structurally related to the non-sulphonylurea part of glibenclamide but do not have a sulphonylurea group. This group includes meglitinide, repaglinide, nateglinide and mitiglinide (Gribble et al., 2003).

The pharmacological properties of K_{ATP} channels found in different areas of the body differ substantially. The cardiac K_{ATP} channels are suggested to be blocked by diazoxide and opened by the channel openers cromakalim and pinacidil, in contrast to the pancreatic K_{ATP} channels (Gogelein et al., 1999). Similarly, both types of K_{ATP} channel are blocked by sulphonylureas although the cardiac SUR2A/Kir6.2 channel is less sensitive to the sulphonylurea drug glibenclamide than the pancreatic SUR1/Kir6.2 channel (Inagaki et al., 1996). Second generation sulphonylureas such as glibenclamide are more potent blockers than first generation sulphonylureas like tolbutamide (Gogelein

et al., 1999). Glibenclamide was found to block both β-cell and cardiac K_{ATP} channel currents with high affinity in giant excised membrane patches of Xenopus oocytes expressing SURx with the mouse Kir6.2 subunit (K_i was 4.2 nM for SUR1/Kir6.2 channels and 27 nM for SUR2A/Kir6.2 currents) (Gogelein et al., 1999). The cardiac SUR2A/Kir6.2 channel appears to be unique in that this channel exhibits differing sensitivities to glibenclamide depending on its expression system (Gogelein et al., 1999). For example when the SUR2A/Kir6.2 channel is expressed in HEK293T cells, the resultant K_{ATP} channel could be blocked by glibenclamide with a K*i* of 160 nM when activated by pinacidil (Gogelein et al., 1999).

The exact binding regions for sulphonylureas have yet to be established but it has been found that TMD2, specifically the site between TM15 and TM16 is crucial for the sulphonylurea binding (Babenko et al., 1999). Both SUR1 and SUR2 are thought to possess a benzamido binding site but only SUR1 has a sulphonylurea binding site. Glibenclamide is thought to interact with two binding sites, compared to tolbutamide, which has only one binding site. Glibenclamide is thought to bind to two regions of the SUR1 subunit; the tolbutamide binding site and the binding site for the benzamido derivative meglitinide (Ashcroft and Gribble, 2000a).

Regulation of the various K_{ATP} channels through nucleotides is via both the Kir and SUR subunits. Tucker et al. (1997) found that the C-terminal truncated Kir6.2 subunit was inhibited by ATP and therefore concluded that Kir6.2 conferred the ATP sensitivity of the K_{ATP} channel. Subsequent investigations have found that over expression of the

Kir6.2 subunit without the SUR subunit in mammalian cells (John et al., 1998) or in the insect line Sf9 (Mikhailov et al., 1998) resulted in K_{ATP} channels, albeit at low density. The exact site for ATP binding is yet to be elucidated, but mutation of both R50G and K185Q produced a decrease in ATP-binding, suggesting that the N-terminal and C-terminal regions of Kir6.2 interact to inhibit channel activity by ATP (Tanabe et al., 2000). Only one molecule of ATP is required to close the K_{ATP} channel, although there are potentially four sites, one for each Kir subunit.

Experiments to characterize the nucleotide binding sites of SUR found that SUR1 binds ATP at NBF-1 and MgADP at NBF-2 (Ueda et al., 1997). It was suggested that either the direct binding of MgADP or the hydrolysis of MgATP at NBF-2 causes a conformational change that stabilises the binding of ATP at NBF-1. Using photo labelling experiments with 8-azido-[α-^{32}P]-ATP and 8-azido-[β-^{32}P]-ATP it was shown that NBF-2 of the SUR1, SUR2A and SUR2B subunits have ATPase activity and NBF-1 has little or none (Matsuo et al., 2000; Seino and Miki, 2003). It is thought that when the ratio of ATP/ADP is decreased, NBF-1 binds the ATP and NBF-2 binds MgADP, resulting in a conformational change where the interaction of the SUR1 subunit with the Kir6.2 subunit leads to the opening of K_{ATP} channels through a reduction of the affinity of Kir6.2 to ATP (Ueda et al., 1999b). Alternatively, when the ratio of ATP/ADP is increased, the associated reduction in MgADP results in a dissociation of bound MgADP from NBF-2 and therefore ATP is released from NBF-1 and the K_{ATP} channels close.

K_{ATP} channels can also be regulated by other factors such as protein kinase A (PKA), membrane phospholipids such as PIP_2 and PIP_3 and trimeric GTP-binding proteins. Protein kinase phosphorylation has been found to have different affects upon the Kir and SUR subunits. Protein kinase A has been found to increase K_{ATP} channel activity through phosphorylating the Kir6.2 subunit in β-cells. The site of PKA phosphorylation on the Kir subunit has yet to be determined, evidence so far has led to the suggestion of two possible sites; Ser372 (Beguin et al., 1999) and Thr224 (Lin et al., 2000). The phosphorylation of the SUR subunit affects the basal channel properties, such as decreasing burst duration, interburst interval, open probability and increases the functional channels at the cell membrane surface (Beguin et al., 1999).

The membrane phospholipid PIP_2 has been found to decrease the ATP-sensitivity of the K_{ATP} channels via the Kir6.2 subunit. The breakdown of PIP_2 by phospholipase C (PLC) has been shown to enhance the ATP-sensitivity of K_{ATP} channels (Xie et al., 1999). Effects of tolbutamide are also reduced as PIP_2 stabilizes the open configuration of the channel (Koster et al., 1999).

GTP-binding proteins have also been shown to alter K_{ATP} channel activity. The $G_{\alpha i1}$ subunit has been shown to stimulate both Kir6.2/SUR1 and Kir6.2/SUR2A channel complexes, contrasting with the $G_{\alpha i2}$ subunit that only increases the activity of Kir6.2/SUR2A (Sanchez et al., 1998). Wada et al., (2000) found that the ATP-sensitivity of the channel was reduced, producing a decrease in ATP-induced inhibition of the Kir6.2/SUR channel complex.

1.5 The effect of ischaemia in the heart- Cellular mechanisms occurring during late metabolic inhibition

In recent years, the cardiac K_{ATP} channel has been implicated in the phenomenon known as 'ichaemic preconditioning', whereby brief periods of ischaemia can protect the heart against a longer sustained period of ischaemia. Before describing the role of the K_{ATP} channel in ischaemic preconditioning (IPC), I will describe the events that occur during myocardial ischaemia. Myocardial ischaemia is a combination of oxygen deprivation of the heart muscle and inadequate removal of metabolites due to reduced blood flow or perfusion.

To enable scientists to study ischaemia in isolated cardiac myocytes, the conditions that produce ischaemic responses must be replicated in isolated cardiac tissue. To mimic ischaemia, a combination of cyanide and iodoacetic acid are often used to block electron transport and glycolysis respectively. Cyanide acts by blocking complex III of the electron transport system, preventing the extrusion of hydrogen ions, resulting in a reduction in the proton-motive force and hence the mitochondrial membrane potential. Consequently, production of ATP by the F_0/F_1 ATP is inhibited, which under normal conditions generates ATP through the flow of hydrogen ions back into the mitochondria. The effects of cyanide result in the dissipation of the mitochondrial membrane potential, a fall in ATP, NADH and $FADH_2$ as the F_0/F_1 ATP synthase is inhibited and the inability to utilize pyruvate may result in an increase in lactate production and an intracellular acidosis.

Iodoacetic acid blocks glycolysis preventing glycolytic production of ATP. As intracellular acidosis increases during metabolic inhibition the strength of contraction in individual myocytes reduces due to acidification reducing the sensitivity of the myofilaments to calcium (Orchard and Kentish 1990). Calcium transients also decrease in size which is thought to be due to a decreased efficiency of the SERCA pump on the sarcoplasmic reticulum (SR) resulting in less calcium being returned to the SR and therefore less calcium being released. Stern et al. (1988) suggested that the gradual decrease in calcium release and eventual failure of the action potential under anoxic conditions was due to alteration of the action potential. They showed that depolarizing the cell following contractile failure could restore contraction, therefore leading to the suggestion that contractile failure was due to shortening and eventual failure of the action potential. More recently, Diaz et al. (2002) suggested that under hypoxic conditions, calcium is released by the ryanodine receptors after direct activation by adjacent L-type calcium channels. It was suggested that the changes in systolic calcium observed under these stressed conditions were due to changes in the open probability of the ryanodine receptors.

These combined effects result firstly in depolarisation of the mitochondria and then cellular contractile failure. Shortly afterwards, individual myocytes rapidly shorten to a state known as rigor, due to reduced availability of ATP. Griffiths et al. (1998) suggested that during hypoxia and following rigor, calcium enters the mitochondria primarily via the reversal of the Na^{+}-Ca^{2+} exchanger and not via the calcium uniporter. In a further study, Griffiths et al., (1999) found that the reversal of the inhibition of the calcium

uniporter was due to the dissipation of the membrane potential. The inner mitochondrial membrane potential depolarises to approximately 0 mV, leading to a reversal of the F_0/F_1 ATP synthase, resulting in the consumption of ATP. During metabolic inhibition the decrease in ATP inhibits the Na, K-ATPase preventing the extrusion of intracellular sodium. Intracellular sodium increases due to the reversal of the Na-H exchanger as a result of the increase in lactic acid and associated hydrogen ions. Further, the rise in intracellular sodium increases intracellular calcium via the sarcolemmal sodium-calcium exchanger (figure 1.5). The decrease in ATP inhibits the Ca-ATPase on the SR and sarcolemma and therefore the intracellular calcium continues to rise.

1.6 The effect of ischaemia in the heart-cellular mechanisms occurring during reperfusion

Reperfusion is achieved in isolated tissue by removal of the metabolic inhibition (CN + IAA) and the addition of the substrates pyruvate and glucose, which rapidly re-energizs the mitochondria (Rodrigo & Standen, 2005). Upon reperfusion, the mitochondrial membrane potential initially repolarises. The pyruvate in the reperfusate is rapidly metabolised by the Krebs cycle, producing NADH and $FADH_2$. These are required by the electron transport system to re-establish the mitochondrial membrane potential. The rapid repolarisation of the mitochondrial membrane potential leads to an increase in ATP production due to activation of the F_0/F_1 ATP synthase. Intracellular calcium rapidly increases in the mitochondria due to uptake of calcium via the sarcolemmal sodium/calcium exchanger (Griffiths, 1999). However, Duchen et al., (1999) suggests that the rise in intracellular ATP leads to a fall in cytoplasmic calcium due to increased

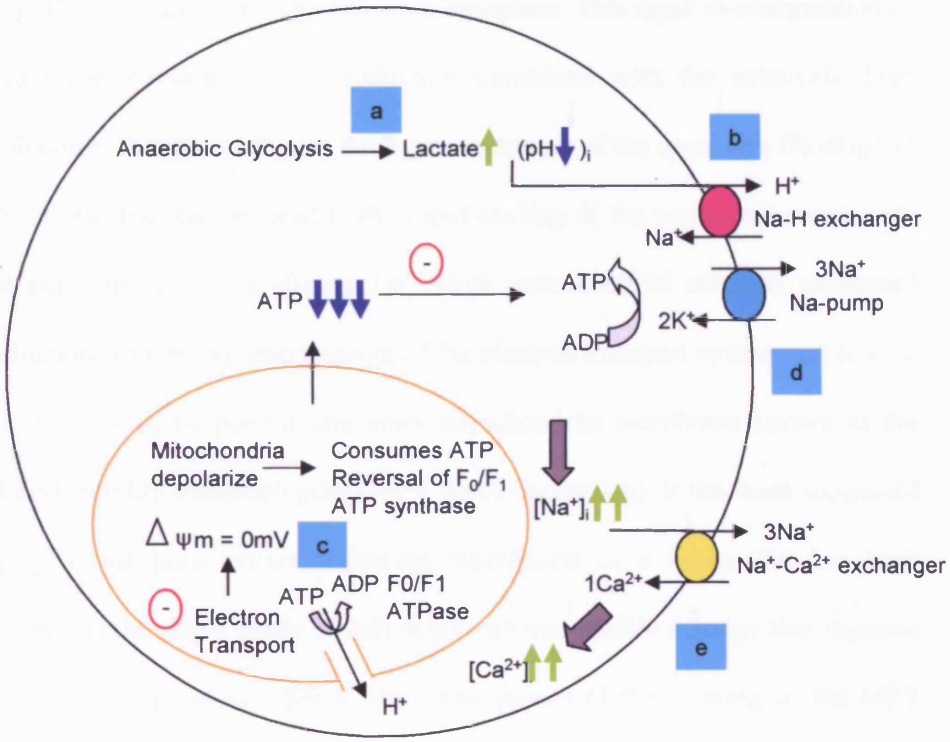

Figure 1.5 Cellular mechanisms occurring during late metabolic inhibition

During late metabolic inhibition, inhibition of glycolysis and the electron transport system by cyanide and iodoacetic acid leads to a fall in intracellular pH due to the increase in lactate (a). The rise in intracellular H^+ increases intracellular sodium levels via the sodium hydrogen exchanger (b). Simultaneously, inhibition of the electron transport system and consumption of ATP by the F0/F1 ATP synthase acting in reverse to oppose the depolarization of mitochondrial membrane potential causes dissipation of the mitochondrial membrane potential and dramatic fall in ATP (c). The decrease in intracellular ATP inhibits the sodium pump contributing to a further increase in intracellular sodium (d). The rise in intracellular sodium causes reversal of the sodium-calcium exchanger, increasing intracellular calcium (e).

activity of the SERCA pump on the sarcoplasmic reticulum. This rapid re-energization of the mitochondria and resulting ATP production combined with the relatively high intracellular calcium is thought to trigger the hypercontrature of the myocytes (Rodrigo & Standen, 2005). These two factors lead to the rapid cycling of the contractile machinery leading to a hypercontracted state (figure 1.6). High mitochondrial calcium, combined with ROS production from the re-energisation of the electron transport system can lead to the opening of a non specific pore in the inner mitochondrial membrane known as the mitochondrial permeability transition pore (MPT pore) (figure 1.6). It has been suggested that the opening of the pore occurs following reperfusion of a tissue that has been ischaemic and may be the major cause of cell death and irreversible damage that happens upon reperfusion (Halestrap et al., 2003). The consequence of the opening of the MPT pore is that the mitochondria are no longer able to produce ATP, which is vital to the repair of damage caused by the calcium-dependent proteases, nucleases and phospholipases activated during ischaemia/reperfusion. This leads to almost certain death due to the discrepancy between the cell's inability to produce ATP and its consumption. Halestrap et al. (1997) showed by using a technique applicable to perfused hearts that the MPT pore opens in reperfusion and not ischaemia. This was based upon experiments where the levels of [^{3}H]-DOG (Deoxyglucose) were measured following ischaemia and reperfusion of intact ex-vivo hearts. As [^{3}H]-DOG is a non metabolised glucose derivative, this compound could only enter the mitochondria through the MPT pore. Indeed, their evidence showed that the level of [^{3}H]-DOG did not increase immediately following an ischaemic period, but increased significantly after reperfusion. The mitochondrial permeability transition pore is thought to be constructed from a voltage-

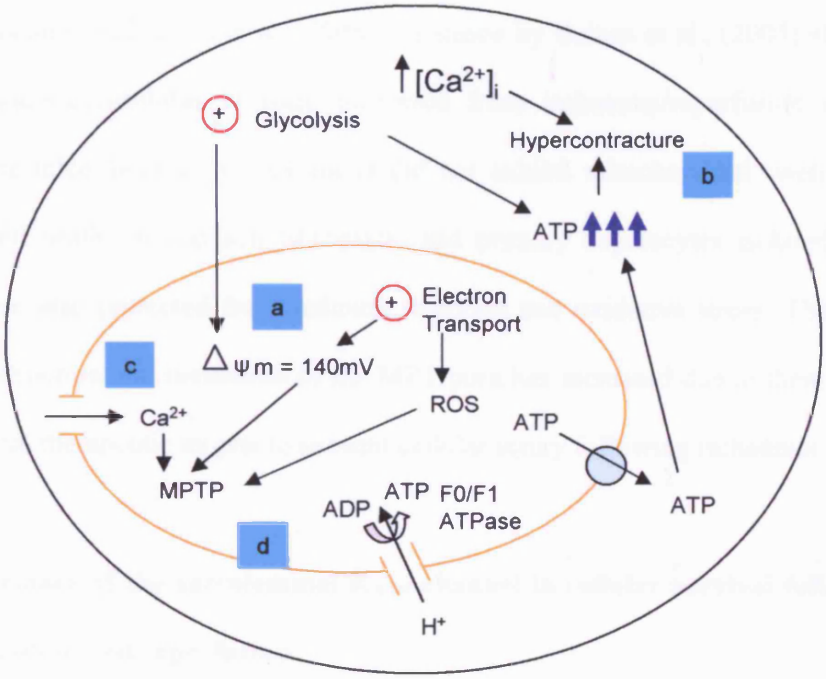

Figure 1.6 Cellular mechanisms occurring during reperfusion

During reperfusion, the substrates in the perfusate restart glycolysis and the electron transport system leading to the re-establishment of the mitochondrial membrane potential (a). Due to the increased intracellular calcium and availability of ATP, this results in a massive cellular hypercontracture (b). Re-establishment of the mitochondrial membrane potential drives calcium into the mitochondria, down its electrochemical gradient (c). High intracellular calcium and production of ROS by the electron transport system, coupled to the negative mitochondrial membrane potential renders the opening of the MPTP more likely (d).

dependent anion channel, the adenine nucleotide translocator, cyclophilin D and additional molecules (Tsujimoto et al., 2006). Evidence by Baines et al., (2005) showed that mice lacking cyclophilin D were protected from ischaemia/reperfusion injury. Specifically, the mice lacking cyclophilin D did not exhibit mitochondrial swelling or spontaneous cell death. In addition fibroblasts and primary hepatocytes isolated from these mice were also protected from calcium overload and oxidative stress. Therefore interest in the structure and regulation of the MPT pore has increased due to them being possible potential therapeutic targets to prevent cellular injury following ischaemia.

1.7 The importance of the sarcolemmal K_{ATP} channel in cellular survival following metabolic inhibition and reperfusion

As the previous discussion has shown, the regulation of the Na^+/Ca^{2+} exchanger is crucial to whether a cell survives metabolic inhibition and reperfusion. At rest when the membrane potential is approximately -70 mV, the reversal potential for the sodium-calcium exchanger is -32.6 mV as illustrated below:

$E_{Na/Ca} = 3E_{Na} - 2E_{Ca}$

Where; $E_{Na} = 63 \log_{10} [Na]_o/[Na]_i$

$E_{Ca} = 31.5\log_{10} [Ca^{2+}]_o/[Ca^{2+}]_i$

At rest $E_{Na/Ca} = -32.6$ mV

Outside sodium concentration is 140 mM and inside is 8.9 mM.

Outside calcium concentration is 2 mM and inside is 150 nM

(Values for internal Na^+ and Ca^{2+} taken from Bers, D.M (2003) Excitation-Contraction Coupling and Cardiac force. Kluwer Academic Publishers.)

Therefore under normal conditions, where outside sodium is 140 mM and inside sodium is 8.9, 3 sodium ions enter the cell in exchange for 1 calcium ion being extruded. However, under conditions of metabolic inhibition, lactic acid increases leading to an increase in intracellular hydrogen ions, which are extruded in return for sodium ions via the sodium-hydrogen exchanger leading to a rise in intracellular sodium. The increase in intracellular sodium affects the reversal potential of the Na^+-Ca^{2+} exchanger due to its effects on the Na^+-equilibrium potential (E_{Na}). Consequently, once intracellular sodium increases to 30 mM, the reversal of the Na^+-Ca^{2+} exchanger is -125 mV. Baczko et al. (2003) demonstrated the dependence of Na^+-Ca^{2+} exchanger on membrane potential during hypoxia-reoxygeneration. They clearly showed that hyperpolarization of the membrane potential protected the cell from calcium overload and hypercontacture. It was shown that the increase of intracellular calcium was due to reversal of the Na^+-Ca^{2+} exchanger, and therefore membrane potential determines the extent of intracellular calcium loading.

The sarcolemmal K_{ATP} channel is known to open under conditions of metabolic stress, when intracellular ATP is low. The importance of the sarcolemmal K_{ATP} channel under these conditions is that the opening of this channel reduces calcium influx via the L-type calcium through the shortening of the action potential duration and via the sodium-calcium exchanger. Baczko et al. (2004) showed that the hyperpolarization of the membrane potential resulting from the opening of the sarcolemmal K_{ATP} channels prevented calcium overload. It was suggested that hyperpolarization towards the E_K for

potassium (-93 mV), favours the calcium extrusion mode of the Na^{+}-Ca^{2+} exchanger, therefore limiting cellular calcium load, hypercontracture and death in contrast to conditions where the sarcolemmal K_{ATP} channel is not opened and the membrane potential is therefore more positive (figure 1.7).

1.8 Ischaemic preconditioning of the heart

Myocardial ischaemic preconditioning is a phenomenon whereby brief periods of ischaemia protect the heart against loss of cardiovascular function following longer periods of ischaemic injury. Ischaemic preconditioning was initially described by Murry et al. (1986) in a canine infarct model, where brief periods of ischaemia due to coronary occlusion reduced the infarct size after a subsequent 40 minute ischaemic insult. Subsequent experiments have shown that protection can be produced in a wide range of species and in isolated myocytes as well as whole hearts. Protection can be divided into two types; classical or early preconditioning and delayed preconditioning. Classical preconditioning is protection afforded up to about twelve hours, after which it disappears. Delayed preconditioning then reappears 24-72 hours after the initial stimuli (Yellon and Downey, 2003). Protection has been measured in a number of different species not only in whole hearts but isolated myocytes including the rat (Ganote et al., 1993, dog (Murry et al., 1986) and rabbit (Cohen et al., 1991). Protection has been measured in a number of ways which include the reduction of reperfusion arrhymias (Shiki and Hearse, 1987) and increased resistance of isolated myocytes to hypoxic injury (Armstrong and Ganote, 1994) in addition to the classical finding of a decrease in infarct size (Yellon and Downey, 2003).

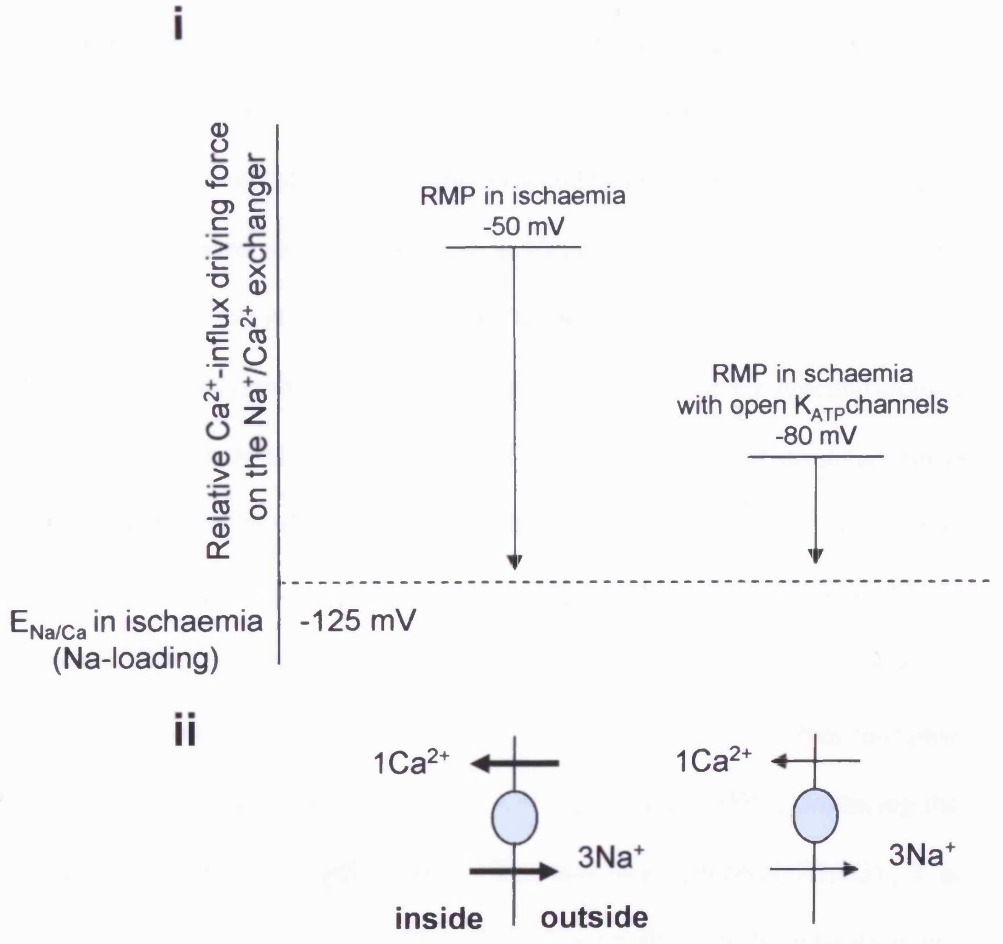

Figure 1.7 The effect of opening of the K_{ATP} channel on Ca-flux on the Na^+-Ca^{2+} exchanger

i, Schematic showing that opening of the K_{ATP} channels clamps the resting membrane potential towards E_K for potassium (-93 mV) and reduces the driving force for Ca-influx via the Na^+-Ca^{2+} exchanger. ii, Ca-influx is reduced when K_{ATP} channels are opened.

A number of trigger and mediator mechanisms for ischaemic preconditioning have been implicated, based mainly upon the ability to either activate or inhibit a preconditioning response through the use of specific receptor and/or channel activators or blockers. Liu et al. (1991) were the first to suggest that ischaemic preconditioning is triggered by receptor occupation. This was based on experimental evidence whereby activation of the adenosine A_1 receptor resulted in protection similar to that of preconditioning. Following this observation, many investigations have led to the suggestion that for preconditioning to occur, multiple receptors must activate in parallel to reach a threshold stimulus. These receptors include, adenosine, bradykinin, angiotensin AT_1, receptors for ET_1, muscarinic and opioid receptors; specifically any G_i-coupled receptor (Yellon and Downey, 2003). Once the threshold for activation of preconditioning has been met, then a number of mediator signals are activated, probably via a phospholipase C pathway. Phospholipase C catalyses the hydrolysis of phosphatidylinositol 4,5-bisphosphate (PIP_2), producing the second messengers, inositol 1,3,4-triphosphate (IP_3) and diacylglycerol (DAG). It is thought that DAG then stimulates protein kinase C (PKC), resulting in the activation and translocation of specific PKC isoforms from the cytosol to anchoring proteins on the membrane cytoskeleton (Dempsey et al., 2000). PKC is then thought to activate a kinase cascade, possibly through the activation of each of the MAPK families, specifically the 42/44-kDa extracellular receptor kinase (ERK), the 46/54-kDa c-*jun* (JNK) and p38 MAPK (Maulik et al., 1998). In addition, Tong et al. (2000) presented evidence of a role for phosphatidylinositol 3-OH kinase (PI 3-kinase) in preconditioning. This was based upon evidence whereby a PI 3-kinase inhibitor (wortmannin) was found to block pre-

conditioning. PKA is also thought to have a role as a mediator in preconditioning, independent of PKC, based upon evidence which demonstrated that the activation of PKA had cardioprotective effects, possibly due to the inhibition of Rho-kinase (Sanada et al., 2004).

Reactive oxygen species (ROS) are also thought to act as mediators in preconditioning, specifically activating various kinases such as PKC. Baines et al. (1997) showed that preconditioning could be blocked by a free radical scavenger. Cohen et al. (2001) showed that ROS were downstream of triggers such as bradykinin, opioids and acetylcholine as application of these agonists resulted in the production of ROS. The complete downstream components of the preconditioning pathway are unknown but are likely to include PKC, specifically PKCε (Baines et al., 2002), which may translocate to the mitochondria (Baines et al., 2003).

Transient opening of the mitochondrial permeability transition pore (MPTP) during the preconditioning phase has been suggested to be cardioprotective as it prevents increased opening during the index ischaemia (Hausenloy et al., 2004; Juhaszova et al., 2004). It has been suggested that ROS could activate PKC and other kinases, leading to the increased open probability of mitochondrial K^+ channels (see section 1.10), resulting in an uncoupling of the mitochondria and a decrease in the release of ROS following the index ischaemia (Hanley and Daut, 2005). It has been suggested that the influx of potassium into the mitochondria will lead to an increase in matrix volume due to an associated influx of water, which could act as the 'memory' element in preconditioning

(Juhaszova et al., 2004). Other mechanisms leading to inhibition of the MPTP other than via K^+ channels have also been suggested. These include, the phosphorylation of GSK-3β, the downsteam mediator of PI 3-Kinase by PKC and other kinases, can also lead to an increase in the threshold for activation of the MPTP by ROS during reperfusion (Juhaszova et al., 2004). Inhibition of the MPTP is also suggested to be due to the ROS dependent translocation of PKCε to the mitochondria, which is suggested to interact and inhibit the VDAC1 component of the MPTP (Clerk and Sugden, 1998). Current research is focused upon investigating what uncouples the mitochondria, whether that it is indeed ROS or K^+ channels in the mitochondrial membrane or an as yet unidentified mechanism (see section 1.10). In addition sarcolemmal K_{ATP} channels are also thought to be involved in preconditioning, however their role in this phenomenon will be discussed at depth in section 1.10.

1.9 Mechanisms of delayed preconditioning

The delayed phase of preconditioning, also known as the second window of protection (SWOP), occurs following a 24 hour delay between the preconditioning and the test ischaemia, resulting in a more prolonged yet less powerful protection (Kuzuya et al., 1993; Yellon and Downey, 2003) The main difference between classical and delayed preconditioning is that the increased time till the SWOP means that there is sufficient time for the possibility of new protein synthesis, post translational protein modification, and a change in the compartmentalization of existing proteins (Yellon and Baxter, 1995;Yellon and Downey, 2003).

In delayed preconditioning, the triggers are very similar to those of classical preconditioning; receptor mediated triggers such as the adenosine, bradykinnin and opioid receptors have all been implicated (Baxter et al., 1994). However, the importance of each trigger appears to vary enormously according to the species under investigation. Other triggers such as nitric oxide (NO), prostanoids and catecholamines have all been suggested to act as both triggers and mediators in the second window of protection (SWOP) (Sun et al., 1996). The mediators in SWOP are also similar to those in classical preconditioning, namely PKC, tyrosine kinases and MAPKs (Imagawa et al., 1997).

The end effectors of delayed preconditioning are thought to include an upregulation of the 72-kDa inducible heat stress protein, hsp72i (Dillmann et al., 1986) and the mitoK_{ATP} channel, with the latter being activated by a kinase dependent mechanism (Takashi et al., 1999). Nitric oxide is thought to act as an end effector of delayed preconditioning, therefore being unique in possessing a dual role as both a trigger and effector of delayed preconditioning (Bolli et al., 1998) It is thought that preconditioning produces an upregulation of inducible nitric oxide synthase (iNOS) and associated increase in nitric oxide synthase (NOS) (Vegh et al., 1994). However, the exact role of NOS is unclear because SWOP can still be exhibited by animals administrered with adenosine receptor agonists in which the iNOS gene has been disrupted (Bell et al., 2001). Adenosine receptor agonists appear to produce SWOP via a non NOS dependent mechanism, as preconditioning under these conditions was not inhibited by iNOS inhibitors (Dana et al., 2001).

1.10 History of the involvement of K_{ATP} channels in cardioprotection

It has been proposed that there are two types of K_{ATP} channel in cardiac myocytes; sarcolemmal and mitochondrial. The hypothesized roles for these channels in ischaemic preconditioning are based upon pharmacological research. The sarcolemmal K_{ATP} channel is thought to be opened by a number of KCOs such as pinacidil, cromakalim, aprikalim, nicorandil and diazoxide if the ADP is increased (Rodrigo and Standen, 2005). Sarcolemmal K_{ATP} channels are blocked by sulphonylureas such as glibenclamide and novel sulphonylureas such as HMR1883 and 1402, designed specifically to target the channel. By contrast the mitochondrial K_{ATP} channel is thought to be opened by diazoxide at concentrations 1000 times lower than those which open the sarcolemmal K_{ATP} channels. There are also other openers of the mitochondrial K_{ATP} channel that include cromakalim, pinacidil, P-1075 and nicorandil, but which also open the sarcolemmal K_{ATP} channel. The blocker (5-HD) is generally accepted to be a blocker of the mitochondrial K_{ATP} channels. However, for the mitochondrial channels to be sensitive to 5-HD, the presence of either a pharmacological opener, ATP, Mg^{2+} or GTP are required (Rodrigo and Standen, 2005). The sarcolemmal K_{ATP} channel is thought to be protective as opening of this channel is thought to shorten the action potential under hypoxic conditions, therefore conserving the energy and calcium reserves and preventing cell necrosis. In addition, opening of the sarcolemmal K_{ATP} channel is also thought to be protective as it hyperpolarizes the membrane potential, which favours calcium extrusion via the Na^{+}-Ca^{2+} exchanger, thereby preventing cellular calcium overload, hypercontracture and death (Baczko et al., 2004). Opening of the mitochondrial K_{ATP} channel is thought to be protective because by opening, the membrane potential is

depolarized and therefore there is a reduced drive for calcium into the mitochondria which could lead to opening of the MPT pore upon reperfusion (Hanley and Daut, 2005). Another suggestion is that opening of the mitochondrial K_{ATP} channels and subsequent increase in matrix volume acts as a 'memory' element in preconditioning leading to a decrease in ROS following the index ischaemia, which prevents opening of the MPTP (Hanley and Daut, 2005). Consequently, molecular and pharmacological techniques have been used to investigate the role of both the sarcolemmal and mitochondrial K_{ATP} channels in ischaemic preconditioning.

Initially it was thought that the sarcolemmal K_{ATP} channel was the channel involved in the preconditioning phenomenon, based upon evidence by Gross et al.(1992) that showed that the K_{ATP} channel openers and blockers could mimic and inhibit preconditioning respectively. Other studies also demonstrated that inhibition of the sarcolemmal K_{ATP} channel, through the application of K_{ATP} channel blockers, such as glibenclamide, prevented action potential duration shortening during ischaemia and consequently impaired recovery of ventricular function following reperfusion (Cole et al., 1991). Cole et al., (1999) also demonstrated that pre-treatment with the K_{ATP} channel opener pinacidil resulted in an accelerated APD shortening and an associated improvement in ventricular function following reperfusion (Cole et al., 1991). The link between K_{ATP} channel openers and ischaemic pre-conditioning was illustrated by Tan et al. (Tan et al., 1993), who showed that both increased the time to electrical uncoupling and associated APD shortening. Suzuki et al. (2001) found that the Kir6.2 subunit is important for the reduction of cardiac excitability and contractility which is induced by potassium channel

openers. This was shown through the application of potassium channel openers, such as pinacidil, P-1075 and diazoxide to Kir6.2-deficient mice; the subunit from which the sarcolemmal channel is thought to be composed. In wild-type mice pinacidil produced an outward current and action potential shortening, which was not observed in the Kir6.2 knockout mice. Gene transfer of subunit Kir6.2 into neonatal ventricular cells could produce similar responses to the wild-type mice when P-1075 was applied. Further investigation found that pinacidil reduced force generation in the wild type but not the Kir6.2-deficient mice. The importance of the sarcolemmal K_{ATP} channels in cardioprotection was further emphasized in latter research conducted by Suzuki et al. (2002) who found that application of metabolic inhibition using a glucose-free, dinitrophenol-containing solution resulted in the activation of the sarcolemmal K_{ATP} current and shortening of the action potential of the ventricular cells in wild-type but not Kir6.2-deficient mice. They also showed that preconditioning reduced infarct size in the wild type but not Kir6.2-deficient mice. Recovery of contractile function after global ischaemia/reperfusion was found to be worse in the Kir6.2-deficient mice compared to the wild type mice, suggesting a role of the sarcolemmal K_{ATP} channels in recovery of contractile function following ischaemia. However, it has also been suggested that the high heart rate of the mouse in general, exagerates the role of the sarcolemmal K_{ATP} channel in protection (Suzuki et al., 2002). In addition, diazoxide-induced protection could only be produced in the wild type not in the Kir6.2 knock out mice. However protection could be abolished by pre-treatment with HMR1098 but not 5-HD in wild-type hearts, suggesting that the sarcolemmal K_{ATP} channel is central to protection (Suzuki et al., 2003). Jovanovic et al., (1998) showed that application of pinacidil to COS-7 cells

transfected with SUR2A and Kir6.2 genes, resulted in inhibition of Ca^{2+} loading upon hypoxia-reoxygeneration. COS-7 cells are non-contracting, therefore the sarcolemmal K_{ATP} channel may afford cardioprotection other than through shortening of the action potential duration. Rainbow et al., (2004) found that down regulation of the expression of the sarcolemmal K_{ATP} channel through SUR2A fragments also reduced cardioprotection during ischaemia, further supporting a role for sarcolemmal K_{ATP} channel in protection. Together, this research suggests that the sarcolemmal K_{ATP} channel may be important in reducing injury caused by ischaemia/reperfusion.

Increased pharmacological evidence has suggested that the ATP-sensitive potassium channel in the mitochondrial membrane may have a role in cardioprotection (Liu et al., 1998; Sato et al., 1998). Mitochondrial ATP-sensitive potassium channels were first described by Inoue et al. (Inoue et al., 1991) as single channels using patch clamp to record from giant mitoplasts formed by fusion of mitochondrial membranes from rat liver mitochondria (Rodrigo and Standen, 2005). Due to the difficulty in recording from these channels, further work on the mitoK_{ATP} channel used purified mitochondrial inner membranes reconstituted into vesicles or lipd bilayers. As yet the actual molecular structure of the mitoK_{ATP} channel has yet to be determined. Yao and Gross (1994) were the first to suggest that a shortening of the action potential duration (APD) due to the sarolemmal K_{ATP} channel was not responsible for cardioprotection. They demonstrated that a low dose of the nonselective K_{ATP} channel opener bimakalim did not effect APD shortening, but still resulted in a cardioprotective effect comparable to that of two higher doses of bimakalim where there was an APD shortening. Other studies also suggested

another intracellular site of cardioprotection other than the sarcolemmal K_{ATP} channel, such as shown by Grover et al. (1995). Grover et al., (1995) showed that APD shortening and cardioprotection were not correlated as the cardioprotective effects of both cromakalim and Ischemic Preconditioning (IPC) were not reduced by dofetilide, a class III antiarrhthmic that prevented action potential shortening. Armstrong et al. (1995) also presented evidence for the role of a K_{ATP} channel in mediating the cardioprotective effects of K_{ATP} channel openers and IPC in the absence of an action potential. Armstrong et al. (1995) showed that pre-incubation of rabbit myocytes with pinacidil prior to ischaemia resulted in cardioprotection.

Garlid et al. (1997) were the first to demonstrate a role for the mitochondrial K_{ATP} channel in cardioprotection. They showed that concentrations of diazoxide that were too low to activate the sarcolemmal K_{ATP} channel produced cardioprotective effects similar to that of cromakaim, whereby there was an increased time to ischaemic contracture and enhanced functional recovery following global ischaemia and reperfusion in isolated rat hearts. These effects could be inhibited by the K_{ATP} blockers, 5-HD and glibenclamide, suggesting a role for the mitoK_{ATP} channel in cardioprotection. Other pharmacological studies have investigated the role of the mitoK_{ATP} channel in cardioprotection using novel pharmacological agents that open the sarcolemmal K_{ATP} channel but inhibit the mitochondrial K_{ATP} channel, such as MCC-134. Sasaki et al. (Sasaki et al., 2003) found that MCC-134 blocked diazoxide-induced flavoprotein oxidation and activated sarcolemmal K_{ATP} channels in rabbit ventricular myocytes, further suggesting a role for mitochondrial K_{ATP} channels in protection. In pioneering work by Marban's group (Liu et

al., 1998; Sato et al., 1998), diazoxide opened and 5-HD could inhibit the mitoK_{ATP} channel in rabbit cardiac myocytes as indicated by the increase and decrease of flavoprotein fluorescence. They suggested that opening of the mitoK_{ATP} channel resulted in dissipation of the mitochondrial membrane potential, leading to the acceleration of electron transfer by the respiratory chain. This in turn was thought to result in an increased production of electron donors and net oxidation of the mitochondria. However, diazoxide was found to have no effect upon flavoprotein fluorescence in either isolated rat (Lawrence et al., 2001) or guinea-pig myocytes (Hanley et al., 2002). Marban stated that his group incubated their cells in substrate-free media overnight which explained the fact that this phenomenon was not reported by the aforementioned groups. Therefore, upon addition of diazoxide (a substrate of β oxidation) this resulted in acceleration of the electron transport system and associated increase in fluorescence.

All the above investigations have suggested a role for the mitochondrial K_{ATP} channel in cardioprotection. However, in recent years it has been shown that the blocker of the mitoK_{ATP} channel, 5-HD has non-specific effects other than on the mitoK_{ATP} channel (Hanley et al., 2005). It has been found that 5-HD can be converted to 5-HD-CoA and can be metabolized by β-oxidation, therefore interfering with the β-oxidation of fatty acids by acting as a metabolite. In addition, diazoxide has also been shown to block the citric acid cycle by inhibiting succinate dehydrogenase, thereby leading to matrix oxidation (Hanley et al., 2002). Consequently the apparent protective effect of the mitochondrial K_{ATP} channel activators in IPC may be due to their effect on mitochondrial metabolism rather than on the mitoK_{ATP} channel.

Another suggestion is that activation of both the sarcolemmal and mitochondrial K_{ATP} channels are required for cardioprotection. Both channels are required to be blocked for preconditioning to occur in dogs (Sanada et al., 2001). Toyoda et al. (2000) investigated the role of the sarcolemmal and mitochondrial K_{ATP} channel before ischaemia, during reperfusion and during ischaemia and reperfusion using non-selective and selective sarcolemmal and mitochondrial blockers; glibenclamide, HMR-1883 and 5-hydroxydecanoate (5-HD) respectively. It was found that mitochondrial K_{ATP} channels affect infarct size reduction mainly during ischaemia whereas sarcolemmal K_{ATP} channels affect functional recovery during ischaemia and reperfusion. This research further supports a role for both sarcolemmal and mitochondrial K_{ATP} channels in ischaemic preconditioning. Tanno et al. (2001) suggested that both the sarcolemmal and mitochondrial K_{ATP} channels might have a role in anti-infarct tolerance. These findings were supported by evidence produced by Sanada et al. (2001) who also concluded that separately, mitochondrial and sarcolemmal K_{ATP} channels might have different roles in limiting the size of the infarct in the canine heart.

Currently, it is generally accepted that the sarcolemmal K_{ATP} channel is involved in protection as demonstrated by Kir6.2 knock-out mice (Suzuki et al., 2002; Suzuki et al., 2003). The role of the mitochondrial K_{ATP} is less established, but it is currently believed that the mitochondrial K_{ATP} channel is one of three potassium channels in the mitochondrial membrane that act together to regulate the volume of the matrix, which would have major effects upon mitochondrial function (Hanley and Daut, 2005). It was

suggested that reactive oxygen species (ROS) could activate PKC and other kinases, leading to the increased open probability of K^+ channels, resulting in an uncoupling of the mitochondria and a decrease in the release of ROS following the index ischaemia (Hanley and Daut, 2005). The other two potassium channels involved are thought to be the BKCa and Kv1.3 (Sieman et al., 1999; Szabo et al., 2005). It is suggested that mitochondrial swelling caused by the influx of potassium ions through these channels down their electrochemical gradients is responsible for cardioprotection. Juhaszova et al. (2004) found that most preconditioning stimuli resulted in a 2.5-4% swelling of the mitochondria. It was found that both swelling and cardioprotection could be abolished by the selective chloride Cl^- channel inhibitor IAA94. This implicates the K^+ channels, as an influx of K^+ into the mitochondria can be linked to an influx in both Cl^- and water. As suggested in section 1.6, the swelling could act as a 'memory' in preconditioning preventing the opening of the MPT pore during the index ischaemia and therefore inducing cardioprotection (Hausenloy et al., 2004).

1.11 The pathways involved in Classical and Delayed preconditioning

The signalling pathway(s) through which the sarcolemmal and mitochondrial K_{ATP} channels are primed for protection in classical preconditioning are still under debate. Different triggers of IPC, such as nitric oxide (NO), adenosine, bradykinin, opioids and catecholamines have been identified, and are thought to be activated during the preconditioning phase. It has been suggested that these triggers may be species dependent and also reliant on the length of the preconditioning stimulus (Yellon and Downey, 2003). A number of mediators have been identified which are involved in the protein

kinase signalling pathway, such as Src tyrosine kinases, p38 mitogen-activated protein kinase (MAPK) and the JAK/STAT pathway (Michel et al., 2001; Ping and Murphy, 2000). In recent years, investigations have focussed on the role of the sarcolemmal and mitochondrial K_{ATP} channel as either trigger or end effector in ischaemic preconditioning.

A synergistic action between adenosine receptor activation and PKC phosphorylation may result in opening of the sarcolemmal K_{ATP} channels. Light et al., (2001) showed a functional coupling between PKC and the sarcolemmal K_{ATP} channel in mediating cardioprotection. IPC has been shown to reduce the inhibition of the sarcolemmal Na-K-ATPase, possibly through phosphorylation by PKC, increasing depletion of subsarcolemmal ATP and enhancing sarcolemmal K_{ATP} channel opening early during ischaemia (Haruna et al., 1998). Tosaki et al. (1997) showed that the production of diacylglycerol by phospholipase D resulted in the activation and transolocation of PKC, which has been implicated in the opening of the sarcolemmal and mitochondrial K_{ATP} channels. There is also evidence to suggest that IPC involves cross talk between the sarcolemmal and mitochondrial K_{ATP} channels. Kong et al., (2001) showed that the protection afforded to rabbits that were raised under hypoxic conditions could not be blocked by either 5-HD, a selective mitochondrial K_{ATP} channel blocker or HMR-1098, a selective sarcolemmal K_{ATP} blocker. Only a combination of both blockers could completely abolish protection. Light et al., (2001) suggested that there was a temporal involvement of sarcolemmal K_{ATP} and mitochondrial K_{ATP} channels.They found that protection by the PKC activator, phorbol 12-myristate 13-acetate (PMA) partially

inhibited by 5-HD during chemically induced hypoxia, whereas HMR-1098, abolished protection during reoxygeneration.

In conclusion, although it is accepted that the sarcolemmal and possibly the mitochondrial K_{ATP} channel are involved in protection, the pathways to their activation and when it occurs are still under invesigation. The main problem with establishing how and when the mitochondrial K_{ATP} channel is opened to produce cardioprotection following preconditioning is that the subunit identity of the mitochondrial channel has not been established, which presently limits investigations into its role. In addition, as previously mentioned, there is currently sceptism concerning the specificity of mitochondrial K_{ATP} openers and blockers, as studies have shown diazoxide and 5-HD to have effects other than the mitochondrial K_{ATP} channel (Hanley et al., 2005).

1.12 Gender differences in cardiovascular disease and cardioprotection

Sex-related differences have been highlighted in relation to cardiovascular diseases due mainly to the observation of an earlier onset of heart disease in men, some 10-15 years earlier to women (Rossouw, 2002). It has been reported that some arrhymias are more common in males than females, such as sudden cardiac death (Shimoni and Xiu-Fang, 2003). This raised the question of whether the presence of the female or male hormone either decreased or increased the risk of heart disease, respectively. The current opinion is that oestrogen may have both genomic and non-genomic effects on the heart. It was known that oestrogen had actions on the vascular system (Barrett-Connor et al., 1991), Stumpf et al., (1977) suggested that oestrogen may also have direct effects on the heart,

shown by radiolabeled 17β-oestradiol binding to the heart. This was later supported by Grohe et al., (1997), who found that oestrogen receptors were present in cardiomyocytes as well as fibroblasts. It must be remembered that when examining the effects of acute applications of oestrogen, studies have varied in the concentrations of synthetic oestrogens used varying for example from 100 nM (Morkuniene et al., 2002) to 10 μM (Meyer et al., 1998). In addition, the length of the estrus cycle of the species under investigation can also differ, for example being four days for rats and nine for dogs. Variation exists between investigators with respect to when in the oestrus cycle experiments were performed and therefore the levels of circulating oestrogen can vary, which has been shown to affect cardiac function differently depending upon when in the cycle investigations occurred (Yang et al., 2006). All the aforementioned can therefore give differing results of sex-dependent effects depending on the species used, where in the estrus cycle an experiment was performed and the level of acute estrogens given during the experiments.

As figure 1.8 shows, oestrogens have varied effects in cardiovascular cells. Further investigations would have been needed to study the precise role of the K_{ATP} channel in gender specific protection, specifically investigating the effects of oestrogen and testosterone on the K_{ATP} channel. Many studies involving oestrogen, progesterone and androgen receptors (ERs, PRs and ARs respectively) have shown that they have varied effects upon genomic, membrane-associated and cytoplasmic signalling pathways in the cardiovascular system They are transcription factors that bind as hetero- or homodimers to initiate the transcription of hormone sensitive genes such as NO synthases (Nuedling et

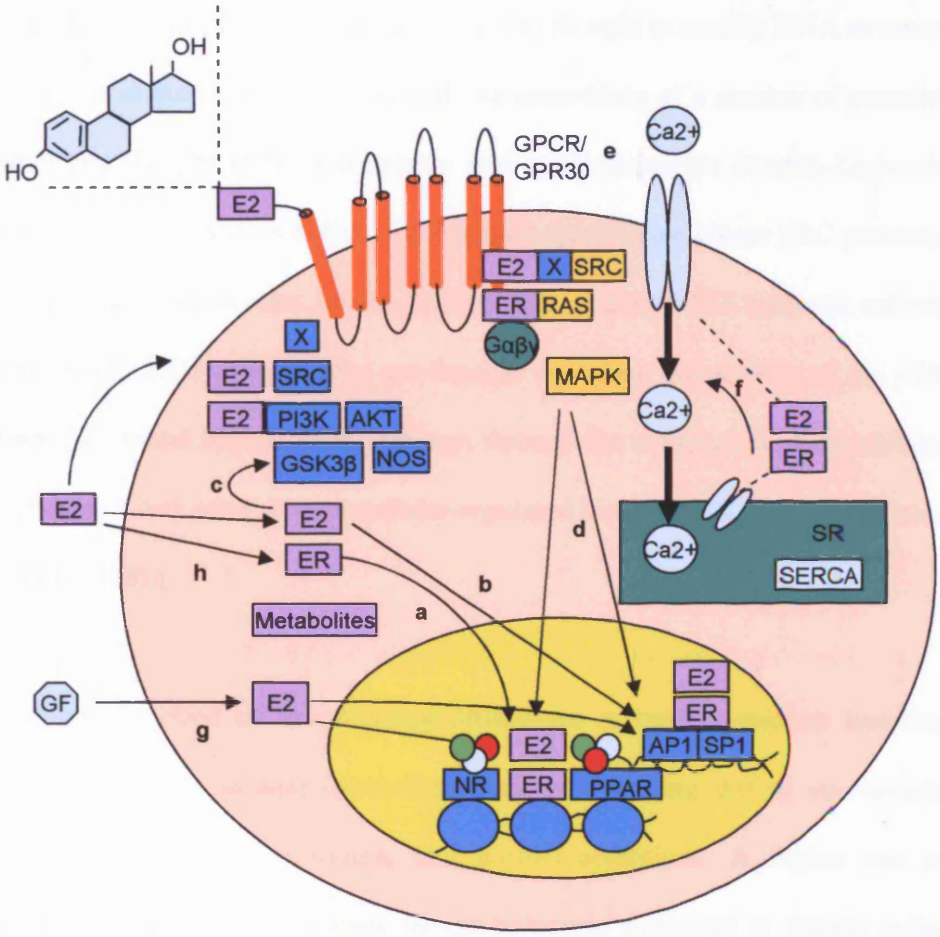

Figure 1.8 The different signalling pathways of oestrogen in cardiovascular cells.

Oestrogen (E2) binds to a cytosolic protein-bound oestrogen receptor (ER) resulting in its activation which results in the activation of gene transcription (a). For gene transcription to occur a number of cofactors are needed, such as peroxisome proliferator-activated receptors (PPARs). ERs can also influence control gene transcription by affecting the activity of other transcriptin factors (b). Oestrogen can induce membrane association of an ER (c), which is facilitated by adaptor proteins suc as caveolin (X), to stimulate SRC, Phosphatidylinositol 3-kinase (PI3K), AKT and glycogen synthase kinase-β (GSK3β), leading to the activation of nitric oxide synthase (NOS) and subsequent production of nitric oxide. Some of these functions of ERα can also be completed by the 46-kDa isoform of ERα. ERα can also activate the mitogen-activated protein kinase (MAPK) pathway (d), with is possibly facilitated by small adaptor and scaffold proteins as well as other membrane receptors (e). The MAPKs pathway is also thought to be activated by the G-protein-coupled receptor GPR30, which is thought to be a new ER. Calcium influx via the L-type calcium channel or calcium handling at the sarcoplasmic reticulum can also be affected by oestrogen (f). Growth factors (GF) can also activate ERs in a ligand-independent manner (g). Finally, metabolites of estrogen such as catechol-estroegens and methoxy-estradiols. ERE, oestrogen-responsive elements; SERCA, sarcplasmic reticulum Ca^{2+}ATPase can exert its effects via receptor-independent mechanisms (h).

Adapted from: Therapeutic implications of the gender-specific aspects of cardiovascular disease. Nature. May, volume 5, number 5, 425-438.

al., 2001; Mendelsohn et al., 2002). Oestrogens are also thought to modify DNA structure and histone proteins in the nucleosomes through the assembling of a number of essential cofactors which are thought to be anti-apoptic and cardioprotective (Regitz-Zagrosek, 2006). They have also been shown to have effects upon the tyrosine kinase SRC pathway, leading to the activation of protein kinase B/AKT and increased NO synthase activity (Camper-Kirby et al., 2001). Oestrogens are thought to reduce the activity of the p38-MAPK pathway, a central hypertrophic pathway, through the stimulation of its inhibitor MAPK phosphatase 1 and controls extracellular-regulated kinase (ERK) phosphorylation (de Jager, T. et al., 2001).

Much research has focussed on investigating differences in cardiac calcium handling between the sexes, mainly because intracellular calcium handling differs enormously between the sexes under both ischaemic and normal conditions. A higher rise in intracellular calcium was reported in male mouse myocytes compared to female under conditions of metabolic stress, which was suggested to be due to the inhibitory effect of oestrogen on the sodium-calcium exchanger (Sugishita et al., 2001). Female rat cardiac myocytes have also been suggested to be able to regulate their intracellular calcium more effectively than male cells in response to increasing extracellular calcium (Curl et al., 2001). This was suggested to be due to a decreased influx of calcium and decreased sarcoplasmic reticulum loading and associated calcium relaese (Curl et al., 2001). The difference in calcium handling between the sexes could also be due to regulation of the L-type calcium channel in females by oestrogen (Johnson et al., 1997). They found that increased expression of the cardiac L-type calcium channel was found in oestrogen

receptor knockout (ERKO) mice. Supporting this observation was evidence that acute application of 17β-oestradiol to cardiac myocytes resulted in an inhibition of L-type calcium channels (Meyer et al., 1998). Chen et al., (2003) suggested that females may also differ from males in their sarcoplasmic reticulum loading capabilities, in that female rabbit cardiac myocytes have a lower sarcoplasmic reticulum calcium loading after application of isoprenaline, compared to males. Chen et al. (2003) found that the decreased calcium loading of the sarcoplasmic reticulum was attributable to a significantly higher level of nitric oxide synthase in female cardiac myocytes. Chu et al., (2005) have found that females have significantly higher levels of proteins constituting the L-type calcium channel, ryanodine receptor and sodium-calcium exchanger, which could also account for the differences in calcium handling between the sexes.

Evidence has shown that apoptosis in ischaemia/repefused heart is triggered by calcium-induced opening of the mitochondrial permeability transition pore (MPTP) and subsequent release of cytochrome c (Halestrap et al., 2003). Female mitochondria have been found to have a lower rate of uptake of calcium in physiological substrate solutions (succinate/pyruvate) and are able to maintain mitochondrial membrane potential more readily than those from males under high calcium conditions, an effect which is thought to be due to the mitochondrial calcium uniporter (Arieli et al., 2004). Morkuniene et al., (2002) showed that physiological concentrations of 17β-oestradiol protected heart mitochondria through block of calcium induced cytochrome c release (Morkuniene et al., 2002). Recent evidence suggests that oestrogen through the beta-oestrogen receptor affords the female heart protection against ischaemia/reperfusion injury (Gabel et al.,

2005). Following ischaemia and reperfusion, post-ischaemic contractile function and infarct size were measured in wild type male and female mice as well as in female hearts that lacked either a functional alpha oestrogen receptor (alpha ERKO) or functional beta oestrogen receptor (beta ERKO). The study found that wild type male hearts showed a significantly less functional recovery and more necrosis compared to females. The alpha ERKO hearts showed similar injury to that exhibited by the wild type females. However, beta ERKO showed significantly less functional recovery than the wild type females, with the injury being more similar to that of the wild type males.

Heart disease is also frequently associated with changes in action potential duration. Potassium currents are the main determinants of cardiac action potential duration, responsible for repolarization and refractory period duration (Keating and Sanguinetti, 2001), and are therefore being investigated for gender specific regulation. Gender differences in the different properties of the potassium channels that are present in the heart have been investigated in many species, such as the guinea-pig (Ranki et al., 2001), rabbit (Liu et al., 1998), dog (Abi-Gerges et al., 2006) and mouse (Trepanier-Boulay et al., 2001). Liu et al., (1998) reported that female rabbit ventricular myocytes have significantly lower I_{Kr} and I_{Kl} outward current densities compared to male cells. These could be contributory factors causing the longer electrocardiographic Q-T interval exhibited by females compared to males. Action potential duration was found to be significantly longer in the female compared to male mouse and there was a significantly lower current density of the ultrarapid delayed rectifier K^+ current, I_{KUR} (Trepanier-Boulay et al., 2001).

The ATP-sensitive potassium channel also contributes to the cardiac action potential, but mainly under ischaemic conditions. Activation of the ATP-sensitive potassium channel results in a large outward $I_{K\ (ATP)}$ current and consequently a shortening of the cardiac action potential duration (APD), associated decrease in the refractory period and consequently a decrease in contraction. Lee et al. (2000) were one of the first groups to report that increased myocardial protection afforded to cardiac cells by K_{ATP} channels was due to oestrogen. They showed that 17β-oestradiol significantly reduced infarct size after ischaemia/reperfusion injury. Application of the presumed mitochondrial K_{ATP} channel specific blocker 5-HD, abolished the protective effect of 17β-oestradiol which reduced the infarct size after ischaemia and reperfusion. Other studies have suggested that testosterone may be protective in cardiovascular cells. Activation of the mitoK_{ATP} by testosterone may improve myocardial protection following ischaemia (Er et al., 2004). This conclusion was based on evidence whereby the mitoK_{ATP} blocker 5-HD prevented the testosterone induced reduction in death of cardiomyocytes following ischaemia, whereas the sarcolemmal K_{ATP} blocker HMR1098 had no effect. Many other studies have also investigated the benefits of testosterone, specifically in its ability to maintain low intracellular calcium following ischaemia-reperfusion injury (Callies et al., 2003), inhibition of L-type Ca^{2+} channels (Scragg et al., 2004) and gene expression regulation of the major calcium regulatory proteins in venricular myocytes (Golden et al., 2004). Investigations by Ranki et al. (2001) have led to the suggestion that there are gender specific differences between the expression and properties of cardiac sarcolemmal K_{ATP} channels. Ranki et al. (2001) found that the density of the pinacidil-sensitive current was

higher in adult female than male guinea-pigs. Ranki et al. (2001) also found there to be higher levels of SUR2A in female tissue relative to male and higher levels of both SUR2A and Kir6.2 proteins in cardiac membrane fractions in female compared to male. They also found increased Ca^{2+} loading in male compared to female cardiomyocytes. Subsequent research has found that 17β-oestradiol regulates expression of K_{ATP} channels in heart-derived H9c2 cells (Ranki et al., 2002). They reported that there were higher mRNA levels of SUR2A and increased level of both SUR2A and Kir6.2 proteins in 17β-oestradiol treated cells.

The gender difference in rates of coronary heart disease (CHD) until the menopause initiated the research into possible cardioprotective effects of oestrogen upon the heart. However, it is now thought that the later onset of CHD in women is due to their higher high-density lipoprotein (HDL) cholesterol levels, which are now being thought to be due to other explanations such as a higher endogenous oestrogen levels (Rossouw, 2002). Evidence has lead to the suggestion that the difference in HDL cholesterol between men and women is an effect of androgen rather than oestrogen (Rossouw, 2002).

This thesis describes studies as to whether there are gender specific differences in the responses of isolated rat cardiac myocytes to simulated ischaemia and reperfusion, and whether there are differences in sarcolemmal K_{ATP} current density. Various aspects of K_{ATP} channels from sarcolemmal membrane of Adult Wistar rat cardiac myocytes were investigated using mainly electrophysiological and fluorence techniques. In addition I also investigated the role of PKC in the possible internalisation of the K_{ATP} channel as a

possible mechanism to prevent excessive activation of the channel that could lead to arrhythmias.

CHAPTER 2

METHODS

Chapter 2 Methods

2.1 Isolation of cardiac myocytes

Rats were killed by cervical dislocation in accordance with Home Office regulations. The heart was removed from the rat and placed into cold nominally zero calcium Tyrode's (see Table 2.1 for constituents). The aorta was cannulated immediately, from which the heart was perfused for 6 minutes with zero calcium Tyrode's solution. All solutions used during the isolation of the cardiac myocytes were kept at approximately 34°C and bubbled with oxygen continuously. The atria were rapidly removed and discarded and pressure released from the ventricles by placing a p10 pipette tip into the heart. After perfusing the heart for 6 minutes with zero calcium Tyrode's, the perfusing solution was then changed to zero calcium Tyrode's solution containing enzymes (BSA (prepared from factor V albumin) 50 mg, protease (type XIV) 20 mg and collagenase type I 30 mg in 30 ml zero calcium Tyrode's,) for between 8 and 15 minutes. For the first minute the perfused enzyme solution was discarded, and then the perfusate was collected and recycled through heart. The length of time for which the enzyme perfused the cannulated heart was dependent upon the time at which the first rod shaped ventricular myocytes were visible in the enzyme perfusuate. Therefore following approximately 8 minutes of perfusate, drops of the recirculated enzyme solution were examined under magnification for the appearance of the rod-shaped myocytes. Following the appearance of rod shaped myocytes and softening of the heart tissue, the solution was changed to normal Tyrode's solution (containing 2 mM calcium chloride) for three minutes. The heart was then cut from the cannula, placed into a conical flask with 2 mls of normal

Tyrode's and shaken in a 37°C water bath for five minutes. The solution was then poured into a new conical flask and another 2mls of normal Tyrode's was added to the remainder of the heart tissue. This process was continuously repeated until there were six or eight fractions. Each of the fractions was individually sieved to remove the remnants of the heart tissue and poured into an individual test tube and allowed to settle for approximately 10 minutes. The supernatant was then removed and the cells resuspended in normal Tyrode's and allowed to settle again for 10 minutes. This process was repeated twice before the supernatant was removed from each test tube and the cells placed into a 75 mm petri dishes with 3 ml of normal Tyrode's. The cells from pairs of adjacent test tubes were combined together, for instance the cells from test tube one and two were combined to produce fraction one and so forth. Each dish had 200 µl of 10,000 U/ml penicillin and streptomycin added. Typically, there was a 70-90% yield of quiescent, rod-shaped cells. Cells were resuspended in normal Tyrode's each evening and stored at room temperature. Cells were used for the first day subsequent to isolation as it been shown that cultering cells in a medium for more than a day has been shown to affect cell morphology (Mitcheson et al., 1996).

2.2 Patch-clamp equipment and methods

Established by Neher and Sakmann (1976), the patch clamp technique can be used to measure changes in membrane current while the membrane potential of the cell is clamped at different voltages.

2.2.1 Formation of a "gigaohm" seal

The patch clamp technique enables the direct measurement of the current flowing through single channels; typically of 1 or 2 pA in amplitude. There were two limitations to previous voltage clamp techniques, which prevented the measurement of single channel current; level of noise and membrane area of the cell. In a voltage clamped muscle fiber the typical root-mean-square noise level is found to be approximately 70 pA, with the use of intracellular microelectrodes and without acetylcholine, this equates to a value of 200 pA from peak to peak (Anderson and Stevens, 1973; Aidley and Stanfield, 1996). The 100-fold difference between the noise level of the muscle fiber and the single channel current must therefore be reduced if single channel activity is to be measured; a reduction of 1000-fold would enable accurate detection of the current. Some of the noise can be attributed to Johnson noise, named after its discoverer; this is the noise caused by thermal agitation of electrical charges. A bandwidth of 1 kHz an internal resistance of 2 GΩ or higher would be required to resolve a channel at 1 pA.

Using a fire polished pipette coated in Sylgard resin and filled with a saline solution,, a gigaohm seal is obtained by suction of the membrane of the cell onto the tip of the pipette forming a Ω shape, reducing the distance between the cell membrane and glass rim of the electrode to approximately 1 Å (Aidley & Stanfield, 2000). This gigaseal reduces the noise level of the recording and so subsequent recordings of single channel currents can be obtained due to the increased resolution. (Hamill, Marty, Neher, Sakmann & Sigworth. 1981). The gigaseal can be used to make different patch clamp configurations (figure 2.1). The cell-attached configuration is where the cell membrane remains in the

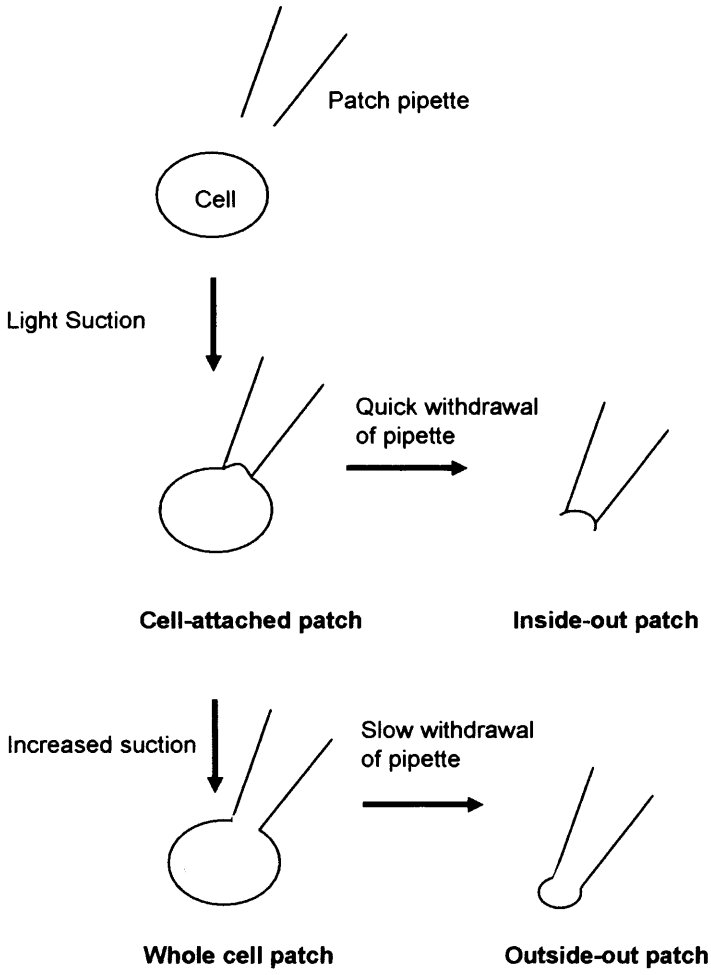

Figure 2.1 Different patch clamp configurations

Following the formation of a Giga Ohm seal, various patch clamp configurations can be made, depending on the type of recording required. For single channel recording, the cell-attached patch is used; breakage of the seal with increased suction results in a whole cell configuration, used for recording whole cell currents. The inside-out patch is formed from a cell-attached patch, which has been quickly extracted from the cell by the pipette. The outside-out patch is formed from a whole-cell patch configuration where the pipette was slowly pulled away from the cell, resulting in a stretching of the sarcolemmal membrane, which breaks and then rejoins to form a small vesicle of membrane.

position it was when a gigaseal was made. This technique as well as the inside-out and outside-out patch may be used to measure single channel activity. The inside-out patches are made by quick retraction of the pipette from a cell-attached configuration. This configuration is useful for investigating the effect of changing both the internal and external environment of the cell, as the cytoplasmic membrane of the cell is in contact with the perfusate and the extracllular face is in contact with the pipette solution. Strong suction or a pulse of up to 1 V applied to the patch to break the cell membrane produces the whole cell technique which is used to measure changes in the whole cell current. The outside-out patch is produced through retraction of the pipette away from the cell which had a whole cell configuration. This leads to a stretching of the membrane which eventually joins as the membrane breaks and reforms with the extracellular face of the cell in contact with the perfusate. Another configuration is the perforated patch, which uses pore-forming antibiotics to allow the perfusate access to the cytoplasmic face of the cell with little disturbance to the intracellular environment. It also results in the cell having low resistance to current flow and therefore the whole cell can be voltage clamped. Once a gigaseal is formed, antibiotics such as amphotericin which are present in the pipette act upon the cell membrane allowing monovalent ions access. My investigations into the K_{ATP} channel used both the whole cell and cell-attached patch configurations.

2.3 Patch –Clamp Equipment and Methods

2.3.1 The Electrophysiology Rig

Figure 2.2 shows a typical rig used for a patch clamp experiment. Two additions to this equipment are a Faraday cage, which is needed to reduce noise caused by electrical interference, and an air table essential for reducing vibrations. The recording system is designed to further decrease the noise, which was initially lowered by the formation of a gigaohm seal.

2.3.2 Bath

Figure 2.3 shows the arrangement of the bath I used for my experiments, including the inflow, outflow, earth and silver/silver chloride wire. The bath consisted of a Perspex sheet with a diamond-shaped hole in the middle. The bottom of the bath, through which cells were viewed, was formed by a coverslip. At one end of the diamond-shaped bath was the inflow and the opposite contained the outflow. For patch-clamp experiments the bath electrode was a silver/silver chloride wire held in place over the edge of the bath, so upon perfusion it was in contact with the bath solution.

2.3.3 Flow system

The experimental bath was perfused by a gravity-fed flow system. The gravity feed system consisted of a polythene tube, which was in contact with the solution reservoir, leading to a bubble trap via a metal needle. The bubble trap was composed of a 1ml

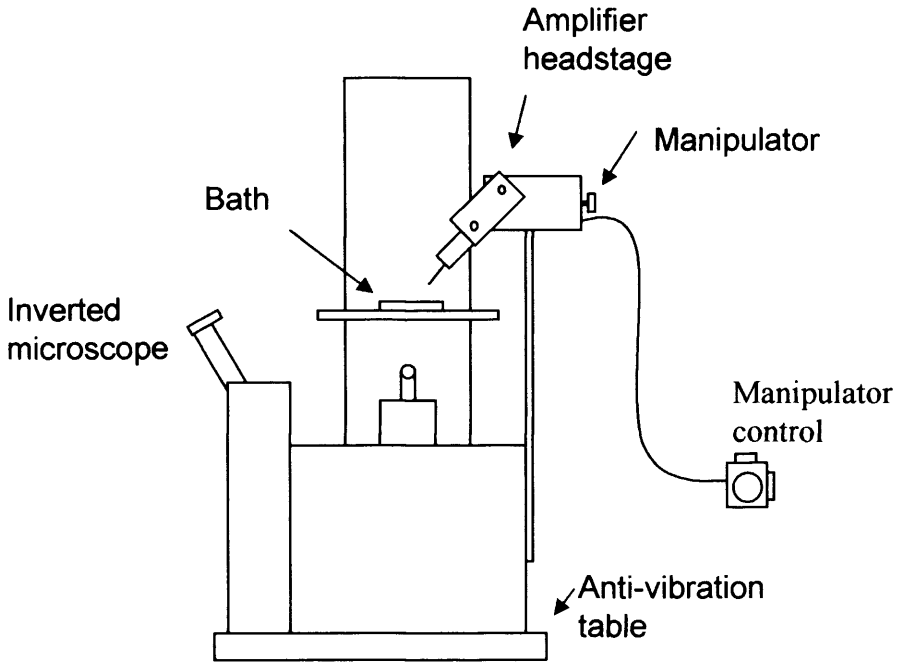

Figure 2.2 The patch clamp set-up

The patch clamp set-up consists of an inverted microscope mounted upon an anti-vibration table. The cells to be viewed are placed in the bath and continuously perfused by solution which can be heated prior to its entry. The pipettes, which are used to measure changes in cellular current, are controlled by a hydraulic manipulator

Adapted from Aidley & P.R.Stanfield (1996) Ion channels: Molecules in action, Cambridge University press, Great Britain. pg. 50.

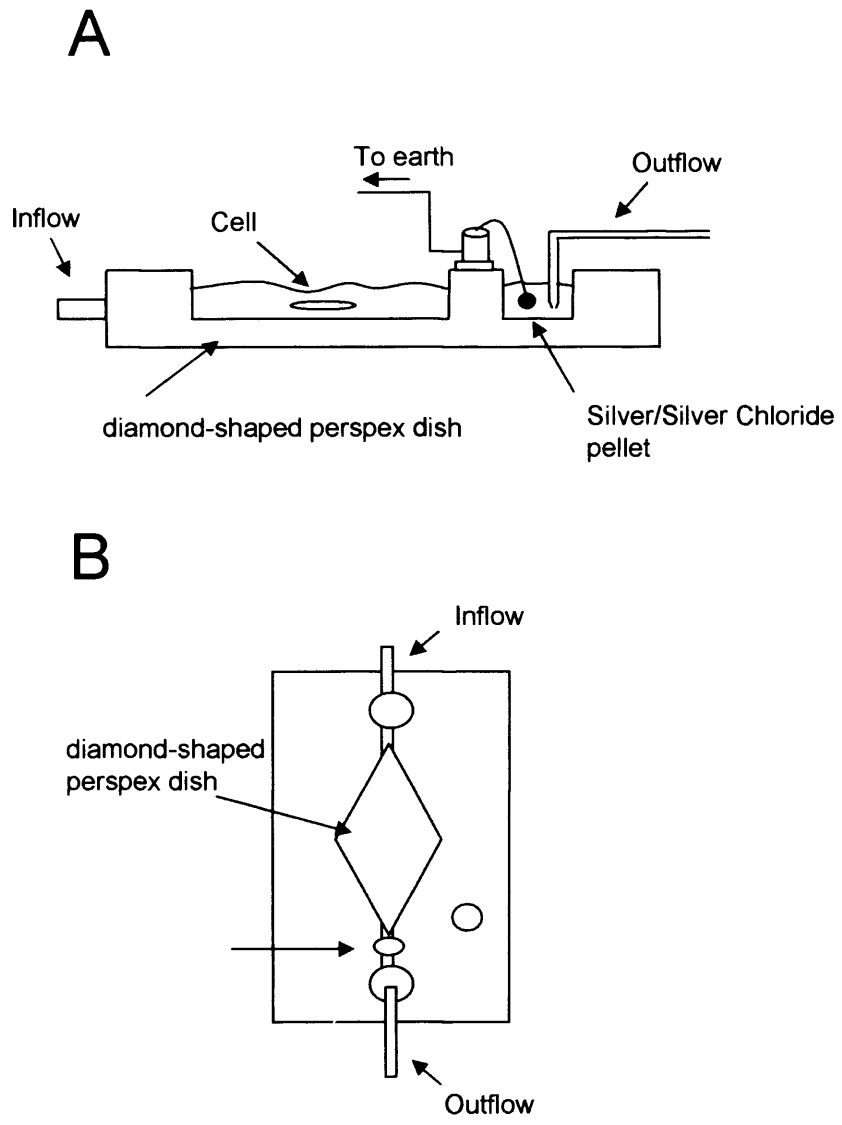

Figure 2.3 The bath

A, Side view of the bath, which is a diamond shape made from perspex. The solution enters the bath through the inflow via a heated element. The solution then bathes the cells contained in the bath and exits through the outflow. The outflow consists of a bent pipette which sucks the bath solution from a chamber in the perspex, separate from the bath. The earth, which has a silver/silver chloride pellet is also in contact with the solution in the same chamber.

B, View of the bath from above.

Gilson tip with a silicone bung, which was pierced by the needle. The needle was connected to further polythene tubing via flexible tubing which led to the inflow of the bath via a heated element.

The outflow from the bath was constructed from a 1.5 mm (O.D) x 0.86 mm (I.D) borosilicate capillary glass rod, the end of which had been placed over a Bunsen burner to heat the glass, decreasing the size of the hole. The Bunsen burner was again used to heat the section of the capillary rod that contained the decreased size in the opening so that it was bent in a 90° angle with respect to the rest. The untouched end of the borosilicate capillary was attached to polythene tubing via flexible tubing to a 1.5 L conical flask.

The solution was subsequently sucked through the polythene tubing and bath by negative pressure inside the 1.5 L conical flask. The negative pressure was due to the air being pumped out of the 1.5 L conical flask via an aquarium pump. The degree of suction was controlled by varying the size of the hole in the borosilicate glass capillaries used as the outflow.

2.3.4 Fabrication of pipettes

Patch pipettes were made from filamented thick-walled 1.5 mm (O.D) x 0.86 mm (I.D) borosilicate capillaries (GC150F-7.5, Harvard Equipment Ltd.). The patch pipettes were produced in two stages using a Narashige vertical pipette puller (Narashige Instruments Ltd., Tokyo, Japan). For single channel recordings, the tips of the electrodes were then coated in Sylgard resin to reduce noise and the capacitance of the pipette. Under

magnification, Sylgard resin was coated near the tip of the pipette using a looped wire and cured by pulling the pipette through a heated coil.

The final stage was to fire polish the tip of the pipette under microscopic observation using a red hot filament and micromanipulators to control the distance between the filament and pipette. Each pipette was filled with a saline solution from a syringe just before use.

For whole cell experiments the pipettes had a resistance of 4-8 MΩ when filled with solution, whereas the pipettes used for cell-attached patches had resistances of 5-10 MΩ when filled.

2.4 Patch-Clamp Experiments

The whole cell configuration of the patch-clamp technique (Hamill et al., 1981) was used to record the whole cell current from individual cardiac myocytes. The cell-attached configuration was used to record current from up to eight K_{ATP} channels at one time. The cardiac myocytes were viewed under phase contrast with a Nikon Diaphot inverted microscope. The patch pipette was moved into the solution and positioned near the cells by a hydraulic manipulator, while maintaining a constant positive pressure to prevent the end of the pipette being contaminanted. When in the solution the pipette tip potential was nulled, and seals were formed by placing the tip of the pipette against the sarcolemmal membrane of the cardiac myocyte and applying gentle suction through a syringe. Seal formation of 1-10 GΩ was monitored via the pClamp8 programme and viewed on the

computer by following the reduction in pipette current in response to a 5 mV hyperpolarizing pulse. As suction was increased, the current pulse decreased in amplitude and sealing was confirmed by montoring the pClamp8.0 on the computer and observing a gigaolhm seal with capacitance spikes. The difference with cell-attached patches is that the seal to the cell membrane is maintained.

Voltage was controlled and membrane currents recorded using an Axopatch 200B amplifier (Axon Instruments). Currents were filtered at 5 kHz and analogue signals were collected and digitised using a Digidata 1200 Series interface. Records were aquired and analysed using either pClamp 8 (Axon) or custom software, Excel 2000 (Microsoft) and SIGMAPlot 5.0 (Jandel Scientific). Cell capacitance was measured using pClamp software as described in figure 2.4.

2.5 Measurement of cell capacitance

The electrical capacitance of cell membrane arises primarily from the phospholipid bilayer and is directly proportional to the membrane area. Therefore capacitance can be used to normalise membrane current to membrane area and so obtain current density as pA/pF.

Membrane capacitance can be measured from the current in response to a small voltage-clamp pulse. The membrane can be approximated by a resistor and a capacitor in parallel, as shown in figure 2.4A. Applying a square voltage pulse to such a circuit leads to a spike of capacity current, I_c, followed by a constant pedestal of current I_r that flowing through Rm (membrane resistance).

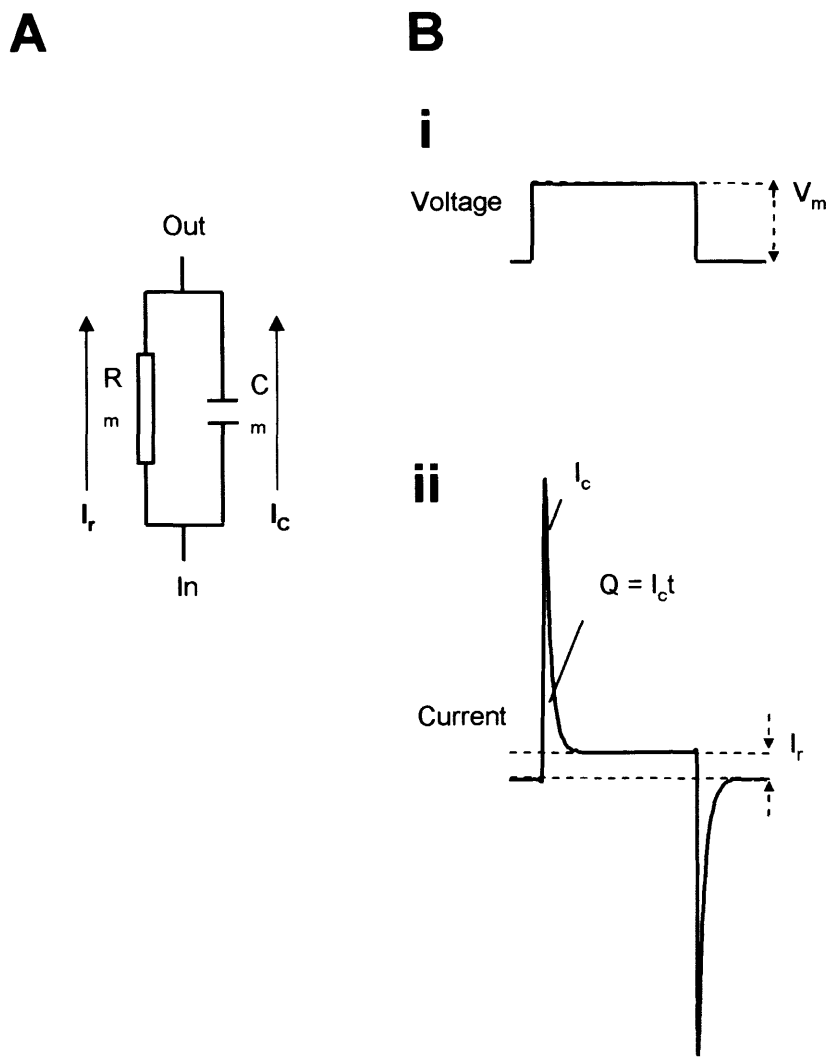

Figure 2.4 Cell capacitance compensation circuit

A, The equipment used for detecting and compensating for cell capacitance consists of a resistor and capacitor in parallel.

B, (i) shows the 5 mV hyperpolarizing pulse in the pClamp8.0 program used to elicit a membrane current (ii).

In these experiments, capacitance was measured using a program provided within PClamp8.0. A 5 mV voltage pulse (V_m) was applied to the cell and the resulting membrane current measured. The cell capacity is measured from the area under the transient capacity current, which is obtained by fitting an exponential to the decline in the current of the form (figure 2.4B).

$$I(t) = I(0)\, e^{-t/\tau}$$

where I(0) is the initial current, I(t) is the current at time t, and τ is the time constant. The area under the curve is obtained by integrating this exponential to give the charge Q on the membrane capacitor, since $Q = I_c t$.

Capacitance, charge, and voltage are related by the expression

$$Q = C\, V$$

where C is capacitance and V voltage. Thus the membrane capacitance is obtained from the charge and the voltage pulse as

$$C_m = Q/V_m$$

The value delivered by the PClamp8.0 program was used to set whole-cell capacitance compensation.

2.6 Series resistance

Series resistance (resistance in series with the cell membrane that is being clamped) arises primarily in the patch pipette. Figure 2.5 shows that the amplifier controls the voltage at its input, which is the same as that of the wire in the pipette, Vpip. Series resistance, Rs, is often 2-3 x the initial resistance of the pipette. When no current is flowing the voltage across the cell membrane, Vcell is equal to Vpip. However, when a current, Im, flows across the cell membrane and so through the pipette tip, there is a voltage drop across Rs equal to ImRs. So Vcell now differs from Vpip by ImRs. Series resistance compensation feeds a signal proportional to Im into the voltage command circuit to (partially) compensate for this voltage error. PClamp8.0 has a program which estimates the series resistance, I therefore used the generated values to compensate approximately 60% for series resistance.

2.7 Solutions

The solutions were made using MilliQ distilled water. All solution components were added as solids except $MgCl_2$ and $CaCl_2$ which were added in the calculated volumes from 1 M stock solutions.

Internal solution for whole cell experiments was frozen at -10°C. All other solutions were stored at 4°C. In both instances, solutions were allowed to reach room temperature (18-

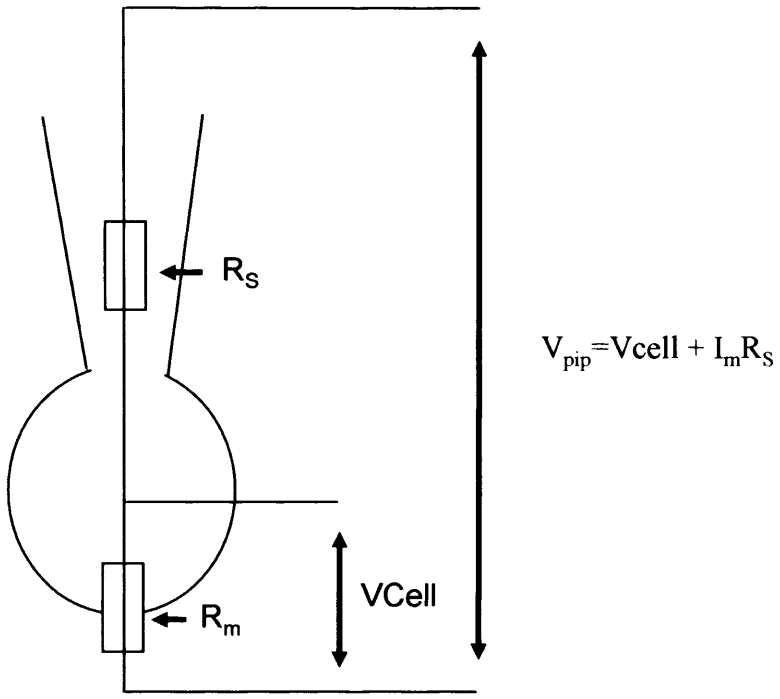

Figure 2.5 Series resistance circuit

The equipment used for detecting and compensating for series resistance where R_s is the pipette resistance and R_m is membrane resistance. The potential drop across the micropipette is compensated for by a positive feedback mechanism, whereby the amplifier subtracts the pipette potential (R_s) to generate the current output (Vout). A fraction of Vout is combined with the command voltage used to control Vpip. This results in a transient and steady state increase in Vpip.

Adapted from Aidley & P.R.Stanfield (1996) Ion channels: Molecules in action, Cambridge University press, Great Britain. pg. 57.

25°C) before an experiement was carried out. Table 2.1 gives details of the composition of normal Tyrode's and substrate-free Tyrode's. Table 2.2 shows the composition of the internal solution, and the solution used for cell-attached recordings.

Table 2.1

External Solutions

Substance	**Normal Tyrode's (mM)**	**Substrate-free Tyrode's (mM)**
NaCl	135	140
KCl	6	6
Na_2HPO_4	0.33	0.33
Na-pyruvate	5	0
Glucose	10	0
$MgCl_2$	1	1
$CaCl_2$	2	2
HEPES	10	10
Sucrose	0	10

Metabolic Inhibition (MI) was produced by adding 2 mM sodium cyanide (NaCN) and 1 mM iodoacetic acid (IAA) to the appropriate volume of Substrate-free Tyrode's.

The external solutions were made to pH 7.4 with either NaOH or HCl.

Table 2.2

Pipette Solutions

Substance	**Whole cell solution (mM) 140 K^+**	**Cell-attached solution (mM) 140 K^+**
$MgCl_2$	1	2
Tetrapotassium Bapta	5	
ATP	0.3	
ADP	0.1	
GTP	0.1	
HEPES	10	10
KCl	140	140
$CaCl_2$		2

An in-house program was used to calculate the ion concentrations in the solutions used.

The internal solutions were titrated to pH 7.2 with either KOH or HCl for whole cell experiments. For cell-attached pipette solutions were made to pH 7.4 with either KOH or HCl.

2.8 Statistical Analysis

Data are represented as mean ± SEM and values of n refer to the number of patched cells or hearts examined as indicated in the text or figure legends.

Mean values obtained were compared by the paired or unpaired Student's t-test where appropriate. Values where $p<0.05$ were considered statistically significant. All experiments were done at 34 ± 2°C.

2.9 Drugs

Pinacidil, glibenclamide, P-1075, chelerythrine and Phorbol-12-mystrate-13-acetate (PMA) were obtained from SIGMA. Drugs were dissolved in dimethylsulphoxide (DMSO) (SIGMA) as stock solutions and diluted in Tyrode's on the day of experimentation.

2.10 Measurements of cell morphology and contraction

Measurements of cell morphology and contraction are described in Chapter 3.

2.11 Fluorescence measurement of cytoplasmic calcium

Fluorescence measurements of cytoplasmic calcium are described in Chapter 3.

2.12 QPCR techniques

2.12.1 RNA isolation and RT-PCR

Ventricular myocytes were dissociated from the animals using an established enzymatic procedure requiring a Langendorff technique with collagenase (type 1, Sigma) and protease (type XV, SIGMA) as described previously (Lawerence & Rodrigo, 1999). Cells were allowed to settle in normal Tyrode's at the bottom of two 15ml falcon tube. Excess normal Tyrode's was removed using a pipette and the concentrated cells formed a 1cm^2 layer. Total RNA was isolated from cells with TriZOL Reagent (Life Technologies), according to the manufacturer's protocol with the following adaptations. The cardiac myocytes were aliquoted into four 1.5 ml microfuge tubes and suspended in 1ml of Trizol with the resultant suspension being sonicated for 2 x 5 second bursts on level 2. During the sonication, the cells were kept cool by placing the microfuge tubes on ice. The cells were centrifuged at 12,000 rpm for 10 minutes at 4°C then incubated for 5 minutes at room temperature. The supernatant was removed, transferred to a fresh microfuge tube and 0.2 ml of chloroform per ml of TriZOL reagent was applied. The samples were shaken vigorously by hand for 15 seconds and then incubated at room

temperature for 2 minutes. Samples were centrifuged at 12,000 rpm for 15 mins at 4°C. The middle phase was then extracted and the RNA was precipitated by adding 0.5 ml isopropyl alcohol per ml of TriZOL and incubated at room temperature for 30 minutes. The samples tubes were then centrifuged at 12,000 rpm for 10 minutes at 4°C. The supernatant was removed and the pellet was washed once with 75% ethanol. 1ml of ethanol was used per ml of TriZol and vortexed. The samples were then centrifuged at 7,500 rpm at room temperature for 5 minutes. The supernatant was then removed, the samples were centrifuged again and any remaining supernantant removed. The pellet was air dried and dissolved in 50µl RNase free water by passing solution up and down the pipette. The RNA was stored at -70°C.

2.12.2 Spectrophotometric quantification of RNA

RNA concentrations were quantified at 260 nm using an UV/visible spectrophotometer (Ultrospec 3000, Pharmacia Biotech). RNA was prepared as a 1:200 dilution of RNA and RNase-free water and placed inside a quartz cuvette. Sterile distilled water was used as the blank. The absorbance of the RNA was measured at 260 nm and 280 nm. The concentration of RNA in the sample was calculated from the equation:

RNA ($\mu g\ ml^{-1}$) = A_{260} x 40 x dilution factor.

The ratio of absorbance at 260 nm and at 280 nm was recorded to assess the purity of the RNA solution. A pure RNA solution has an A_{260}:A_{280} absorbance ratio of at least 1.8; ratio below this may indicate protein contamination.

2.12.3 Turbo DNA-free

RNA was treated with TURBO RNase-free DNase (Ambion) according to the manufacturer's protocol to eliminate any contamination by DNA. 0.1 volume 10x TURBO DNase buffer and 1µl Turbo DNase (2 U/µl) was added to each 50µl RNA sample. Each sample was incubated at 37°C for 30 minutes, before 0.1 volume DNase Inactivation Reagent was added and incubated for 2 minutes with occasional mixing at room temperature. Each sample was then centrifuged at 10,000 rpm for 1.5 minutes at room temperature and the supernatant was transferred to a new microfuge tube.

2.12.4 Omniscript Reverse Transcription procedure

Omniscript reverse transcription was used to produce a cDNA pool from the total RNA template. Once a cDNA pool had been made, the normal PCR reaction could take place. Each omniscript reverse transcription reaction was 40µl in volume, consisting of 2µg of template RNA and the mastermix shown in Table 2.3. I quantified the total RNA and then used 2µg of RNA per omniscript reverse transcription procedure. Where possible I used concentrated total RNA but this was not always possible if it was dilute, consequently I varied the amount of mastermix put into each omniscript reverse transcription procedure to ensure the final weight of total RNA in each reaction was 2µg.

Table 2.3 Composition of the RT-PCR reaction mastermix

Component	Volume/reaction
10x Buffer RT	17
DNTP mix (5mM each dNTP)	16
Oligo-dt primer (10 μM)	8
Omniscript Reverse Transcriptase	6
RNase-free water	43
Total volume	90

2.12.5 QPCR of Beta Actin, Kir6.2 and SUR2A

The QPCR reactions were performed to amplify the genes that constitute the cardiac K_{ATP} channel; Kir6.2, SUR2A and the control gene Beta Actin. The sequences for which were obtained from GenBank (www.ncbi.nlm.nih.gov) accession numbers D86039, D83598 and V01217 J00691 respectively. Primer sets were designed using primer http://operon.com/oligos/toolkit.php software. The oligonucleotide primer sequences used are shown in Table 2.4.

Table 2.4 Nucleotide sequences of cardiac K_{ATP} channel used in QPCR reaction

Nucleotide sequence name	Sense sequence 5'-3'	Antisense sequence 5'-3'
Kir6.2	ATCCTTCCACCTCAGTTCCACCCC	TCAGCCTTCCAGCAGAGTCAGGAG
SUR2A	CATGACAGCCTTTGCGGATCGCACGG	GGTTTGGACCAGTATCGCACTCCAC
β-Actin	CGGACTCATCGTACTCCTGCTTGC	TGCTCCTCCTGAGCGCAAGTACTC

2.12.6 Quantification of both the cardiac K_{ATP} channel subunits Kir6.2 and SUR2A

A rapid real-time PCR assay was used to investigate whether there was a difference in the relative transcript abundance of the two genes that constitute the K_{ATP} channel (SUR2A and Kir6.2) between male and female rats. The housekeeping gene β-actin was used as an internal control.

The Quantitative polymerase chain reaction was carried out using the Taqman reverse transcription polymerase chain reaction (RT-PCR). This method enables measurement of an accumulating PCR product in real-time. Primers selective to the cardiac K_{ATP} channel subunits Kir6.2, SUR2A, and β-Actin were designed based on rat sequences obtained from the Genbank database (see Table 2.4). Initially the PCR efficiencies and specificities of primer sets were tested for each primer set (see figures 2.6 and 2.7) using SYBER®-Green Mastermix (Applied Biosystems) described below. This confirmed that Kir6.2, SUR2A, and β-Actin primer sets amplified PCR products with a similar efficiency between different animals and between the duplicate reactions. To validate that

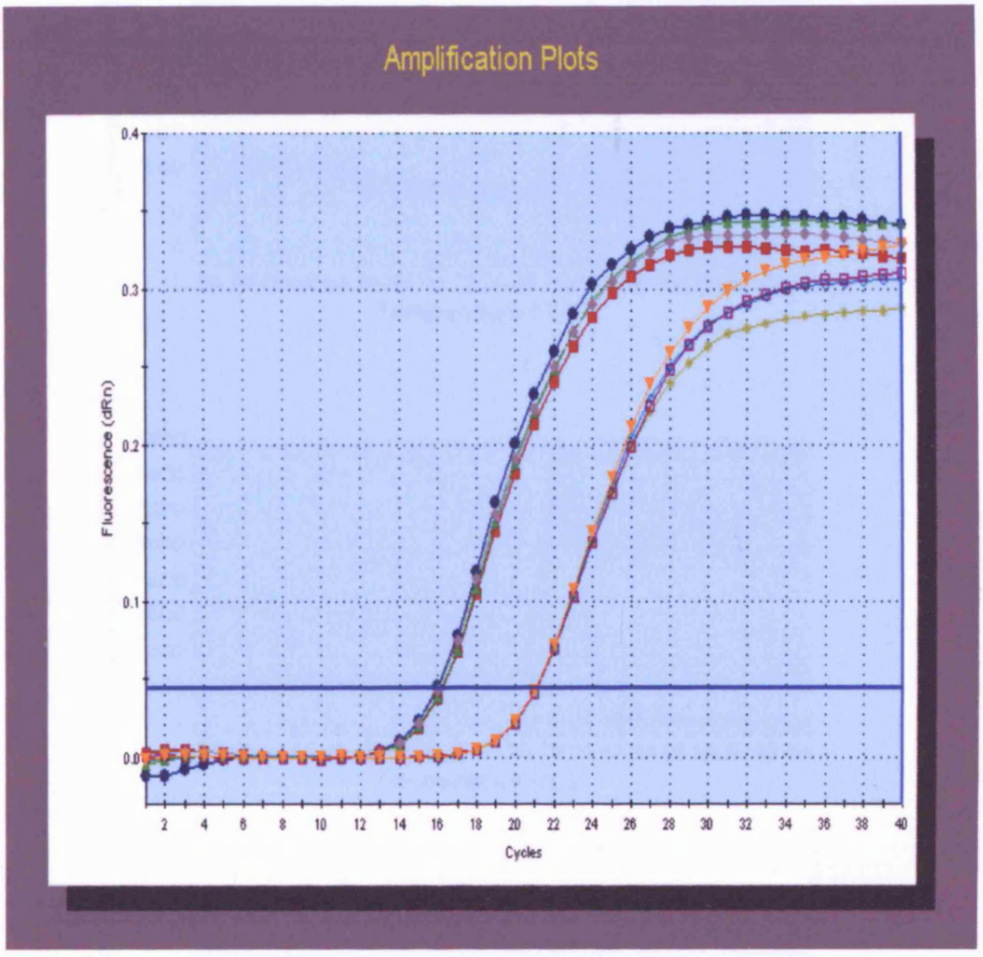

Figure 2.6 Validating the efficiency of Beta-Actin, SUR2A, and Kir6.2 primers using real-time PCR.

Oligonucleotide primers were obtained for quantitative PCR to evaluate specific Kir6.2, SUR2A and Beta-Actin mRNA expression levels in cardiac myocytes from four male and four female rats (see chapter 3). Shown are representative screenshots taken from Sequence Detection Software. For each sample, an amplification plot was generated showing the increase in reporter dye fluorescence (triangle) with each cycle of PCR (A). The figure above shows two distinctive groups of amplification plots. The first group of amplification plots (left) represent four amplification plots of beta-actin from four animals. Similarly, the second group of amplification plots (right) represent four amplification plots of Kir6.2 from four animals.

i

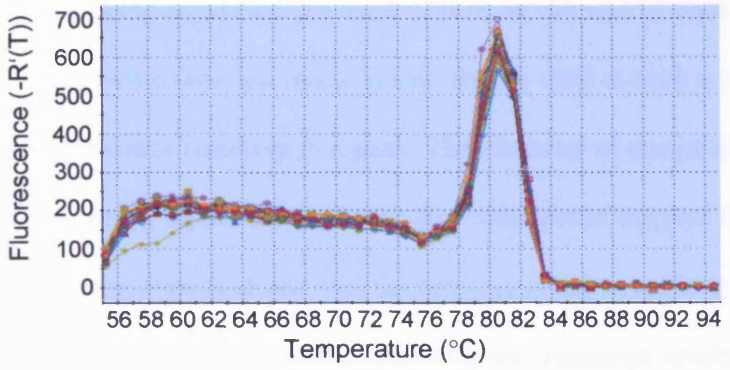

ii

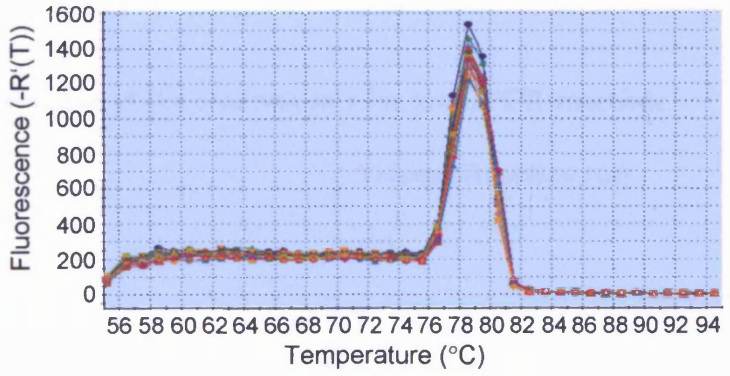

iii

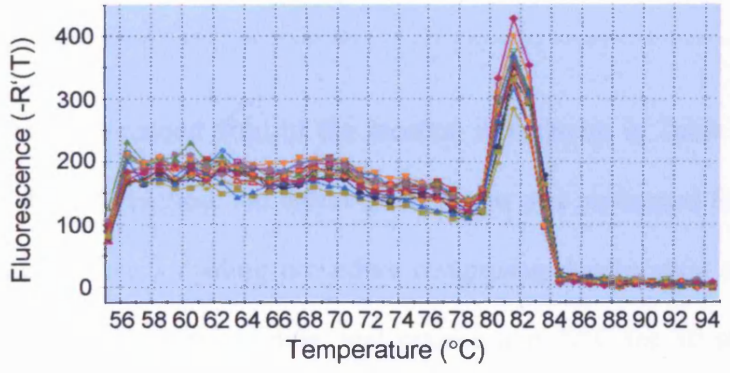

Figure 2.7 Validating the specificity of Beta-Actin, SUR2A and Kir6.2-selective primers using real-time PCR.

Each sample also gave a dissociation curve (i, Beta-Actin; ii, SUR2A; iii Kir6.2) for each primer set. The presence of one peak indicates that there was one product amplified.

only one product was being amplified for each primer, at the end of each of the QPCR experiments, the temperature was increased by one degree until at such a point there is a rapid increase in fluorescence resulting in a peak. The presence of one peak indicates that only one product was being amplified, however any other peaks suggest that there are a number of products being amplified and that the reaction is not specific to those primers only and would therefore give false results regarding the transcript levels of the genes. The composition of the reaction mix for the QPCR reaction is shown in Table 2.5.

Table 2.5 Composition of the reaction mix for the QPCR reaction.

Component	**Volume/Reaction (µl)**
Syber Green	425
Reference	7
Primers (sense and anti-sense)	18
RNAse-free water	400

Each QPCR reaction contained 50µl of the reaction mix shown in Table 2.5 and 1.5µl (3000 µg/ml) of the RT reaction. An initial denaturation was performed for one cycle at 95°C for 10 minutes, then a cycling procedure comprising denaturation at 95°C for 30 seconds, annealing at 58°C for 1 minute, and extension at 72°C for 30 seconds, which was repeated for 40 cycles, then 95°C for a one minute cycle and a final extension at 55°C, increasing in 1°C increments. The amplification was carried out on a Thermocycler PCR machine (PTC-200, MJ Research). Real-time PCR data were captured using sequence Detection Software (PE Applied Biosystems) to obtain Ct (threshold cycle)

values for the genes of interest. The threshold cycle is the cycle at which a statistically significant increase in ΔRn is first detected (associated with an exponential increase in PCR product). Values were expressed as fold difference from the housekeeping gene, beta-actin. All measurements were performed in quadriplicate.

2.13 Western blotting procedure

2.13.1 Sample preparation

Cardiac myocytes were isolated from a whole rat heart using the protocol as stated in methods. Cells were separated into three fractions and each fraction was incubated for 20 minutes under one of the following conditions, 100nM PMA, 10μM chelerythrine and the amount of DMSO used for the fractions treated with PMA and chelerythrine. Cells were spun down for one minute using a bench top centrifuge at 4°C and 5000 rpm. Cells were then washed with 1ml PBS and Ca^{2+}. 300μl of cells were lysed with 1ml of ice-cold hypertonic buffer (composition in mM, unless otherwise stated: Tris 100, EDTA 10, NaCl 150, 1% (v:v) NP40, 0.1%; (w:v) SDS, 5mg ml^{-1} deoxycholic acid, 200μg ml^{-1} benzamidine, PMSF 1, and 10μl of protease inhibitor cocktail pH 7.4). Cell lysates were homogenised using a hand-held homogeniser and were then fractionated by centrifugation (30,000 rpm for 30mins, 4°C). The CB-Protein Assay (EMD Biosciences, Inc.) was used to determine the protein (ml^{-1}) concentrations of both the soluble and insoluble fractions. Fractions were diluted to the same concentration using hypertonic lysis buffer.

A 50µl aliquot of each sample was mixed with an equal volume of sample buffer (composition in mM, unless otherwise stated: Tris-HCl 100, DTT 200, 4% (w:v) SDS, 0.1% (w:v) bromophenol blue, 20% (v:v) glycerol) and boiled for five minutes.

2.13.2 Gel Electrophoresis

A soluble and insoluble 18 µl volume of boiled sample for each condition (100 nM PMA, 10µM Chelerythrine and DMSO) was separated by sodium dodecyl sulphate polyacrylamide gel electrophoresis (SDS-PAGE) using the mini-Protean II electrophoresis system (Bio-Rad). Initially, the glass plates used for making the 10% resolving gel were washed with 70% ethanol to ensure good adhesion between the plates and gel. Once the plates were dry, a large glass plate was combined with a small plate and clamped together using gel cast apparatus. A 10% acrylamide resolving gel (composition in mM, unless otherwise stated: 3.3 mls acrylamide, 2.5 mls resolving buffer [1.5 mls Tris-HCL, pH 8.8], 0.1 mls SDS, 3.97 mls H_20, 0.1 mls APS, 0.005 µls TEMED [N',N,N'-tetramethylethylenediamine]) was prepared and pipetted into the space between the large and small glass plates, until the solution was approximately 2 cm from the top of the small plate. To avoid the formation of bubbles in the gel, 70% ethanol was pipetted on top of the resolving gel. Ammonium persulphate and TEMED were added to the solution last and just prior to it being pipetted between the glass plates. This is because the gel sets due to the polymerisation of the acrylamide by the ammonium persulphate and TEMED. Once the gel has set, the apparatus holding the glass plates in position were tilted to discard the ethanol layer on top of the resolving gel. Distilled water

was then pipetted into the space which previously contained ethanol and again tilted, to ensure all reminants of ethanol had been washed from the gel.

A 4% acrlyamide stacking gel (composition in mM, unless otherwise stated: 1.3 mls acrylamide, 2.5 mls stacking buffer [0.5 mls Tris-HCL, pH 6.8], 0.1 mls SDS, 6.0 mls H_20, 0.1 mls APS, 0.010 µl of TEMED) was then prepared and pipetted on top of the resolving gel. A ten-well comb was then inserted into the stacking gel and allowed to set. Once set, the comb was carefully removed, taking care not to damage any of the wells. The wells were then washed with distilled water to remove any remnants of the stacking gel that had not set.

A running buffer (composition in mM, unless otherwise stated: Tris Base 20, NaCl 137, 0.1% Tween 20, pH 7.4) was prepared and poured to fill one quarter of the electrophoresis tank. The glass plates, containing the stacking and resolving gels were then removed from their respective setting frames and clipped into the frames used to suspend the plates in the running buffer. Once the plates were placed into position in the electrophoresis tank, the running buffer was poured into the inside and outside reservoirs to completely fill the electrophoresis tank. The gels were then loaded with the samples into specific wells using a special loading pipette tip. The molecular mass of proteins was determined by running pre-stained proteins of known molecular mass (Full Range Rainbow™ Molecular Weight Markers). The electrophoresis tank was then ran at 120V for approximately 90 minutes.

2.13.3 Transfer of proteins

Proteins were transferred from gels to nitrocellulose membranes using the Wet transfer system. While the electrophesis tank is running, four pieces of blotting paper, one piece of nitrocellulose and two sponges are soaked in the transfer buffer (composition in mM, unless otherwise stated: Trizma-base 25, Glycine 192, 20% (v:v) methanol, pH 7.4). Following electrophoresis, the glass gel plates were separated using the comb and the stacking gel removed using a transfer comb. The resolving gel was gently removed from the glass plate into a small plastic container containing the transfer buffer and also left to soak. Using a transfer cell, a sponge is placed on the anode side followed by two pieces of blotting paper. A piece of nitrocellulose with the top left corner cut is then placed on top of the blotting paper, followed by the gel, remembering the orientation of the samples and marker. Finally two pieces of blotting paper and the other sponge are placed over the gel and the cathode plate closed over it to form the transfer 'sandwich'. Bubble trapping was always avoided by rolling a glass tube over the various additional layers of the transfer sandwich. The transfer cells were then placed into the electrophoresis tanks and filled with the transfer buffer. The electrophoresis tanks were then set to run at 100 V for an hour. The tank was then surrounded with ice to keep the system cool.

Following transfer of the proteins to the nitrocellulose paper, the nitrocellulose paper was cut around the outline of the gel and the gel disgarded.

2.13.4 Western blotting procedure

Each piece of nitrocellulose paper was washed in a blotting buffer for two hours at room temperature in TBS-Tween (composition in mM, unless otherwise stated: Tris-base 20, NaCl 137, 0.1% (v:v) Tween-20 containing 5% (w:v) dried milk). Membranes were then washed for three 10 minute washes in excess TBS-Tween. Each nitrocellulose membrane was placed in a heat sealed plastic pocket with the respective goat polyclonal anti-sera, specific for the delta (diluted 1:500) and episilon (1:1000) isoforms of PKC in 5ml TBS-Tween (composition in mM, unless otherwise stated: Tris-base 20, NaCl 137, 0.1% (v:v) Tween-20 containing 1% (w:v)) dried milk overnight at 4°C with gentle rocking. Membranes were then washed for three 10 minute washes in excess TBS-Tween before incubation with horseradish peroxidase (HRP)-conjugated anti-mouse secondary antibodies (1:1000 dilution) in 5ml TBS-Tween (composition in mM, unless otherwise stated: Tris-base 20, NaCl 137, 0.1% (v:v) Tween-20 containing 1% (w:v)) for approximately 60 minutes at room temperature with gentle rocking.

2.13.5 Protein detection

The ECL reagents kit from Amersham (Bucks, U.K.) was used (according to the manufacturer's instructions) to develop the blot. The reagents were removed from the fridge and allowed to equilibrate to room temperature. A large piece of Cling film was then placed upon the lab bench, which had been previously cleaned with 70% ethanol. The nitrocellulose was removed from the blocking buffer and excess buffer allowed to drain and then the membrane was placed with the protein face up on the Cling film. The solutions were then mixed and poured onto the cling film and left for 5 minutes. The

Cling film was then lifted slightly to remove excess reagents and wrapped over the nitrocellulose membranes. The wrapped nitrocellulose membrane was then placed inside an x-ray film cassette, which was then taken to a dark room. Under the safety red lights of the dark room, a sheet of autoradiography film (Hyperfilm™) was placed over the protein side of the nitrocellulose membrane and the cassette was shut. The film was then left in the cassette for approximately 7 minutes before it was removed and developed using an Amersham Hyperdeveloper. The exposure time for other pieces of autoradiography film was adjusted depending upon the appearance of previous exposures.

2.13.6 Western blot analysis

Comparison of the different densities of the protein bands of the samples on the autoradiography film was achieved using the densitometry measuring program NIH ImageJ.

CHAPTER 3

GENDER DIFFERENCES: INTRACELLULAR CALCIUM AND ITS RELATIONSHIP TO CELLULAR SURVIVAL

Chapter 3 Gender differences: Intracellular calcium and its relationship to cellular survival

3.1 Introduction

Isolated cell models have long been used as a means to examine the effect of ischaemia, mainly due to the fact that the external environment can be controlled in a way which it can not be in vivo. To mimic ischaemia, workers have often used metabolic inhibition or hypoxia; of course certain aspects are hard to reproduce in vitro such as CO_2 and lactate accumulation, cellular K^+ loss, and extracellular retention (Silverman, 1994). Many of the studies into the effect of ischaemia at the single cell level have found that hypoxia or metabolic inhibition causes the cell to rapidly shorten while maintaining its organised sarcomere pattern and intact sarcolemma. The disagreements have been over the effect of reperfusion following either metabolic inhibition or hypoxia. In some studies, cells were shown to exhibit an 'oxygen paradox' prior to reperfusion, whereby the cells shorten upon perfusion with metabolic inhibition or hypoxia but developed a rounded hypercontracted structure upon reperfusion (Haworth et al., 1981; Stern et al., 1985). In contrast, investigations using graded hypoxia to mimic ischaemia have shown that the cells rounded into hypercontracted states at different times during the actual hypoxia while exhibiting no further morphological changes upon reperfusion (Piper et al., 1984). Therefore the main focus of subsequent studies has been to investigate what are the determing cellular factors in whether a cell survives ischaemia and reperfusion or not. Many studies have shown that injury following metabolic inhibition, hypoxia or anoxia is dependent upon calcium. A study by Nishioka et al. (1984) showed that the recovery of

mechanical function of an isolated arterially perfused rabbit septal preparation was inversely related to the increase in cellular calcium. However, an investigation by Murphy et al., 1985 has shown that cellular survival following ischaemia and reperfusion may not be solely reliant upon the level of intracellular calcium but due to an interaction been intracellular calcium and ATP. It was found that myocytes that had been perfused with metabolic inhibitors had a level of lactate dehydrogenase release (an index of injury) twice that of cells that had been treated with ouabain, even though intracellular calcium was four-fold higher in the ouabain treated cells. More recent studies have used techniques such as spectrofluorometry to study changes in intracellular calcium during and following ischaemia and reperfusion. These studies have been useful for identifying the role of particular channels and exchangers, such as the Na^{+}-Ca^{2+} exchanger, in calcium homeostasis during hypoxia and ischaemia (Pei et al., 2003). Consequently knowledge of the role of calcium overload during ischaemia and reperfusion and what may cause it has improved, establishing a better understanding of ischaemia and reperfusion injury.

Much research has focussed on comparing calcium handling between the sexes, mainly because intracellular calcium handling differs enormously between the sexes under both ischaemic and normal conditions. Regulation of intracellular calcium is imperative to the cell, as high intracellular calcium can result in apoptosis and subsequent cell death (Dong et al., 2006). A higher rise in intracellular calcium was reported in male mouse myocytes compared to female under conditions of metabolic stress, which was suggested to be due to the inhibitory effect of oestrogen upon the sodium-calcium exchanger (Sugishita et al.,

2001). Female rat cardiac myocytes have also been suggested to be able to regulate their intracellular calcium more effectively than male cells in response to increasing extracellular calcium (Curl et al., 2001). This was suggested to be due to a decreased influx of calcium and decreased sarcoplasmic loading (Curl et al., 2001). The difference in calcium handling between the sexes could also be due to regulation of the L-type calcium channel in females by oestrogen (Johnson et al., 1997). Johnson et al., 1997 found that increased expression of the cardiac L-type calcium channel was found in oestrogen receptor knockout (ERKO) mice. In addition, there was evidence that acute application of 17β-oestradiol to cardiac myocytes resulted in an inhibition of L-type calcium channels (Meyer et al., 1998). Chen et al. (2003) suggested that female rabbits may also differ from males in their sarcoplasmic reticulum loading capabilities in that female cardiac myocytes have a lower sarcoplasmic reticulum calcium loading, compared to males after application of isoprenaline. Chen et al. (2003) found that the decreased calcium loading of the sarcoplasmic reticulum was attributed to a significantly higher level of nitric oxide synthase in female cardiac myocytes. Chu et al., (2004) have found that females have significantly higher levels of proteins constituting the L-type calcium channel, ryanodine receptor and sodium-calcium exchanger, which could also account for the differences in calcium handling between the sexes.

Mitochondrial damage is an essential event in ischaemia cell injury and apoptosis (Dong et al., 2006). Apoptosis in ischaemia/repefused heart is triggered by calcium-induced opening of the mitochondrial permeability pore (MPTP) and subsequent release of cytochrome c (Dong et al., 2006). Female mitochondria have been found to have a lower

rate of uptake of calcium in physiological substrate solutions (succinate/pyruvate) and are able to maintain mitochondrial membrane potential more readily than males under high calcium conditions (Arieli et al., 2004). Morkuniene et al., (2002) showed that physiological concentrations of 17β-oestradiol protected heart mitochondria through block of calcium induced cytochrome c release (Morkuniene et al., 2002). Recent evidence suggests that oestrogen acting through the β-oestrogen receptor affords the female heart protection against ischaemia/reperfusion injury (Gabel et al., 2005).

Other studies have suggested a difference in calcium handling between the sexes attributable to differences in the Na^+-Ca^{2+} exchanger (Cross et al., 1998) in addition to calcium handling in cardiac mitochondria (Arieli et al., 2004), and L-type calcium channel density (Johnson et al., 1997). Ranki et al., (2001) suggested that a higher K_{ATP} channel current density in females was linked to a lower intracellular calcium concentration following ischaemia and reperfusion. As previously mentioned in Chapter 1, the K_{ATP} channel may be protective by hyperpolarising the membrane potential, thereby reducing the drive of calcium into the cell via the Na^+-Ca^{2+} exchanger.

In the present study, to investigate differences in calcium handling between the sexes, Ca^{2+} homeostasis was assessed from the ability of cells to recover a low diastolic $[Ca^{2+}]_i$ after metabolic inhibition (MI) and reperfusion. The percentages of male and female cells that survived MI and reperfusion were also studied. The times at which contractile failure and rigor occurred and whether the cells regained the ability to contact in response to stimulation following MI reperfusion were measured.

I found a significant difference between male and females with respect to cellular survival when using metabolic inhibition (CN and IODOACETIC ACID) followed by perfusion with normal Tyrode's. Specifically, females had a higher rate of functional recovery compared to males following metabolic inhibition and reperfusion, indicated by a higher percentage of cells that regained the ability to contract in response to stimulation following reperfusion. In addition female cells were found to have a significantly lower intracellular calcium concentration during and after MI and reperfusion compared to males.

3.2. Methods

Ventricular myocytes were dissociated from the animals as described in chapter 2.

3.2.1 Measurement of cell morphology and contraction

Myocytes were placed in a diamond-shaped perspex superfusion chamber mounted on the stage of a Nikon TMS inverted microscope, which were continuously superfused with normal Tyrode's at a rate of 5 ml/min and maintained at 34 ± 2°C. The cells were also continuously field stimulated at 1Hz. Changes in cell morphology were assessed by viewing the cells with the aid of a CCTV camera. Metabolic stress was induced by superfusing the cells with substrate-free Tyrode's for 3 minutes then MI-Tyrode's for 7 min followed by reperfusion with normal Tyrode's for 10 minutes. From video images, the cells were classified as either normal rod-shaped, in rigor, or hypercontracted. Cells were also classified as either contractile or non-contractile in response to stimulation.

3.2.2. Fluorescence measurement of cytoplasmic calcium

To measure $[Ca^{2+}]_i$, myocytes were loaded with Fura-2 at room temperature (20°C) using the membrane permeant AM-ester form of fura-2 (2 μM) for 25 minutes. Myocytes were excited alternately at 340 and 380 nm with light from a monochromator (PTI deltaRAM) and viewed with a x20 fluor objective (Nikon, Kingston-upon-Thames, UK). The output to the photo-multiplier tube or camera was collected at > 510 nM. Fluorescence intensity was measured with a photomultiplier tube or from images of myocytes viewed with a video imaging system (Photon Technology International, Lawrenceville, NJ, USA).

Metabolic stress was induced as described above. In some experiments, contraction in individual mycytes was determined from changes in cell length using a video-edge detection system (Crescent Electronics). Changes in cell length were measured in conjunction with the measurement of intracellular calcium from one cell at a time, using the photomultiplier tube and a dichromatic mirror to visualise the cell.

To reduce background fluorescence, experiments were carried out in a light-proof chamber. Background fluorescence was measured and subtracted from measured calcium signals. In addition, autofluorescence, was <2% of the measured signal, which was also ignored in analysis. Additional Light exposure of the cells, which could cause photodamage when using Fura-2 was also limited by reducing the light intensity via the iris and also exposure time to 33 ms at 0.2 Hz.

The imaging system enabled the fluorescence signal from up to 5 myocytes in the field of view to be measured independently and simultaneously, whereas only one cell's fluorescence signals were measured using the photomultiplier.

3.2.3 Analysis

Fluorescence images were analysed using PTI FELIX or Imagemaster software. Fluorescence intensity was measured from a region of interest drawn around each whole cell. To subtract the background fluorescence a region of the field that did not contain cells was used. The ratio of the 340:380 nm calcium images of the cells were then converted to estimated free calcium values using a look up table generated with a fura-2

imaging calibration kit (Molecular Probes). This is only an estimation of the free calcium concentration as the K_D of fura-2 may differ from cell to cell, therefore the values give an indication of $[Ca^{2+}]_i$ rather than the exact intracellular calcium concentrations.

Data are represented as mean ± SEM and values of n refer to the number of cells examined as indicated in the text or figure legends.

Mean values obtained were compared by the paired or unpaired Student's t-test where appropriate. Values where $p<0.05$ were considered statistically significant. All experiments were done at 34 ± 2°C.

3.3 Results

3.3.1 Cellular responses to metabolic inhibition in male and female ventricular myocytes.

To investigate possible gender-specific differences in the responses of rat cardiac myocytes to metabolic inhibition, metabolic inhibition and reperfusion were achieved by application of MI-Tyrode's, as described in the methods. Figure 3.1A shows a typical recording of cell length from a myocyte during superfusion with MI-Tyrode's. The amplitude of contractions increased over a period of about 2 minutes and then declined rapidly, culminating in contractile failure followed shortly afterwards by the development of a sustained rigor contraction (figure 3.1B, photograph ii). Rigor, in which cells retained a rectangular shape with visible striations, was observed in all cells under such conditions. Reperfusion with normal Tyrode's induced rapid hypercontracture (within 1 minute) in which cells shortened further, associated with the development of membrane blebs (figure 3.1B, photograph iii) and failure to contract in response to electrical stimulation.

In these experiments I measured the times to contractile failure, rigor and the percentage of cells that recovered contractile function after the cells had been metabolically inhibited using a substrate-free solution containing 2mM cyanide and 1mM iodoacetic acid. Contractile failure was measured as the time (minutes) at which the cell stopped contracting in response to electrical stimulation. The times given for that of contractile failure and rigor were measured from the time at which the cells were perfused with the metabolic inhibitor.

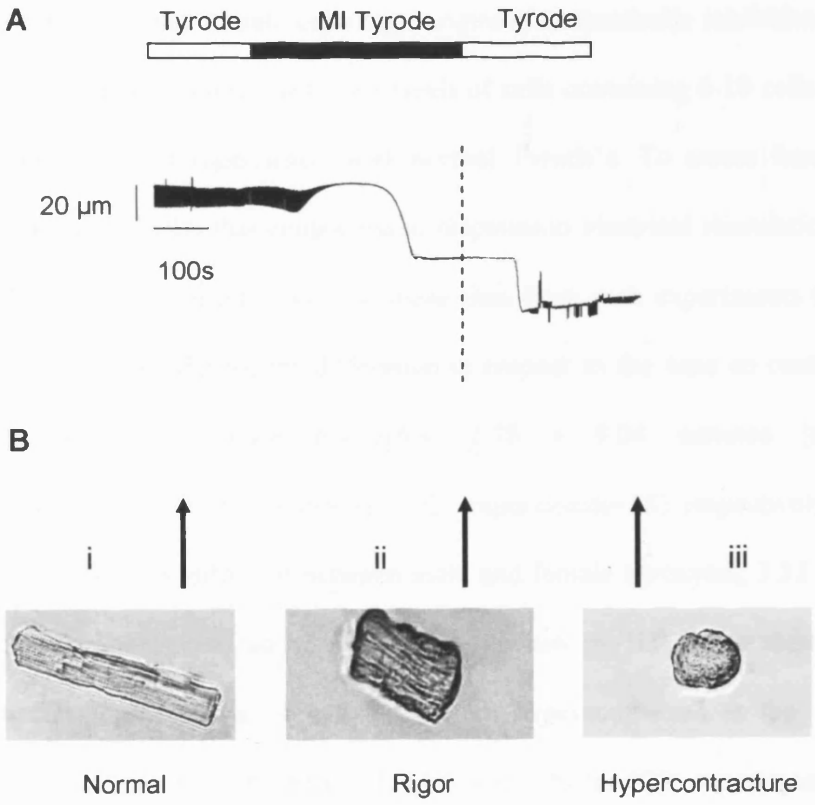

Figure 3.1. Effect of metabolic inhibition and reperfusion on cell contraction.

A, Record of cell length from a male myocyte superfused with MI-Tyrode for 8 mins and reperfused with normal Tyrode as indicated in the bar above. Measurement of cell length was made in conjunction with changes in intracellular calcium, as can be seen in figure 3.4. Field stimulation was applied at 1 Hz throughout. A decrease in cell length is seen as a downward deflection, so that the top of the trace represents diastolic length and the bottom systolic length. The individual contractions in response to stimulation fuse into a solid block on the line scale used. The dashed line shows the time of reperfusion with normal Tyrode.

B, show the three different morphological changes in the shape of the myocyte that occur at different times throughout the experiment. In normal Tyrode, the cell has an oblong shape and striated pattern (i), which contracts to a square shape upon perfusion with MI Tyrode (ii). Upon reperfusion with normal Tyrode the cell hypercontracts into a rounded appearance and characterised by a loss of the straited pattern and the appearance of membrane blebbing (iii).

In experiments where male and female cells were exposed to metabolic inhibition for 7 minutes, cell morphology was determined from fields of cells containing 6-10 cells at the end of a 10 minute period of reperfusion with normal Tyrode's. To assess functional recovery, the percentage of cells that contracted in response to electrical stimulation was measured after 10 minutes of reperfusion. The mean data from such experiments (figure 3.2) show that there was no significant difference in respect to the time to contractile failure between male and female myocytes, 2.78 ± 0.04 minutes (n=100, experiments=16) and 2.81 ± 0.05 minutes (n=102, experiments=18) respectively. The time to rigor was significantly different between male and female myocytes, 3.32 ± 0.04 minutes (n=100, experiments=16) and 3.57 ± 0.06 minutes (n=102, experiments=18) respectively ($p<0.05$). The number of cells that were hypercontracted at the end of reperfusion were highly significantly different, 68.8 ± 6.5 % (n=100, experiments=16) and 11.9 ± 3.4 % (n=102, experiments=18) ($p<0.01$) respectively for male and female myocytes respectively (figure 3.3). Female cells also showed increased functional recovery: (figure 3.3) 73.6 ± 7.2 % (n=102, experiments=18) of female myocytes recovered contractile function compared to 42.4 ± 9.1 % (n=100, experiments=16) of male cells.

3.3.2 Intracellular calcium following metabolic inhibition and reperfusion was lower in female myocytes

Previous studies by Ranki et al., (2001) suggested that a higher K_{ATP} channel current density in female guinea-pigs was linked to a lower intracellular calcium concentration

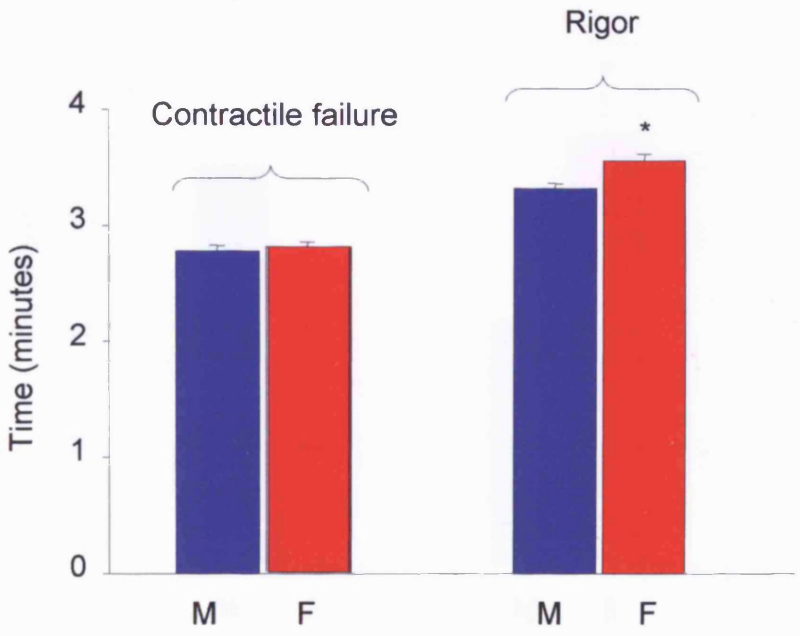

Figure 3.2 The time (mins) to contractile failure and rigor of male and female cardiac ventricular myocytes.

In this figure, the blue bar shows the mean (± s.e.m.) time at which male cells (n =100, experiments = 16) and female (n = 102, experiments = 18) exhibited contractile failure (left) and rigor (right), following three minutes of Normal Tyrode, seven minutes of Metabolic Inhibition (2mM $NaCN^-$ and 1mM IAA^-) and ten minutes of reperfusion with Normal Tyrode, field stimulated at 1 Hz throughout. Time zero was the time at which the cells began to be perfused with MI. (* $p<0.05$). The time (mins) is measured from of application of MI Tyrode.

Male Female

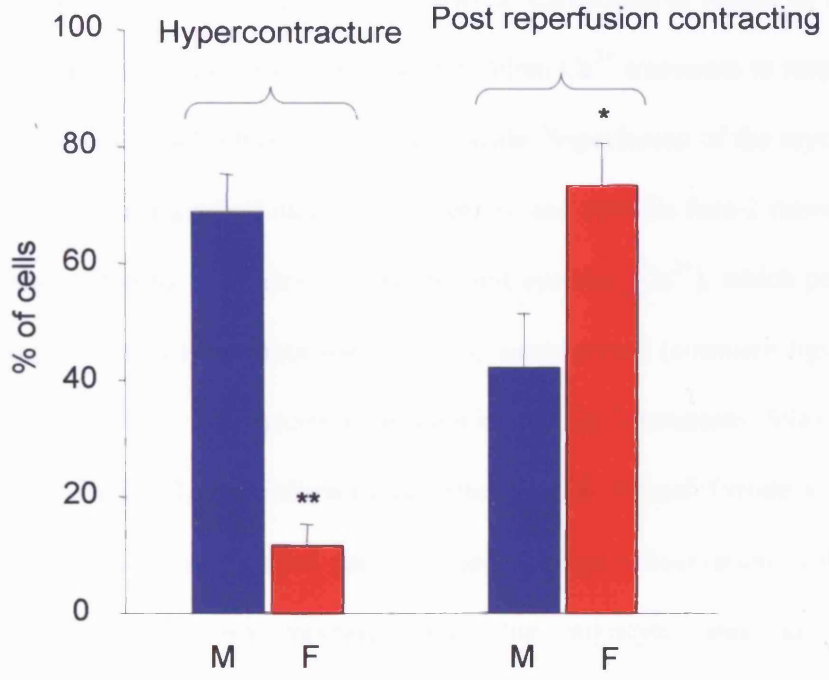

Figure 3.3 Effect of reperfusion injury on cellular survival rate of male and female cardiac ventricular myocytes.

In this figure, the blue bar shows the percentage of male cells (n =100, experiments = 16) and female (n = 102, experiments = 18) which had hypercontracted (left) or which contracted in response to electrical stimulation (right) after 7 minutes with MI-Tyrode and 10 minutes with Normal Tyrode, field stimulated at 1 Hz throughout. (** $p < 0.01$, * $p<0.05$).

Male Female

following reperfusion. To investigate whether there was a difference between cells from male and female rats with respect to their calcium handling following reperfusion injury, cells were metabolically inhibited for seven minutes and reperfused for 10 minutes with normal Tyrode's (Figure 3.4A). Figure 3.4B shows a representative record of the fura-2 ratio (340/380 nM) from a male myocyte. The individual Ca^{2+} transients in response to 1 Hz stimulation fuse into a solid block on this time scale. Superfusion of the myocyte with MI-Tyrode's resulted in a gradual increase in diastolic and systolic fura-2 ratios over the initial 2 minutes, reflecting increases in diastolic and systolic $[Ca^{2+}]_i$ which presumably underlie the increased cell shortening seen over the same period (compare figure 3.4A). Continued superfusion with MI-Tyrode's caused a loss of Ca^{2+}-transients, followed by an increase in $[Ca^{2+}]_i$ (figure 3.4B). Following reperfusion with normal Tyrode's, there was a fall in $[Ca^{2+}]_i$, followed by a gradual and sustained increase. Observation of the cell by conventional light microscopy revealed that the myocyte was in sustained hypercontracture with blebbing of the sarcolemmal membrane. There was no recovery of Ca^{2+}-transients in response to electrical stimulation.

To compare differences in calcium handling during metabolic inhibition (MI) and reperfusion, intracellular calcium concentration was measured before the application of MI, at the end of 7 minutes of MI and at the end of reperfusion with normal Tyrode's (figure 3.4 i, ii and iii). Figure 3.5 shows recordings of intracellular calcium from a field of cells using the imaging system (A, 7 male, B, 5 female cardiac ventricular myocytes) exposed to metabolic inhibition for seven minutes and reperfusion for ten minutes. The cells were also field stimulated at 1 Hz throughout. Each trace shows a recording from a

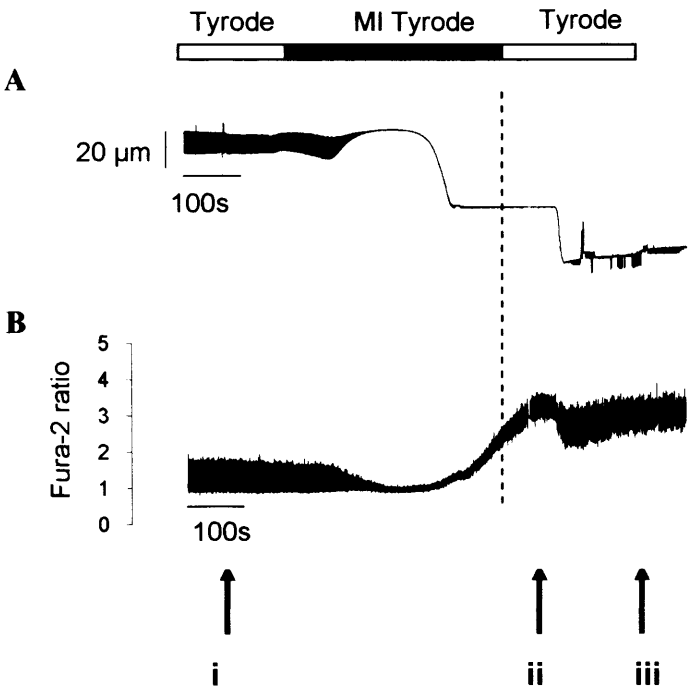

Figure 3.4 The effect of metabolic inhibition and reperfusion on cell length and Ca^{2+} homeostasis in isolated ventricular myocytes.

A, Record of cell length from a male myocyte superfused with MI-Tyrode for 8 mins and reperfused with normal Tyrode as indicated in the bar above. Field stimulation was applied at 1 Hz throughout. A decrease in cell length is seen as a downward deflection, so that the top of the trace represents diastolic length and the bottom systolic length. The individual contractions in response to stimulation fuse into a solid block on the tine scale used. Same record as that of figure 3.1A.

B, Record showing the associated changes in intracellular calcium in a single myocyte under the same conditions as in A. The calcium rises during metabolic inhibition, then decreases rapidly following reperfusion with normal Tyrode, before rising slowly again. The cell had a square appearance in normal Tyrode but developed rigor during metabolic inhibition and hypercontracture on reperfusion as indicated by i,ii and iii respectively, the photos of which are in figure 3.1. The dashed line indicates the time at which reperfusion occurred.

different cell. Images were collected at 10 s intervals and the peaks in the early sections of the records arise from aliasing of the calcium transients, due to differences between the sampling and stimulation rates. It can be seen that female cells maintained a lower intracellular calcium concentration during metabolic inhibition and reperfusion compared to males. The female cells are seen to recover following reperfusion as indicated by the reappearance of the calcium transients at the end of reperfusion, this is in contrast to the male myocytes where calcium remained high in all but one cell (figure 3.5). It can also be seen that the fall in intracellular calcium appears simultaneous in all cells in the field of view. However, there was slight variation of between 10-20 seconds, but this is not easily distinguishable due to the compressed time base.

Figure 3.6 shows that the intracellular calcium concentration, measured in experiments like those of figure 3.5 following metabolic inhibition and reperfusion was significantly lower in females compared to male myocytes; 164 ± 5 nM (n=137, expts=19) in male myocytes compared to 149 ± 4 nM (n=100, expts=15) in female myocytes. At the end of reperfusion intracellular calcium was significantly lower in the female (186 ± 6 nM, n=100, expts=3) compared to male myocytes (279 ± 18 nM, n=137, expts=3) ($p<0.5$). Cells that had an intracellular calcium concentration above 250 nm, when viewed by conventional microscopy were non-contractile, hypercontracted with membrane blebbing (Rodrigo and Standen, 2005). Therefore I compared the numbers of male and female myocytes that had a calcium concentration above 250 nM after 10 minutes of reperfusion as an indication of recovery of calcium homeostasis. Figure 3.7 shows the percentage of male and female myocytes that had an intracellular calcium concentration above 250 nM

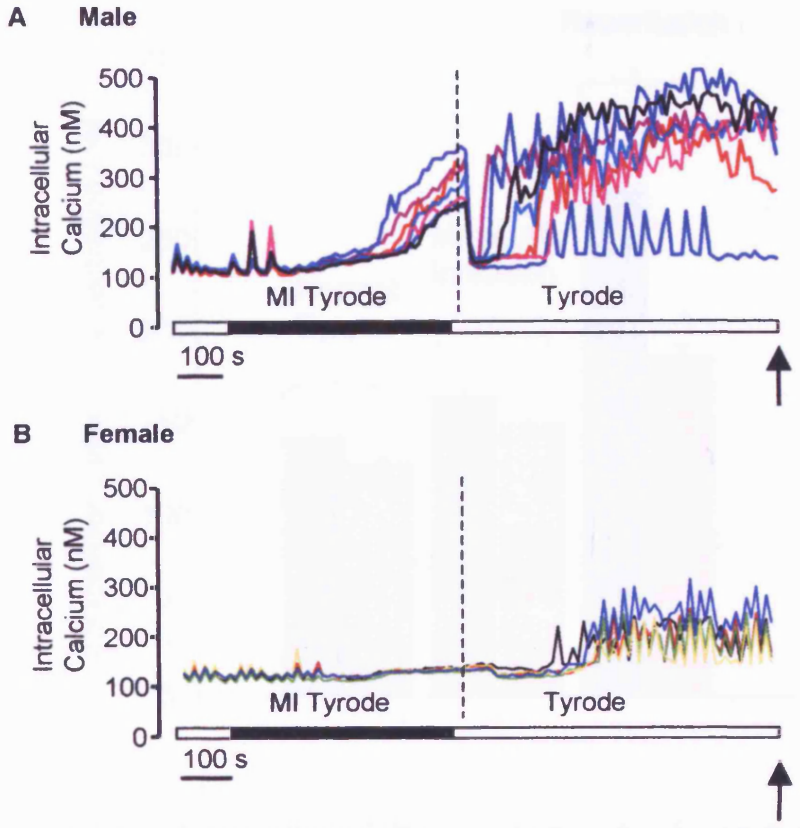

Figure 3.5 Effect of metabolic inhibition and reperfusion on Ca^{2+} homeostasis in isolated ventricular myocytes

Recordings of intracellular calcium in fields of cardiac ventricular myocytes exposed to metabolic inhibition and its removal whilst field stimulated at 1Hz throughout (A, male, B, female). Each trace shows a recording from a different cell. Images were collected at 10-s intervals and the peaks in the early sections of the records arise from aliasing of the calcium transients, due to differences between the sampling and stimulation rates. The arrow shows the time at which the measurements shown in figure 3.7 were collected.

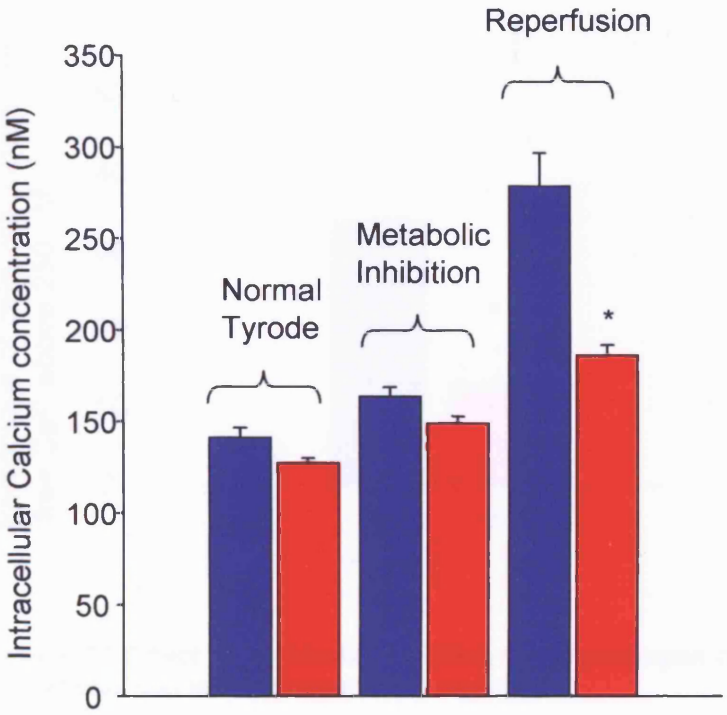

Figure 3.6 Intracellular Ca^{2+} concentration of male and female myocytes during Normal Tyrode, Metabolic Inhibition and following reperfusion.

In this figure, the blue bar shows mean (± s.e.m.) intracellular calcium concentration results from male cells (n =137, experiments = 19) and female (n = 100, experiments = 15) following two minutes of Normal Tyrode, seven minutes of Metabolic Inhibition (2mM $NaCN^-$ and 1mM IAA^-) and ten minutes of reperfusion with Normal Tyrode field stimulated at 1 Hz throughout.(* $p<0.05$).
Male ■ Female ■

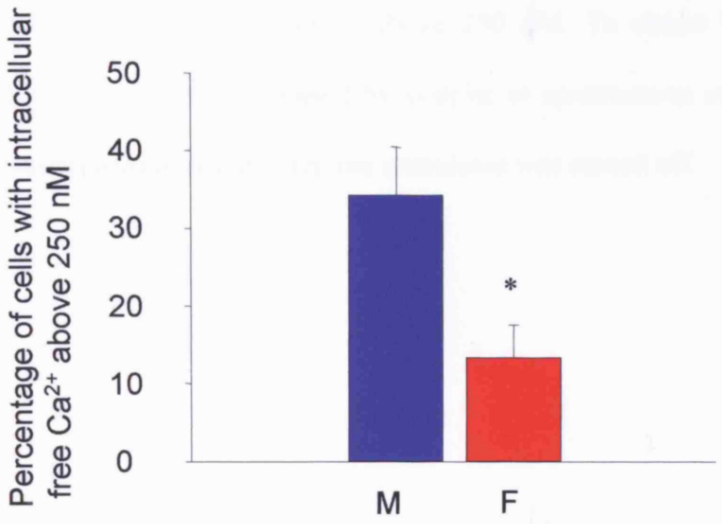

Figure 3.7 Effect of metabolic inhibition and reperfusion on Ca^{2+} homeostasis in isolated ventricular myocytes.

Barchart showing the percentage of male and female cardiac ventricular myocytes that had an intracellular diastolic calcium concentration above 250 nM at the end of 10 minutes reperfusion with normal Tyrode following 7 minutes metabolic inhibition. Male, n=137, experiments=19; Female, n=100, experiments=15 (* $p<0.01$).
Male ■ Female ■

at the end of reperfusion. There was a significant difference ($p<0.5$) between male and female cells, approximately 30% of male myocytes (27 from a total of 75 cells) compared to approximately 10% of female myocytes (13 from a total of 104 cells) had an intracellular diastolic calcium concentration above 250 nM. To obtain basal diastolic calcium concentrations that were not biased by systolic or spontaneous calcium release, measurements of calcium were made when the stimulator was turned off.

3.4 Discussion

3.4.1 The effects of metabolic inhibition and reperfusion on cell morphology and contractile function

Inhibiting cardiac myocytes with a metabolic inhibitor and reperfusing with normal Tyrode's provides an opportunity to study the changes in morphology, contraction and $[Ca^{2+}]_i$ in cells that undergo irreversible damage and those that recover their ability to contract. If female K_{ATP} channel current density is higher in females than males as proposed by Ranki et al. (2001) then contractile failure might be expected to occur sooner. This would be due to an increase in potassium conductance, which would oppose depolarisation and so promote action potential failure thus preventing contractions from occurring. This would reduce any overload of calcium as the voltage-gated calcium channels would be closed. In addition, hyperpolarisation would also reduce the drive of calcium into the cell via the Na^+-Ca^{2+} exchanger. Therefore there should be a higher percentage female cell survival rate as necrosis due to calcium overload is less likely to occur. However, I found no significant difference between male and female cells with respect to time to contractile failure (figure 3.2). Interestingly, there was a significant difference with regard to the time at which rigor occurred (figure 3.2). A higher percentage of female compared to male cells recovered their ability to contract in response to electrical stimulation following metabolic inhibition and reperfusion (figure 3.3). There was also a lower percentage of female compared to male cells that were irreversibly damaged as indicated by a hypercontracted state characterised by the loss of the rectangular shape and visible striations, followed by the development of membrane blebs (figure 3.3).

3.4.2 Changes in intracellular calcium

The pattern of intracellular calcium changes during metabolic inhibition is similar between the sexes. During metabolic inhibition, $[Ca^{2+}]_i$ increases in both male and female cells. However, following reperfusion an initial fall in $[Ca^{2+}]_i$ is seen in both sexes. This is followed by a progressive rise in $[Ca^{2+}]_i$ in all cells during reperfusion. However, the $[Ca^{2+}]_i$ concentration rises to significantly higher levels in males compared to females following reperfusion (figures 3.5 and 3.6). Further, the percentage of male cells considered to have lost calcium homeostasis at the end of reperfusion, indicated by a higher $[Ca^{2+}]_i$ than 250 nM (see section 3.3.2 for explanation), again was significantly higher in males compared to females (figure 3.6). Thus, my results suggest that there are gender differences in the rat in both cellular survival and calcium homeostasis in response to metabolic inhibition and reperfusion. In each case, female myocytes are more resistant to metabolic stress than those from male animals.

Other studies have reported similar differences in calcium handling between the sexes (Ranki et al., 2001, Chen et al., 2003). Therefore the question is what is responsible for controlling the differences in intracellular calcium and cellular survival between the sexes? Many studies have investigated these differences. Ranki et al., (2001) suggested that a higher K_{ATP} channel density in females was linked to a lower intracellular calcium concentration following ischaemia and reperfusion injury. Other studies have suggested a difference in calcium handling between the sexes is attributable to differences in calcium handling in cardiac mitochondria (Arieli et al., 2004), Na^+-Ca^{2+} exchanger (Cross et al., 1998) and L-type calcium channel density (Johnson et al., 1997).

Although there was no difference in the time to contractile failure between the sexes, the K_{ATP} channel could still be protective by being responsible for the lower intracellular calcium concentration following metabolic inhibition and reperfusion in females. As previously explained in chapter 1, the sarcolemmal K_{ATP} channel can be protective in two ways, either by activating earlier to shorten the action potential leading to contractile failure, which would have the effect of decreasing calcium entry into the cell via the L-type calcium channel. Secondly, the K_{ATP} channel could hyperpolarise the membrane potential, thereby decreasing the drive for calcium into the cell via the Na^{+}-Ca^{2+} exchanger. This chapter only presents evidence contrary to the first hypothesis, therefore an investigation of the sarcolemmal K_{ATP} channel density between the sexes is essential, as a higher female sarcolemmal K_{ATP} channel density could be suggested to be protective as there would be an increased drive to hyperpolarise the membrane potential compared to that of the males. In the experiments described in the next chapter, I therefore attempted to determine whether sarcolemmal K_{ATP} channel density also shows gender differences.

CHAPTER 4

GENDER DIFFERENCES: K_{ATP} CHANNEL DENSITY

Chapter 4 Gender differences: K_{ATP} channel density

4.1 Introduction

Sex-related differences have been highlighted in relation to cardiovascular diseases due mainly to the observation of an earlier onset of heart disease in men, some 10-15 years earlier than women (Rossouw, 2002). It has been reported that some arrhythmias are more common in males than females, including those causing sudden cardiac death (Shimoni & Xiu-Fang, 2003). This raised the question of whether the presence of female or male hormone either decreased or increased the risk of heart disease, respectively. The current opinion is that oestrogen may have both genomic and non-genomic effects on the heart. It was known that oestrogen had actions on the vascular system (Stumpf et al., 1977). Barrett-Connor et al (1991) suggested that oestrogen might also have direct effects on the heart, as suggested by radiolabeled 17β-oestradiol binding to the heart. This was later supported by Grohe et al., (1997), who found that oestrogen receptors were present in cardiomyocytes as well as fibroblasts.

Heart disease is also frequently associated with changes in action potential duration. Potassium currents are major determinants of cardiac action potential duration, being responsible for repolarization and refractory period duration (Tseng et al., 1989), and are therefore being investigated for gender specific regulation. Gender differences in the different potassium channels that are present in the heart have been investigated in many species, such as the rabbit (Liu et al., 1998), guinea-pig (Ranki et al., 2001), and mouse (Trepanier-Boulay et al., 2001). Liu et al. (1998) reported that female rabbit ventricular myocytes have significantly lower I_{Kr} and I_{Kl} outward current densities than male cells.

These could be contributory factors causing the longer electrocardiographic Q-T interval exhibited by females compared to males (Chapman et al., 2000). Long Q-T syndrome is when the characteristic electrocardiogram exhibits a prolonged Q-T interval, rendering these people more susceptible to an abnormally rapid heart arrhythmia known as 'Torsades de pointes'. In mice, action potential duration was found to be significantly longer in the female compared to the male and there was a significantly lower density of the ultrarapid delayed rectifier K^+ current, I_{KUR} in females (Trepanier-Boulay et al., 2001).

The ATP-sensitive potassium channel also contributes to the repolarisation of the cardiac action potential, but mainly under ischaemia conditions. Activation of the ATP-sensitive potassium (K_{ATP}) channel results in a large outward $I_{K(ATP)}$ current and consequently a shortening of the cardiac action potential duration. Oestrogen modulates characteristics of ventricular repolarization, an effect which appears to be mediated by blocking ATP-sensitive potassium channels. Lee et al. (1999) provided indirect evidence for the demonstration of the effects of oestrogen upon K_{ATP} channels. Oestrogen was shown to affect the Q-T characteristics of menopausal women with syndrome X. Syndrome X is a clinical condition used to describe angina associated with cardiac ischaemia, in the absence of coronary artery disease. The effects of oestrogen were shown to be blocked by the K_{ATP} channel opener nicorandil. Following this discovery, Tsai (2002) showed that infarct size in dogs following ischaemia/reperfusion was significantly reduced upon application of 17β-oestradiol. Pretreatment with a mitochondrial K_{ATP} channel antagonist, 5-hydroxydecanoate, completely abolished the protection afforded by oestradiol,

suggesting the involvement of the mitochondrial K_{ATP} channel in oestradiol-induced protection. In addition, Tsai (2002) found that activation of the sarcolemmal K_{ATP} channel significantly reduced the incidence and duration of reperfusion-induced ventricular tachycardia and ventricular fibrillation. Investigations by Ranki et al. (2001) have led to the suggestion that there are gender specific differences between the expression and properties of cardiac K_{ATP} sarcolemmal channels. Ranki et al. (2001) found that the density of the pinacidil activated current was higher in adult female than male guinea-pigs. The average current density at +80mV induced after the addition of 100 μM pinacidil was approximately 2 pA/pF and 5 pA/pF for males and females respectively. Using the reverse transcription polymerase chain reaction (RT-PCR), Ranki et al. (2001) also found there to be higher levels of messenger SUR2A in female tissue transcript relative to male. They also found higher levels of both SUR2A and Kir6.2 proteins in cardiac membrane fractions in females compared to males. In addition, they found an increased Ca^{2+} loading in male compared to female cardiomyocytes in response to ischaemia and reperfusion. Subsequent research has shown that 17β-oestradiol regulates expression of K_{ATP} channels in heart-derived H9c2 cells, leading to higher mRNA levels of SUR2A and increased levels of SUR2A and Kir6.2 proteins in 17β-oestradiol treated cells (Ranki et al., 2002).

This chapter describes studies designed to investigate whether a gender specific difference in K_{ATP} channel density exists in the rat. To assess K_{ATP} current density, K_{ATP} currents were elicited by pinacidil, P-1075 or metabolic inhibition (MI) and measured

using whole-cell patch clamp. Sensitivities to pinacidil and P-1075 were compared through construction of dose response curves.

Electrophysiological investigations showed there to be no significant difference between male and females with respect to K_{ATP} channel density when using MI. In contrast there was a significant difference between males and females with respect to sarcolemmal K_{ATP} channel density when using pinacidil and P-1075. However, quantitative PCR did not reveal any gender differences in mRNA levels for Kir6.2 and SUR2A.

4.2 Methods

4.2.1 Isolation of cardiac myocytes

Ventricular myocytes were dissociated from the animals as described in chapter 2.

4.2.2 Solutions

Isolated ventricular myocytes were superfused with normal Tyrode's, the composition of which is described in chapter 2. Other reagents were added to this solution as described in the text. Pinancidil, P-1075 and glibenclamide were obtained from Sigma. Drugs were dissolved in dimethylsulphoxide (DMSO) (Sigma) as stock solutions of 10 mM, 20 mM and 10 mM respectively, and diluted in normal Tyrode's to the required concentrations as specified in the text. Metabolic inhibition was induced by superfusing the cells with metabolic inhibition (MI) Tyrode's, which contained 2 mM NaCN and 1 mM iodoacetic acid (IAA) in substrate-free Tyrode's.

4.2.3 Analysis

Data are represented as mean ± SEM and values of n refer to the number of cells examined as indicated in the text or figure legends.

Mean values obtained were compared by the paired or unpaired Student's t-test where appropriate. Values where $p<0.05$ were considered statistically significant. All experiments were done at 34 ± 2°C.

4.3 Results

4.3.1 K_{ATP} current activated by pinacidil in male and female myocytes

Previous studies by Ranki et al., (2001) in guinea-pig myocytes used a single concentration of pinacidil (100μM) to evaluate K_{ATP} current density in male and female guinea-pigs. However, 100μM may not be a maximal concentration of pinacidil, raising the possibility that potency of pinacidil differs between males and females. Therefore I constructed dose response curves for pinacidil sensitivity for both male and female cells to determine which concentration of pinacidil elicited maximal K_{ATP} current.

K_{ATP} currents were elicited using the K_{ATP} channel opener pinacidil as shown in figure 4.1. Figure 4.1A shows the pulse protocol used to evoke the K_{ATP} current. Cells were held at –70 mV and pulsed every ten seconds to –40 mV for 200 ms and then to 0 mV for 400 ms. The K_{ATP} current was measured at the end of the 0 mV pulse. The pulse protocol was designed to reduce possible activation of other channel currents, thus pulsing from –70 mV to –40 mV inactivates and therefore prevents interference from voltage-activated channels such as sodium channels, voltage-gated potassium channels and calcium channels. To isolate currents through K_{ATP} channels the K_{ATP} blocker glibenclamide, which blocks K_{ATP} currents activated by pinacidil in these cells with an IC_{50} of 7.9 nM (Lawrence et al., 2001) was used as shown in figure 4.1B.

Figure 4.2 shows the effect of increasing the pinacidil concentration from 20-500 μM upon the K_{ATP} current. Following application of each concentration of pinacidil, there

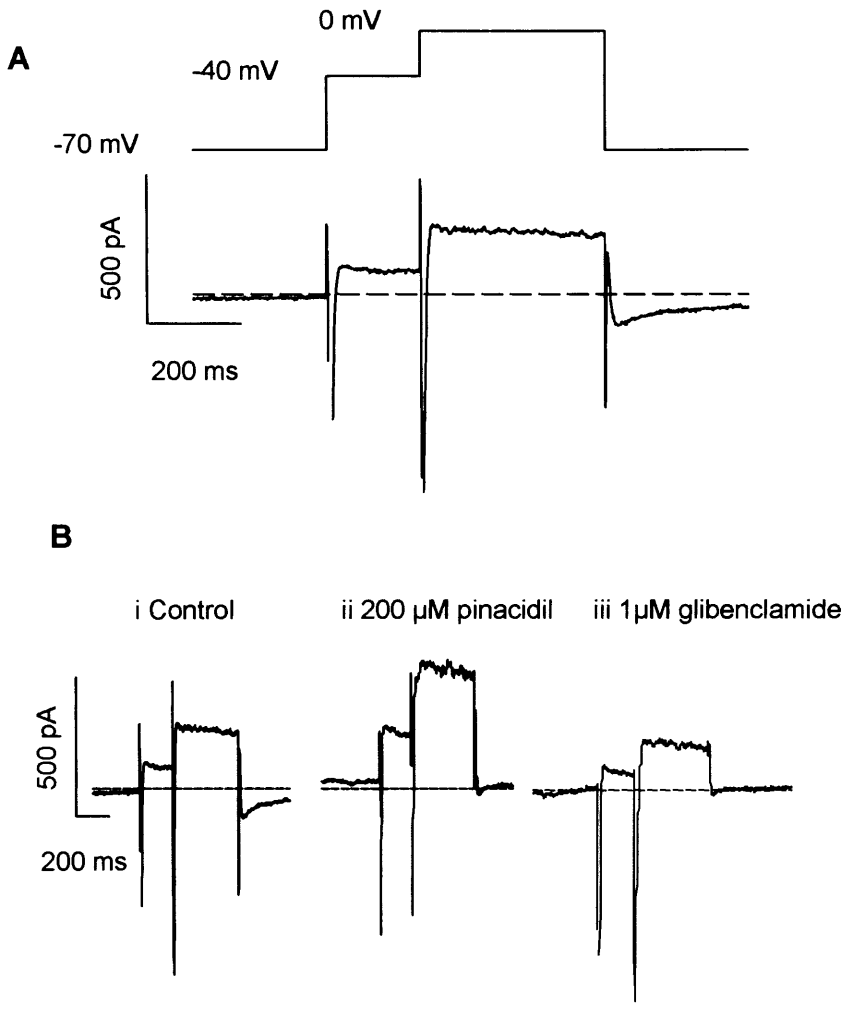

Figure 4.1 K_{ATP} current activation by pinacidil

A, The voltage pulse protocol (above) used to measure K_{ATP} current (below) from a cardiac myocyte (above) and the resulting whole-cell current (below). The voltage was stepped from a holding potential of –70 mV to –40 mV for 200 ms and then 0 mV for 400 ms. This pulse protocol was repeated every 10 seconds.

B, Whole-cell current from a cardiac myocyte (i) in the absence of pinacidil; (ii) 3 minutes after the addition of 200 µM pinacidil; (iii) 3 minutes after the addition of glibenclamide in the continued presence of pinacidil.

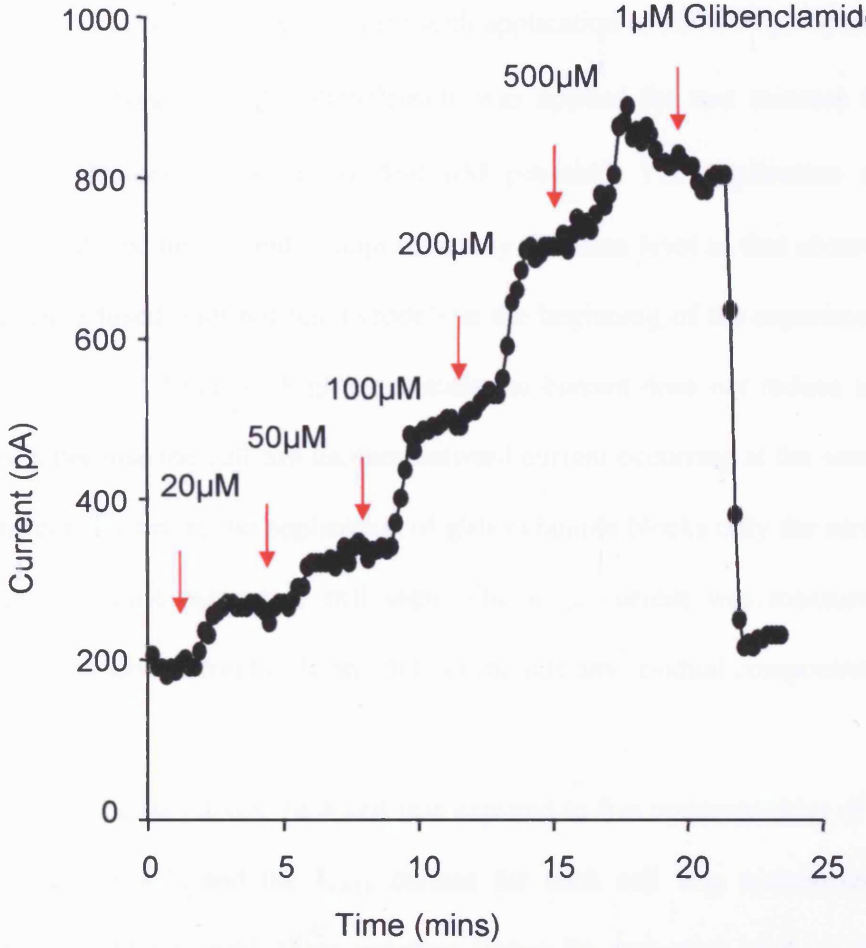

Figure 4.2 The effect of increasing pinacidil concentration on K_{ATP} current

K_{ATP} currents were recorded at 0 mV using the protocol shown in figure 4.1 from a cardiac myocyte superfused with Tyrode solutions containing increasing concentrations of pinacidil as indicated. Each solution was applied for 4 minutes and 1 μM glibenclamide was applied at the end of the experiment to obtain basal current level.

was an increase in current until a plateau was reached, usually after 3 minutes. It can be seen that the current increased with the application of higher concentrations of pinacidil. The most substantial increases in current were seen with application of 100 and 200 μM pinacidil and maximal current was obtained with application of 200-500 μM pinacidil. To isolate the K_{ATP} current, 1 μM glibenclamide was applied for two minutes following maximal K_{ATP} channel activation by 500 μM pinacidil. The application of 1 μM glibenclamide reduced the current to approximately the same level as that observed when the cell was superfused with normal Tyrode's at the beginning of the experiment. It can be seen from figure 4.2 that with glibenclamide the current does not reduce to 0 pA. I suggest this is because the cell has another outward current occurring at the same time as the K_{ATP} current. Therefore the application of glibenclamide blocks only the sarcolemmal K_{ATP} current, so some current is still seen. The K_{ATP} current was measured as the glibenclamide-sensitive current only and did not include any residual component.

To obtain dose-response curves, each cell was exposed to five concentrations of pinacidil as shown in figure 4.2, and the K_{ATP} current for each cell was normalized to that measured in 500 μM pinacidil. Dose response curves for activation of K_{ATP} current by pinacidil were constructed from the currents elicited from myocytes from male and female rats respectively. Figure 4.3 shows mean dose response curves for myocytes from male and female rats. Each point is the mean ± S.E.M current (pA) produced from 16 and 12 male and female cells respectively for a particular pinacidil concentration. The fitted curves are drawn to the equation:

Normalised current = $c^n/(c^n+EC_{50}^n)$

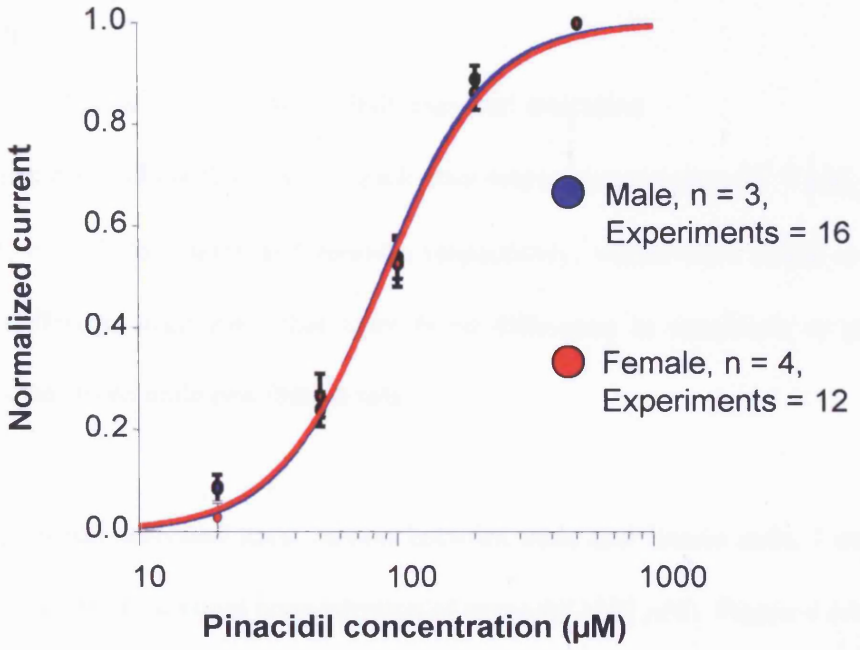

Figure 4.3 Dose-response curves for pinacidil activation of K_{ATP} current in myocytes from male and female rats.

Cumulative dose-response curves were constructed for individual cells as illustrated in figure 1. K_{ATP} current was measured as glibenclamide-sensitive current (after subtraction of the basal current). For each cell, currents were normalized to the value in 500μM pinacidil. The points show mean (± s.e.m.) normalized current in myocytes from male (blue circles, n = 16 cells from 3 animals) and female (red circles, n = 12 cells from 4 animals) rats. The fitted curves are drawn to equation:

$$\text{Normalised current} = c^n/(c^n+EC_{50}{}^n)$$

Where:

n = Hill coefficient

c = the concentration of pinacidil

EC_{50} = the concentration of pinacidil for half-maximal activation

With the previous parameters: male (red curve) EC_{50} = 87.5 μM,

n = 2.14; female (blue curve) EC_{50} = 88.8 μM, n = 2.07.

Where:

n = Hill coefficient

c = the concentration of pinacidil

EC_{50} = the concentration of pinacidil for half-maximal activation

The EC_{50} values and Hill coefficients for each dose response curve were 87.5 μM, n=2.14 and 88.7 μM, n=2.07 for males and females respectively, which were found to not be significantly different, suggesting that there is no difference in sensitivity to pinacidil between myocytes from male and female rats.

To compare pinacidil activated K_{ATP} current between male and female cells, I measured the current elicited by a maximal concentration of pinacidil (500 μM). Figure 4.4A shows that currents were significantly higher in cells from female rats. To allow for possible differences in cell size, I also measured cell capacitance as described in the methods, section 2. Figure 4.4B shows that there was no significant difference between male and female rats with respect to cell capacitance. Current density was measured as pA/pF by dividing maximal current by cell capacitance and is shown in figure 4.4C. Current density was found to be 3.19 ± 0.40 pA/pF (n=16 cells from 3 animals) and 5.51 ± 0.65 pA/pF (n=.12 cells from 4 animals) for male and female myocytes respectively. These results show that maximal pinacidil-activated current density was significantly higher in female than male myocytes ($p<0.05$, unpaired Student's t-test).

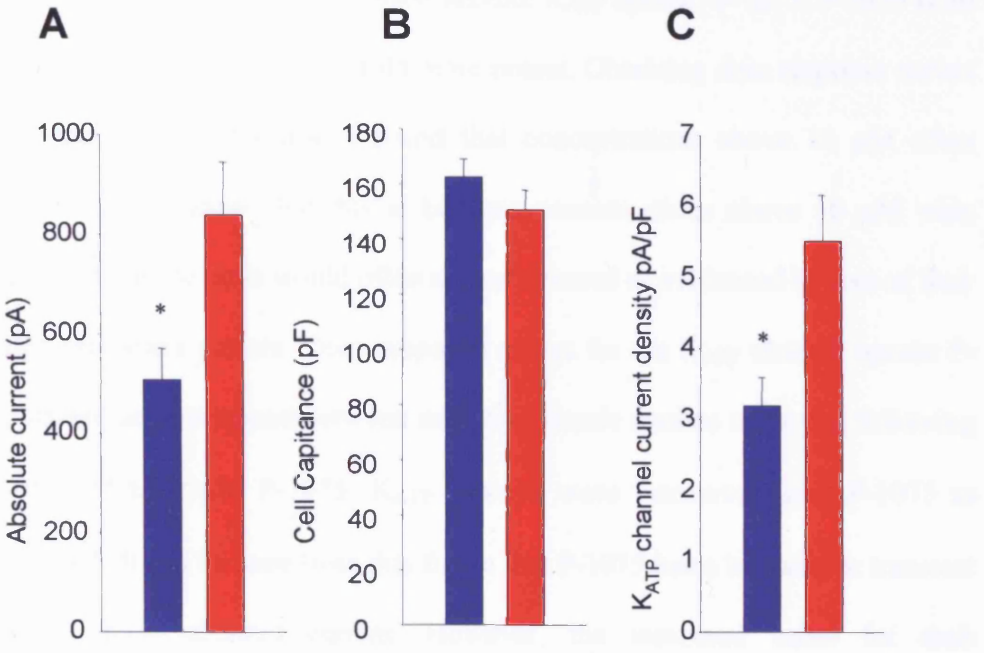

Figure 4.4 Maximal K_{ATP} current activated by pinacidil in myocytes from male and female rats.

A, Mean (± s.e.m.) whole-cell K_{ATP} current activated by 500 μM pinacidil in cells from male and female rats. In this figure and in B and C, the blue bar shows results for cells from male rats (n = 16 cells from 3 animals) and the red bar those from female rats (n = 12 cells from 3 animals). Current was measured at 0 mV using the protocol shown in Figure 4.1.* $p<0.05$

B, Mean membrane capacitance of cells from male and female rats.

C, Mean K_{ATP} current density (pA/pF) for current activated by 500 μM pinacidil in cells from male and female rats, * $p<0.05$.
Male ■ Female ■

4.3.2 K_{ATP} current activated by P-1075 in male and female myocytes

To confirm my finding with pinacidil, I used another K_{ATP} opener, P-1075. P-1075 is an analogue of pinacidil, but is around 10-fold more potent. Obtaining dose response curves using P-1075 was difficult because I found that concentrations above 10 μM often reduced the current. I suggest that this is because concentrations above 10 μM were poisonous to the cell as the cells would often appear stressed as evidenced by loss of their regular striated sarcomere pattern. Dose response curves for the K_{ATP} channel opener P-1075 were obtained and compared between male and female cardiac myocytes following application of 1μM to 20μM P-1075. K_{ATP} currents were measured using P-1075 as shown in figure 4.5. It can be seen from this figure that P-1075 has a biphasic or transient effect upon the K_{ATP} channel current. However, the measured value for each concentration of P-1075 was always taken as the maximum current evoked. A protocol was used where the cell was held continuously held at 0 mV to ensure that calcium channels were inactivated. Dose response curves were obtained by applying the following concentrations of P-1075: 1 μM, 3 μM, 10 μM, 20 μM (figure 4.5). Not every cell was exposed to all the concentrations of P-1075, because the myocytes often died if exposed to too many concentrations in succession. For example, figure 4.5 shows that that particular cell was exposed to only 1,3 and 10 μM P-1075. To isolate the K_{ATP} current, 10 μM glibenclamide was applied for two minutes following maximal K_{ATP} channel activation by 20 μM P-1075. Following application of each concentration of P-1075, there was an increase in current until a plateau was reached after approximately 4 minutes. The most substantial increase was observed following application of 10 and 20μM P-1075, at which concentrations the K_{ATP} current appeared maximal.

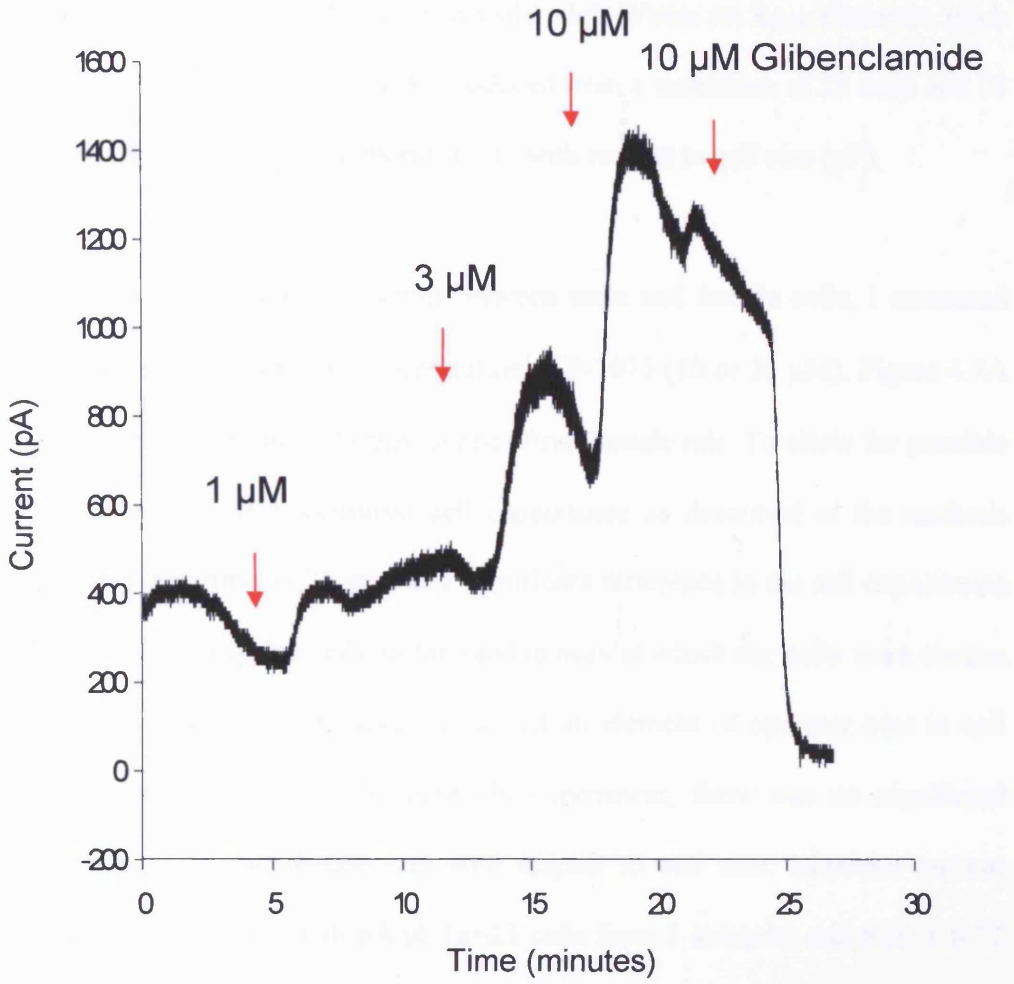

Figure 4.5 The effect of increasing P1075 concentration on K_{ATP} current

K_{ATP} currents were recorded at 0mV from a cardiac myocyte superfused with Tyrode solutions containing increasing concentrations of P1075 as indicated. Each solution was applied for 4 minutes and 10 µM glibenclamide was applied at the end of the experiment to obtain basal current level.

Figure 4.6 shows the mean current density (pA/pF) elicited by the different concentrations of P-1075 for both female and male adult Wistar rat K_{ATP} channels. Each point is the average maximum current (pA) produced from a maximum of 23 male and 18 female cells for a particular P-1075 concentration, with respect to cell size (pF).

To compare P-1075 activated K_{ATP} current between male and female cells, I measured the current in response to a maximal concentration of P-1075 (10 or 20 μM). Figure 4.7A show that current was significantly higher in cells from female rats. To allow for possible differences in cell size, I also measured cell capacitance as described in the methods section 2.6. In these experiments, there was a significant difference in the cell capacitance between the sexes. This was due only to the randomness at which the cells were chosen to be experimented upon and may have introduced an element of operator bias in cell size. Figure 4.7B show that as in the pinacidil experiment, there was no significant difference between male and female rats with respect to cell size. Maximal current density was found to be 6.09 ± 0.46 pA/pF (n=23 cells from 3 animals) and 8.06 ± 0.72 pA/pF (n= 18 cells from 3 animals) for male and female cells respectively ($p<0.05$, t-test) (figure 4.7C). Thus, as for pinacidil, P-1075 elicited a higher maximal K_{ATP} current density in female than in male myocytes.

4.3.3 K_{ATP} current activated by metabolic inhibition in male and female myocytes

To investigate whether the difference in K_{ATP} current was due to a gender difference in channel expression and not a pharmacological phenomenon, I used metabolic inhibition

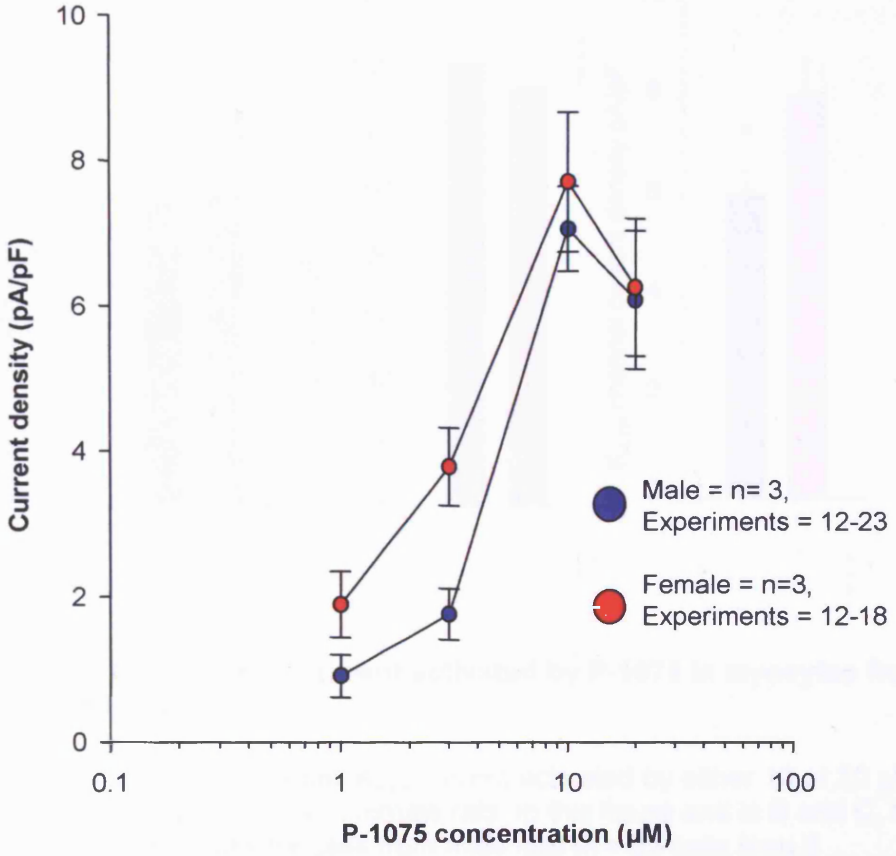

Figure 4.6 Dose-response curves for P-1075 activation of K_{ATP} current in myocytes from male and female rats.

The graph above shows the mean current elicited by different concentrations of P-1075 for both male and female cells (pA/pF).The points show current in myocytes from male (blue circles, n = 12-23 cells from 3 animals) and female (red circles, n = 12-18 cells from 3 animals) rats.

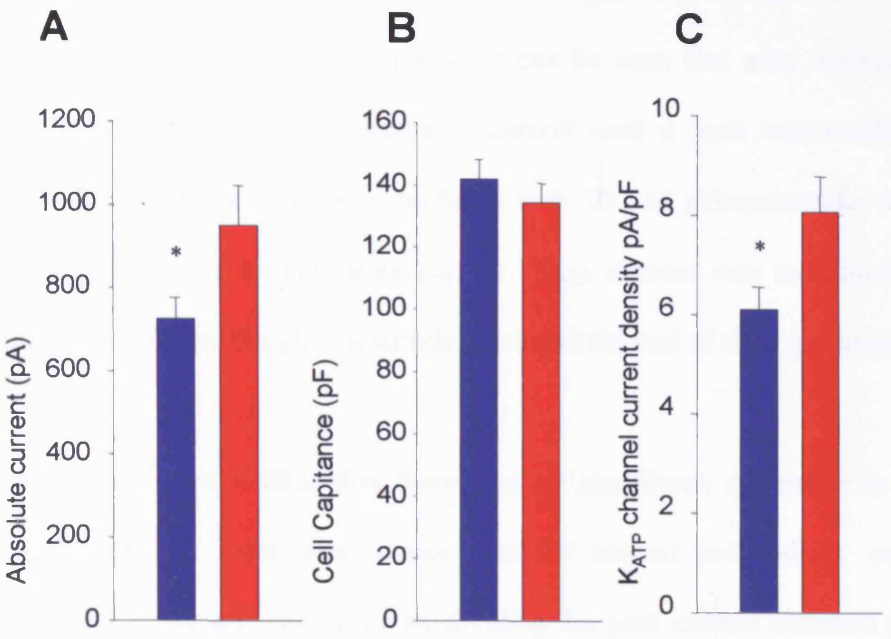

Figure 4.7 Maximal K_{ATP} current activated by P-1075 in myocytes from male and female rats.

A, Mean (± s.e.m.) whole-cell K_{ATP} current activated by either 10 or 20 μM P1075 in cells from male and female rats. In this figure and in B and C, the blue bar shows results for cells from male rats (n = 23 cells from 3 animals) and the red bar those from female rats (n = 18 cells from 3 animals) rats. Current was measured at 0 mV.* $p<0.05$

B, Mean membrane capacitance of cells from male and female rats.

C, Mean K_{ATP} current density (pA/pF) for current activated by either 10 or 20 μM P1075 in cells from male and female rats. (pA/pF), * $p<0.05$.
Male Female

with 2 mM NaCN and 1 mM iodoacetic acid (IAA) to elicit K_{ATP} current. K_{ATP} currents were measured using metabolic inhibition as shown in figure 4.8A. A protocol was used where the cell was held at 0 mV throughout. It can be seen that after application of metabolic inhibition, there was an increase in current until a peak was reached. The current then declined until the cell was perfused with 10 μM glibenclamide, at which point the current was seen to fall more rapidly. K_{ATP} current was measured as the maximal peak current minus the glibenclamide current at the end of the experiment.

It can be seen from figure 4.8Biii that there was no significant difference in current density (pA/pF) between male and female rats for current induced by metabolic inhibition. Current density was calculated by dividing the peak current obtained after the application of metabolic inhibition by the cell capacitance. Current density was found to be 29.82 ± 2.91 pA/pF (n=27 from 3 animals) and 26.83 ± 1.79 pA/pF (n=24 from 3 animals) for males and females respectively. This contrasts with the investigations using pinacidil and P-1075 into the differences in current density between males and females with respect to K_{ATP} current, where there was found to be a significant difference. There was also a much larger current elicited using metabolic inhibition compared to using pinacidil or P-1075; compare figures 4.4A and 4.7A to figure 4.8Bi.

4.3.4 Quantification of the cardiac K_{ATP} channel subunits Kir6.2 and SUR2A

A rapid real-time PCR assay was used to investigate whether there was a difference in the relative transcript abundance of the two genes that constitute the K_{ATP} channel (SUR2A and Kir6.2) between male and female rats. The housekeeping gene β-actin was used as an

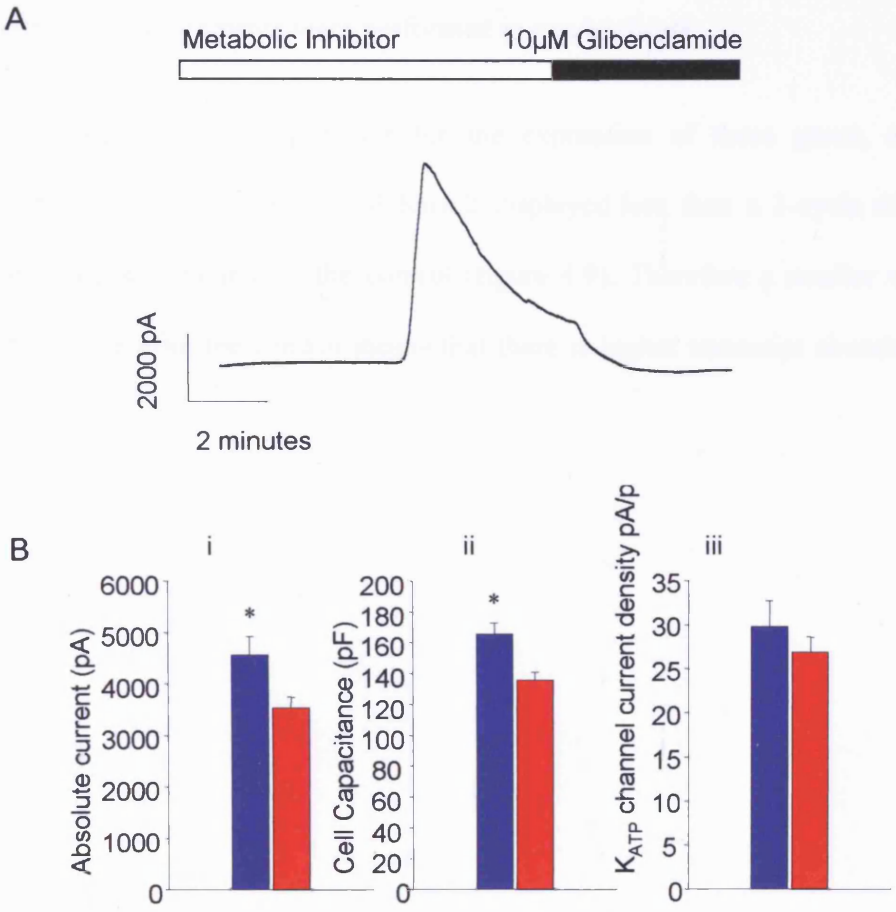

Figure 4.8 K_{ATP} current activated by metabolic inhibition in myocytes from male and female rats.

A, Recording of whole cell current from a male rat cardiac myocyte showing the effect of metabolic inhibition. MI Tyrode and glibenclamide (10 μM) were applied as indicated and the cell was held at 0 mV throughout.

Bi, Peak whole-cell K_{ATP} currents activated by metabolic inhibition in experiments like that of A above. In this figure, the blue bar shows mean (± s.e.m.) results for cells from male rats (n = 27 cells from 3 animals) and the red bars those from female rats (n = 24 cells from 3 animals). * $p<0.05$. ii, Membrane capacitance of cells from male and female rats.* $p<0.05$. iii, K_{ATP} current density (pA/pF) for current activated by metabolic inhibition in cells from male and female rats. Male ■ Female ■

internal control. Values were expressed as cycle difference from the housekeeping gene, beta-actin. All measurements were performed in quadriplicate.

Gender is not a determining factor for the expression of these genes, as both the investigated transcripts SUR2A and Kir6.2 displayed less than a 1-cycle difference in abundance when compared to the control (figure 4.9). Therefore a smaller value in the cycle difference from the control means that there is higher transcript abundance of that gene.

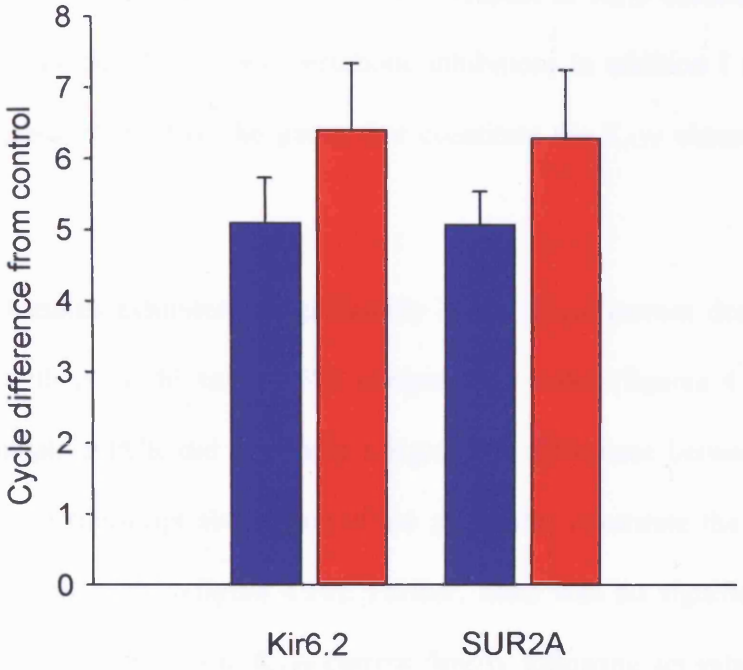

Figure 4.9 Quantitative analysis of genes that constitute the K_{ATP} channel between male and females

Figure shows the mean cycle difference from control (beta-Actin) of the genes that constitute the K_{ATP} channel, Kir6.2 and SUR2A for males and females. Male, n=3, experiments=4; Female, n=3, experiments=4. Male ■ Female ■

4.4 Discussion

Gender specific differences in K_{ATP} channel density have been linked to differences in cellular survival between the sexes (Ranki et al., 2001). Here I investigated whether there was a difference between the sexes in rats with respect to K_{ATP} channel density after application of pinacidil, P-1075 and metabolic inhibition. In addition I used QPCR to compare the transcript level of the genes that constitute the K_{ATP} channel; Kir6.2 and SUR2A.

I showed that females exhibited a significantly higher K_{ATP} current density following application of both pinacidil and P-1075 compared to males (figures 4.4C and 4.7C). However, quantitative PCR did not show a significant difference between the genders with respect to the transcript abundance of the genes that constitute the K_{ATP} channel, namely SUR2A and Kir6.2 (figure 4.10). Further, there was no significant difference between the sexes with respect to K_{ATP} current density following activation of the K_{ATP} channels by metabolic inhibition (figure 4.8Biii).

Numerous studies have shown that pre-menopausal women have a lower incidence of cardiovascular disease compared to age matched men. The cellular mechanisms responsible for the sex differences in the susceptibility of the heart to ischaemia and reperfusion injury have not been elucidated. However, recent evidence has suggested the involvement of the sarcolemmal K_{ATP} channel in this protective phenomenon difference between the sexes. This is based on studies where it has been found that the protein expression of sarcolemmal K_{ATP} channel subunits Kir6.2 and SUR2a is greater in hearts from females (Johnson et al., 2006). It has also been shown that application of an

oestrogen derivative, 17β-oestradiol, to heart-derived H9c2 cells results in an increased expression of Kir6.2 and SUR2A as well as an increased resistance to hypoxia-induced calcium overload (Ranki et al., 2002). Other studies have also suggested there to be a significant difference in K_{ATP} channel density between male and females, which is linked to their cellular survival during metabolic stress (Ranki et al., 2001). Ranki et al., (2001) found K_{ATP} channel currents in female guinea-pig cardiac myocytes to be approximately 5 pA/pF whereas those from male were 2 pA/pF. Infarct size has also been shown to be significantly smaller in female hearts compared to male following ischaemia/reperfusion (Johnson et al., 2006). The administration of the sarcolemmal K_{ATP} channel blocker HMR1098 abolished this difference suggesting that the sarcolemmal K_{ATP} has a central protective role in ischaemia/reperfusion injury. This could partly explain gender-specific differences in susceptibility to heart disease and certain arrhythmias. Therefore for therapeutic reasons with respect to heart disease, investigations into the role of the K_{ATP} channel in cellular survival are very important.

Here I have investigated the differences in K_{ATP} channel density and characteristics between males and females using both electrophysiological and molecular biological techniques. In this study, Q-PCR analysis demonstrated there to be no gender specific differences in the levels of SUR2A and Kir6.2 mRNA. However, post-translational effects could result in higher levels of functional K_{ATP} subunits. Therefore, to test the hypothesis that more K_{ATP} channels are present in the sarcolemma of female cardiac myocytes as opposed to male cells, I measured the K_{ATP} current density directly using pinacidil, P-1075 and metabolic inhibition with iodoacetic acid and sodium cyanide. Investigations into K_{ATP} channel density using pinacidil found there to be a significantly

higher current density in female myocytes than in male cells (figure 4.4C). This is in direct agreement with Ranki et al., (2001) and suggested the presence of more functional cardiac K_{ATP} channels in female cardiac myocytes as opposed to male cells. The apparent discrepancy between the results obtained with a Q-PCR methodology (no differences in the mRNA levels of SUR2A and Kir6.2) and electrophysiology (differences in the current from functional K_{ATP} channels) could be explained by the fact that Q-PCR measured levels of total SUR2A and Kir6.2 mRNA, while patch clamp electrophysiology, measured levels of only those functional channels consisting of SUR2A and Kir6.2 subunits.

Due to the discrepancy between the Q-PCR and electrophysiological investigations, I again investigated whether there was a gender specific difference with respect to K_{ATP} channel density using other methods of opening the K_{ATP} channel; P-1075 and metabolic inhibition. This was also to demonstrate that I was indeed measuring the current elicited from all available K_{ATP} channels and not a submaximal population. The application of P-1075 to both male and female cells resulted in a significantly higher current density in female cells compared to male, whereas there was no significant gender specific difference with respect to K_{ATP} channel density when metabolic inhibition was used to elicit the K_{ATP} current. It was clearly evident that the application of P-1075 resulted in a slightly higher current than that elicited by pinacidil (compare figure 4.7A to figure 4.4A). However, the K_{ATP} current produced through application of metabolic inhibition to cardiac myocytes resulted in a much larger current than that seen with either pinacidil or P-1075 (compare figure 4.8Bi to figures 4.4A and 4.7A).

It can be seen that the whole cell experiments using pinacidil were performed using a pulsing to 0 mV protocol. However, the experiments with P-1075 and metabolic inhibition used a holding at 0 mV protocol. There is no explanation for the implementation of the different protocols. It could be suggested that the differences in the sarcolemmal K_{ATP} channel density could be related to the protocol used, as holding the myocyte at 0 mV could be considered more stressful for the cell as it is being held for a long period of time at a considerably more depolarised potential than it would be at rest (-70 mV). As previously mentioned in chapter 1, depolarisation of the cell membrane potential leads to an increased drive of calcium into the cell via the Na^{+}-Ca^{2+} exchanger. The increase in intracellular calcium could lead to an associated drive of calcium into the mitochondria due to the mitochondria's strongly hyperpolarised potential, which theoretically could uncouple the mitochondria preventing the production of ATP by the F0/F1 ATP synthase. It could therefore be suggested that more sarcolemmal K_{ATP} channels would open due to decreased availability of ATP, as the cell retaliates to try and combat the depolarisation by hyperpolarising the membrane potential. This would be in contrast to using a pulsing to 0 mV protocol, as the cell would spend the majority of the experiment clamped towards its resting membrane potential of approximately -70 mV. This is not surprising as it can be seen that during metabolic inhibition there was an increase in the sarcolemmal K_{ATP} channel density for both males and females compared to pharmacological activation. However, even under these stressful conditions, where the cell appears to be showing a metabolic as well as pharmacological effect, the application of P-1075 still resulted in a difference in K_{ATP} channel density between the sexes, similar to that seen with pinacidil. Interestingly, P-1075 appeared to have a biphasic or transient

effect upon the K_{ATP} current. However, there still was a higher female sarcolemmal K_{ATP} channel density compared to males under the same conditions, indicating that in any case female cells open more sarcolemmal K_{ATP} channels under stress compared to males. As already discussed this could be protective by reducing calcium influx via the Na^{+}-Ca^{2+} exchanger.

I suggest that the differences in the sarcolemmal K_{ATP} channel density observed between the sexes, is probably due to sarcolemmal K_{ATP} channel independent effects of the drugs used to open the channels. For instance, the metabolic inhibitor used in these experiments consisted of cyanide and iodoacetic acid. Cyanide inhibits oxidative metabolism and iodoacetic acid inhibits glycolytic metabolism. Pinacidil at a concentration of 100 μM has been found to accelerate state-four respiration, resulting in a decreased mitochondrial membrane potential, thereby acting like an uncoupler (Hanley & Daut, 2005). Similarly, glibenclamide has been found to reduce the rate of fatty acid oxidation by inhibiting carnitine palmitoyltransferase, block ABC transporters and chloride channels (Hanley & Daut, 2005). Therefore experiments using solely pharmacological methods for assessing the function of the sarcolemmal K_{ATP} channel are not reliable as these drugs clearly affect other cellular sites than this channel.

Conclusion and significance

In conclusion, I found no significant difference between the genders with respect to the mRNA levels of the subunits that constitute the sarcolemmal K_{ATP}, Kir6.2 and SUR2A. However, this does not mean that there is no gender specific difference at the level of the functional channel. Consequently any gender specific differences with respect to

sarcolemmal K_{ATP} channel density might be found using electrophysiological techniques. The application of pinacidil and P-1075 to male and female cells to elicit the sarcolemmal K_{ATP} current resulted in a significantly higher sarcolemmal K_{ATP} current density in female compared to male cells. However, the application of metabolic inhibition to the cells resulted in no significant difference with respect to the sarcolemmal K_{ATP} current density between the genders. Interestingly, there was also no consistency with respect to the amount of current elicited by either pinacidil, P-1075 or metabolic inhibition, suggesting that the current elicited was pathway specific. In particular, currents elicited by MI were much greater than those seen using the pharmacological openers. This makes it clear that even maximal concentrations of sarcolemmal K_{ATP} channel openers do not activate all the sarcolemmal K_{ATP} channels, and questions the use of these openers for assessing relative density of functional channels.

However, although no difference was found between the sexes with respect to the sarcolemmal K_{ATP} channel density in the presence of metabolic inhibition, there may still be sex-specific differences in the activity of the sarcolemmal K_{ATP} single channel. For instance, sarcolemmal K_{ATP} channels could open earlier in females than males that would be undetectable using whole cell electrophysiological techniques. The earlier opening of the K_{ATP} channels could have the effect of hyperpolarising the membrane potential enough to prevent a significant drive of calcium into the cell via the Na^{+}-Ca^{2+} exchanger. Although there may not be a substantial number of single sarcolemmal K_{ATP} channels opening, there may be enough to prevent or delay the increase in intracellular calcium via the Na^{+}-Ca^{2+} exchanger. This could explain why rigor occurred later in females than males upon application of metabolic inhibiton, (figure 3.2) as the calcium load required

in conjunction with high ATP to cause rigor would have required a longer period of time to accumulate. In addition the mean open time of the sarcolemmal K_{ATP} channel may also be longer in females than males, also resulting in the same effect. Therefore in chapter 5, I investigated the kinetics of the sarcolemmal K_{ATP} channel from both males and females.

CHAPTER 5

SINGLE CHANNEL ANALYSIS OF K_{ATP} BEHAVIOUR OF MALE AND FEMALE MYOCYTES

Chapter 5 Single channel analysis of K_{ATP} behaviour of male and female myocytes

5.1 Introduction

The previous results chapters have shown that differences exist between males and females with respect to cellular survival and calcium handling following MI. It has been suggested that the increased female cellular survival following MI reperfusion injury was due to a higher K_{ATP} current density (Ranki et al., 2001). The results presented in chapter 4 are contradictory regarding whether there is a difference in K_{ATP} current density between the sexes. Whole cell experiments, which used pinacidil and P-1075 to activate the K_{ATP} channels, showed that females had a significantly higher K_{ATP} current density than males (figures 4.4C and 4.7C). In contrast, whole cell experiments where metabolic inhibition was used to elicit the K_{ATP} current showed that there was no significant difference between males and females with respect to the K_{ATP} current density (figure 4.8iii). Therefore I investigated whether the differences in cellular survival between the sexes could be due to differences in K_{ATP} channel characteristics. I investigated possible differences in K_{ATP} channel conductance, time to activation and the number of channels activated by MI. I also compared open and closed time distributions between K_{ATP} channels from male and female rats.

5.2 Methods

5.2.1 Isolation of cardiac myocytes

Ventricular myocytes were dissociated from the animals as described in chapter 2.

5.2.2 Solutions

Isolated ventricular myocytes were superfused with normal Tyrode's, the composition of which is described in chapter 2. Metabolic inhibition was induced by superfusing the cells with metabolic inhibition (MI) Tyrode's, which contained 2 mM NaCN and 1 mM iodoacetic acid (IAA) in substrate-free Tyrode's, the composition of which is described in chapter 2.

Single channel currents were recorded from cardiac myocytes using the cell-attached patch clamp configuration as described in chapter 2. Patch pipettes were filled with a solution containing (in mm): KCl 140, $MgCl_2$ 2, HEPES 10, $CaCl_2$ 2 at pH 7.2 and had a resistance of 5-10 MΩ .Voltage was controlled and membrane currents recorded using an Axopatch 200B amplifier (Axon Instruments). Currents were filtered at 2 kHz and analogue signals were collected and digitised at 10 kHz using a Digidata 1200 Series interface. Records were acquired and analysed using either pClamp 8 (Axon) or custom software, Excel 2000 (Microsoft) and SigmaPlot 8.0 (SPSS). All experiments were carried out at 34 ± 2 °C.

5.2.3 Analysis

Data are represented as mean ± S.E.M and values of n refer to the number of patched cells examined as indicated in the text or figure legends. Mean values obtained were compared by the paired or unpaired Student t test where appropriate. Values where $p<0.05$ were considered statistically significant.

5.2.4 Single channel kinetics

Channel openings and closings were detected using the half amplitude threshold crossing method of Colquhoun & Sigworth (1983). When a record crossed the 50% threshold between the open and closed levels of a single channel, then an event was said to have occured. Linear regressions were fit between the data points which spanned the threshold and the duration of an event was estimated from the times when the regressions cut the threshold (Davies et al., 1992). More accurate than evaluating durations as integer data points, linear regressions were used as they allow durations to be measured as fractions of data points and are suggested to not lead to the over-estimation of the durations of brief events unlike the former method (Davies et al., 1992).

5.2.5 Minimum resolution

A minimum resolution of 100 μs was imposed on the data. This value was chosen because it was in excess of the dead time (90 μs), which is 0.538 times the filter rise time (Colquhoun & Sigworth, 1983). A minimum resolution was necessary as it allowed the false events (i.e. those events that could not have been accurately detected by the

recording system) to be excluded from the fit (Davies et al., 1992). Consequently open times of less than the minimum resolution were considered as part of a long closure.

5.2.6 Missed closed events

Following examination of the records and of the closed time distributions of K_{ATP} channels it appears that there are many brief closed events, which are too short to be detected (Davies et al., 1992). Therefore the measured open times are an over estimation as they do not allow for these brief closing events. Consequently an estimation of the real mean open time was calculated by multiplying the measured mean open time by the proportion of closed events detected. The latter value was calculated by integrating the fitted closed time distribution between the minimum resolution of 100 μs and infinity (Davies et al., 1992).

5.3 Results

5.3.1 Gender specific differences in sarcolemmal K_{ATP} channel kinetics

I investigated whether there were differences in the sarcolemmal K_{ATP} channel conductance, the time taken for the channel to open following metabolic inhibition (MI) and the number of channels activated by MI. Although no difference was found between the sexes with respect to the K_{ATP} channel density in the presence of metabolic inhibition (chapter 4), there may still be sex-specific differences in the activity of the sarcolemmal K_{ATP} single channel. I suggest that sarcolemmal K_{ATP} channels could open earlier in females than males that would be undetectable using whole cell electrophysiological techniques. The earlier opening of the sarcolemmal K_{ATP} channels could have the effect of preventing or delaying a significant drive of calcium into the cell via the Na^{+}-Ca^{2+} exchanger by hyperpolarising the membrane potential. This could explain why rigor occurred later in females than males upon application of metabolic inhibition, (figure 3.2) as the calcium load required in conjunction with high ATP to cause rigor would have required a longer period of time to accumulate. In addition the mean open time of the K_{ATP} channel may also be longer in females than males, also resulting in the same effect. Therefore in chapter 5 I investigated the kinetics of the sarcolemmal K_{ATP} channel from both males and females.

It is possible that differences in these components of the sarcolemmal K_{ATP} channel could account for there being no difference between males and females with respect to

sarcolemmal K_{ATP} channel density following metabolic inhibition but that a significantly higher percentage of female cells survive metabolic inhibition compared to males.

5.3.2 K_{ATP} single channel conductance

To measure differences in sarcolemmal K_{ATP} single channel conductance, cell attached patches were obtained with the pipette solution containing 140mM KCl, 2mM $MgCl_2$, 2mM $CaCl_2$ and 10mM HEPES. The bath was perfused with MI-Tyrode's to open the K_{ATP} channels, from which single channel current-voltage relationships were constructed. I measured the single channel conductance of the K_{ATP} channels by applying ramp voltages to cell-attached patches as shown in Figure 5.1. The relation was obtained from the ensemble average of the open-channel current measured in response to 100 ramps in which the voltage applied to the pipette was ramped from +60 to −160 mV over 100ms Since the resting potential of these cells is around −70 mV, the effective voltage change across the patch will be from about −130 to +90 mV. Figure 5.1A, shows the voltage ramp used to measure the single channel current-voltage relation. Figure 5.1B shows an example of a current trace recorded in response to the ramp. Channel openings can be seen early in the ramp and as the voltage passes the reversal potential. To subtract leak and capacity currents, sections of traces where no channels were open were averaged to produce the average leak trace shown in figure 5.1C. This average leak trace was then subtracted from all individual traces. Figure 5.1D shows the trace of figure 5.1B after subtraction of the leak. After subtraction, sections of traces where channels were open were averaged to produce the average single channel current during the ramp, this

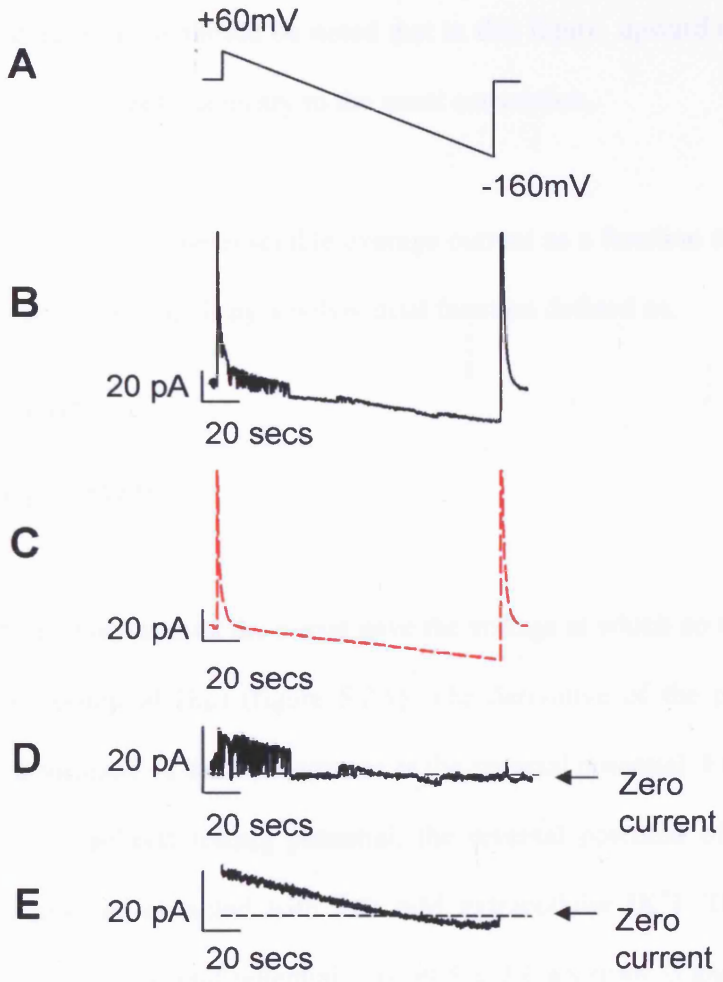

Figure 5.1 Single channel currents recorded in response to voltage ramps in cell-attached patches

A, Cell attached patches were obtained in symmetrical 140mM K^+ solution. K_{ATP} channel activity was evoked by perfusing the cells with MI solution. Once K_{ATP} channels were evoked, voltage ramps from +60 mV to –160 mV were applied to cell-attached patches.

B, Recording of current in response to a voltage ramp.

C, Ensemble average leakage trace obtained by averaging regions from those of B without channel openings.

D, The recording of B after subtraction of the leakage trace.

E, Ensemble average single-channel current obtained by averaging regions of 100 traces like those of D where a channel was open. The relation was obtained from the ensemble average of the open.

average is shown in figure 5.1E. It should be noted that in this figure, upward deflection in current represent inward currents, contrary to the usual convention.

Figure 5.2A shows an example of the ensemble average current as a function of voltage. The ensemble average obtained was fit by a polynomial function defined as:

$$\mathbf{Y = a + bx + cx^2 + dx^3 + ex^4}$$

Where *a*,*b*,*c*,*d* and *e* are constants.

The point where the fitted line crossed the x-axis gave the voltage at which no net current flowed i.e. the reversal potential (E_R) (figure 5.2A). The derivative of the polynomial function was used as a measure of the conductance at the reversal potential. Figure 5.2A shows that, allowing for the cell resting potential, the reversal potential of the K_{ATP} current is close to 0 mV, as expected with 140 mM extracellular [K^+]. The unitary conductance measured at the reversal potential was 99.5 ± 2.6 pS (n=8, 3 animals) and 93.3 ± 3.8 pS (n=7, 3 animals) for males and females respectively, characteristic of the cardiac sarcolemmal K_{ATP} channel (figure 5.2B). There was no significant difference between the genders with respect to the single channel conductance.

5.3.3 Time to activation and number of channels activated

The time to activation of the K_{ATP} channels in response to metabolic inhibition was investigated in cell attached patches held at +40 mV with 140 mM K^+ in the pipette solution. Figure 5.3A shows a recording of K_{ATP} channel openings in response to the application of MI. The times at which the channels activated were measured from the

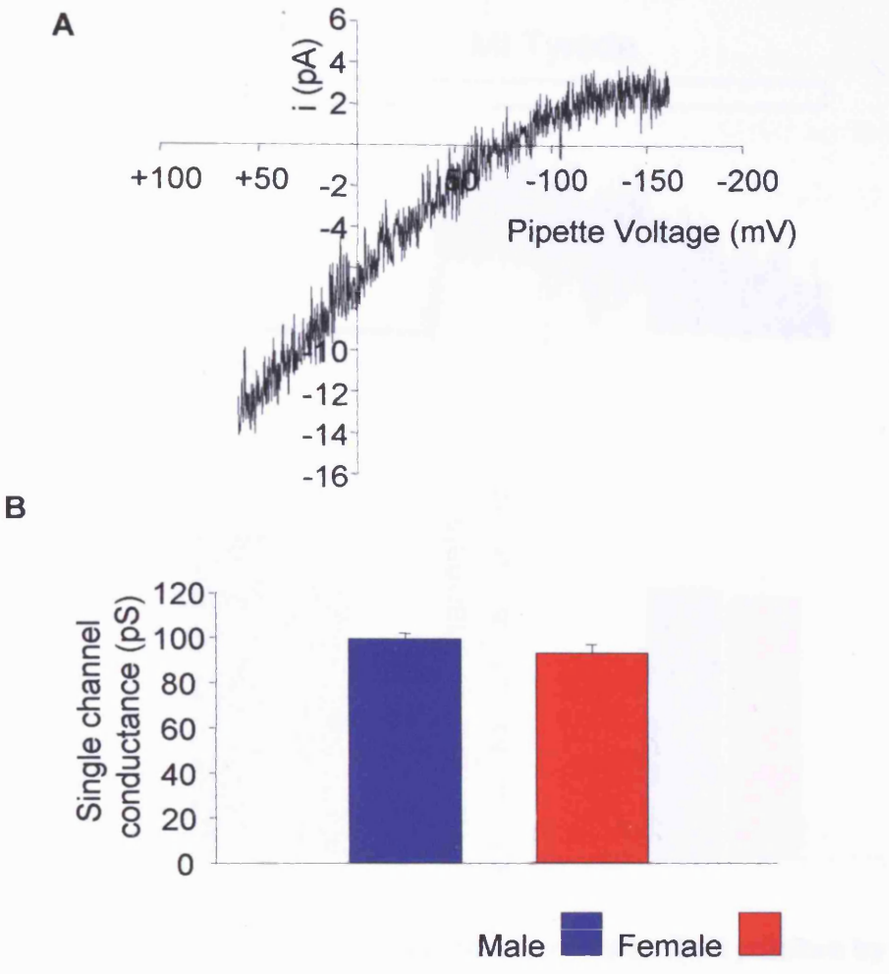

Figure 5.2 Single channel current voltage relation and conductance for the K_{ATP} channels activated by MI Tyrode.

A, The i/V relation obtained from the ensemble average of the open-channel current measured in response to 100 ramps in which the voltage applied to the pipette was ramped from +60 to −160 mV (Fig.5.1A). The relation was fitted with a polynomial function and its derivative was used to calculate the slope conductance at the reversal potential.

B, Mean unitary conductance for males (n=8, 3 animals) and females (n=7, 3 animals) respectively.

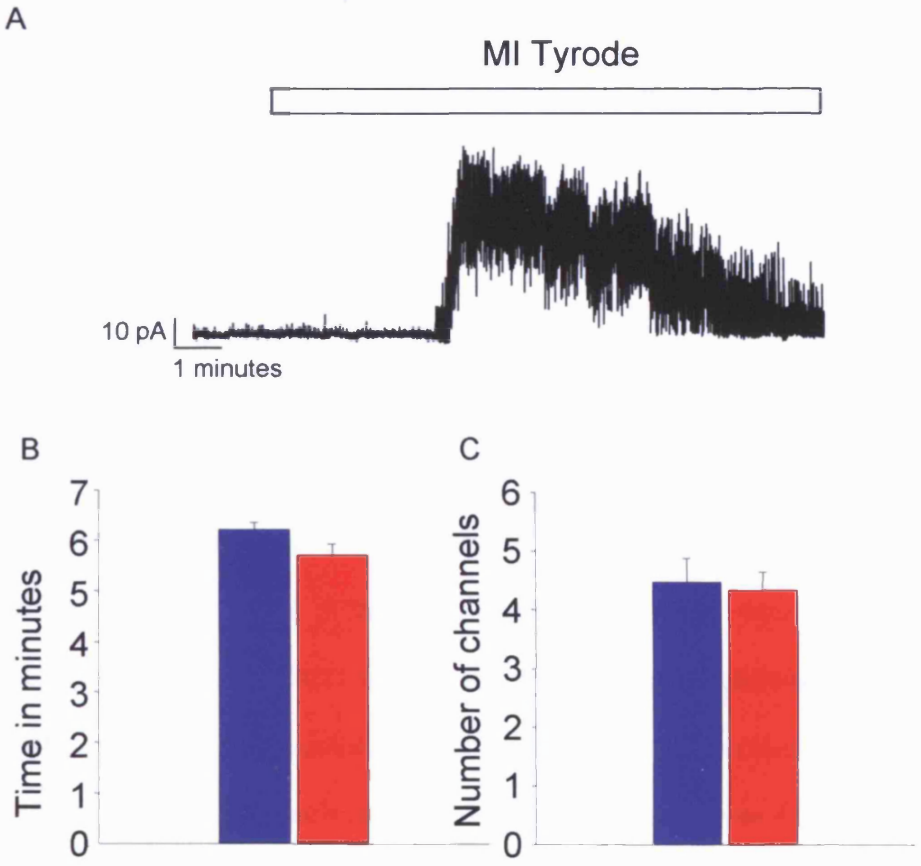

Figure 5.3 Activation of K_{ATP} channels in cell-attached patches by metabolic inhibition

A, Recording of current from a cell-attached patch on a cardiac myocyte from a male rat showing the effect of metabolic inhibition, applied in the solution superfusing the rest of the cell.

B, Mean time from application of metabolic inhibition to K_{ATP} channel activation. In this figure and in figure C below, the blue bar shows results for cells from male rats (n = 17 cells from 3 animals) and the red bar those from female rats (n = 30 cells from 3 animals) . Male Female

C, Mean maximal number of K_{ATP} channels activated by metabolic inhibition in cells from male and female rats.
Male Female

time of the first burst of openings of a K_{ATP} channel. The data shown in figure 5.3B show that there is no significant difference between cells from males and females with respect to the time to K_{ATP} channel activation. The mean time to single channel activation for males and females was 6.2 ± 0.2 minutes (n=17, animals=3) and 5.7 ± 0.2 minutes (n=30, animals=3) respectively.

The maximum number of K_{ATP} channels activated by MI-Tyrode's in cell attached patches was measured by dividing the peak current by the single channel current. Single channel current was measured at the beginning of the recording as current often fell during recording due to changes in the cell's membrane potential, most likely due to stress. Figure 5.3C shows that there was no significant difference between males and females with respect to the maximum number of simultaneously active channels per patch. The mean number of channels activated for male and females was 4.5 ± 0.4 (n=17, animals=3) and 4.3 ± 0.3 (n=30, animals=3) respectively.

5.3.4 Open and closed time distributions

To investigate possible changes in open and closed time distributions, these parameters were measured at the beginning and at the end of cell attached experiments where the channels were opened using MI. Distributions of open and closed times were obtained from sections of recordings where only one channel was open. The current records were used to obtain an idealized trace showing the transitions between the open and closed levels as described in section 5.1. Data, together with the idealized trace, were displayed in segments, and a decision made to accept or reject the idealized trace or to reset the

threshold. This was to allow for and consequently compensate for any changes in the baseline due to drift, sections of the recording which contained anomalities or multiple channel openings. Open and closed times were binned according to the method of Sigworth and Sine (1987) after imposition of a minimum resolution.

I calculated weighted mean values for the parameters of the fitted distributions by weighting the values from each patch in proportion to the total number of events recorded from that patch (Davies et al., 1992). I calculated the weighted variance as:

$$\sigma^2 = \frac{\sum (x_i - x_w)^2 w_i}{N-1}$$

Where w_i is the weight for the ith patch, and so the standard deviation and standard error of the mean.

To investigate possible changes in the open time distributions for a K_{ATP} channel from a male and female rat over the course of an experiment where the K_{ATP} channel was opened by MI, open time distributions were calculated both before and after maximum activation of the K_{ATP} channels. Closed time distributions were not compared between males and females as the information required to perform these analyses was not available. Figures 5.4 and 5.5 show that these open time distributions were similar for both male and female rats. Figure 5.6 shows an example of the distributions of closed times for a male cardiac myocyte. Figure 5.7 shows by way of stability plots, changes in the mean open and

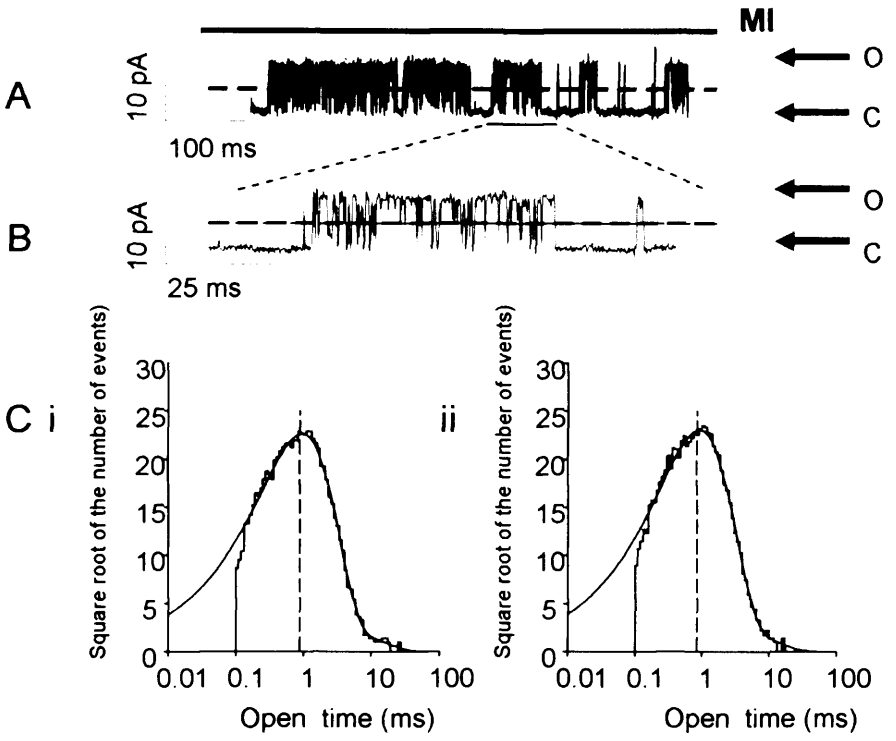

Figure 5.4, Example of K_{ATP} channel activity, recorded from a cell-attached patch of a male cardiac ventricular myocyte.

A, Example segment of recording of single channel activity in a patch on a male myocyte. The trace has been filtered at 2kHz for display and the trace below (B) show the portion of the above trace indicated by the line at an expanded time scale. The holding potential was +40 mV, the patch pipette contained 140 mM K^+ and the bathing solution contained 5 mM K^+. O, open level; C, closed level.

C, Histograms of open time distributions of a K_{ATP} channel obtained under the same conditions as in A. Ci, shows the histogram of open time distributions of a K_{ATP} channel recorded from when the K_{ATP} channels began to open until a second level of K_{ATP} channels were observed. Two exponential components were required to fit the open times distributions. The fitted line is drawn to the sum of two exponential components with normalised area and time constants of a1=0.99; t1=0.95; a2=0.01; t2=4.6. Mean open time=0.96; Corrected mean open time=0.87. Cii, shows the histogram of open time distributions recorded from the same K_{ATP} channel as in Ci, except the recording occurred after maximal opening of the K_{ATP} channels was observed. Two exponential components were required to fit the open times distributions. The fitted line is drawn to the sum of two exponential components with normalised area and time constants of a1=0.99; t1=0.93; a2=0.01; t2=3.72. Mean open time=0.96; Corrected mean open time=0.85.

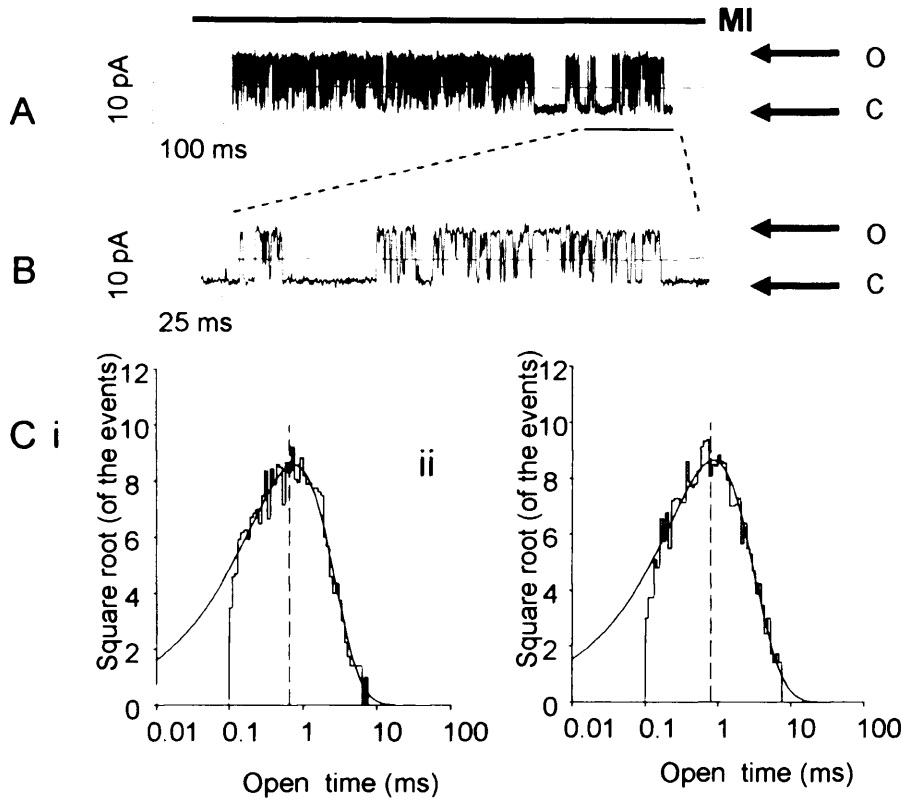

Figure 5.5, Example of K_{ATP} channel activity, recorded from a cell-attached patch of a female cardiac ventricular myocyte.

A, Example segment of recording of single channel activity in a patch on a female myocyte. The recording conditions were the same as those in figure 5.4. The traces have been filtered at 2kHz for display and the trace below (B) show the portion of the above trace as indicated by the line at an expanded time scale. O, open level; C, closed level.

C, Histograms of open time distributions of a K_{ATP} channel obtained under the same conditions as in A. Ci, shows the histogram of open time distributions of a K_{ATP} channel recorded from when the K_{ATP} channels began to open until a second level of K_{ATP} channels were observed. The fitted line is drawn to the sum of two exponential components with normalised area and time constants of a1=0.95; t1=0.74; a2=0.05; t2=1.21. Mean open time=0.75; Corrected mean open time=0.66. Cii, shows the histogram of open time distributions recorded from the same K_{ATP} channel as in Ci, except the recording occurred after maximal opening of the K_{ATP} channels was observed. Two exponential components were required to fit the open times distributions. The fitted line is drawn to the sum of two exponential components with normalised area and time constants of a1=0.79; t1=0.80; a2=0.21; t2=1.314. Mean open time=0.90; Corrected mean open time=0.80.

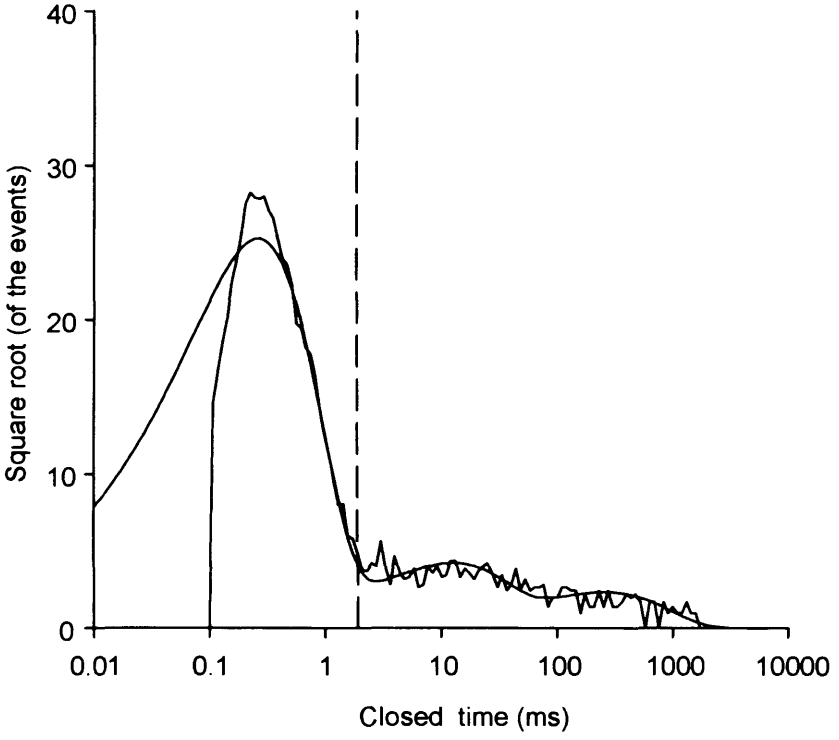

Figure 5.6, Closed time distribution measured from a male cardiac myocyte

A, Histogram of closed time distribution of a K_{ATP} channel obtained under the same conditions as in figure 5.4A. Three exponential components were required to fit the closed times distribution. The fitted line is drawn to the sum of three exponential components with normalised area and time constants of a1=0.97; t1=0.27; a2=0.03; t2=12.21; a3=0.01; t3=256.47. Mean closed time=2.71; Corrected mean closed time=1.90. The dashed line shows the corrected mean closed time.

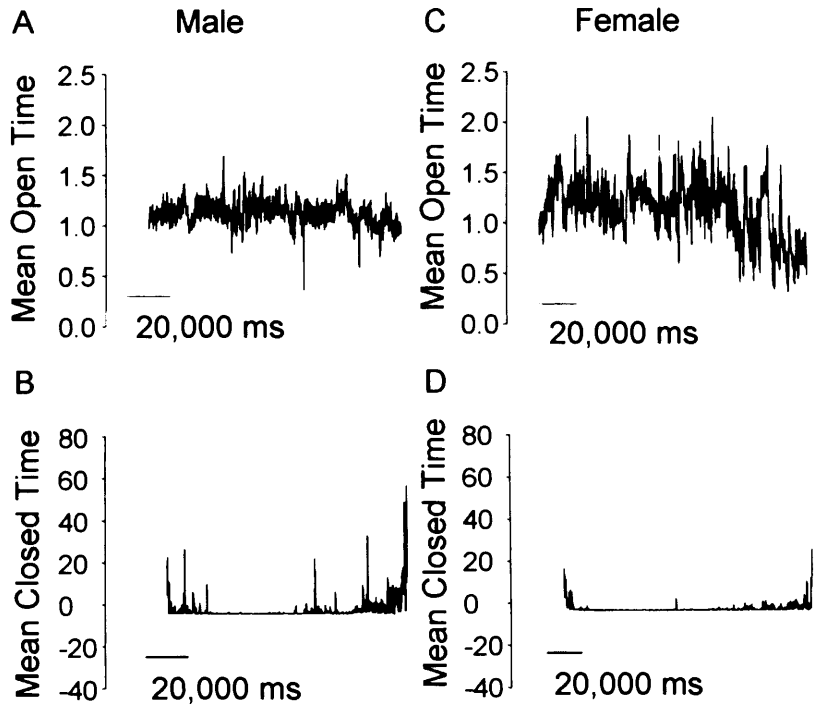

Figure 5.7, Stability plots for mean open and closed times in patches from male and female myocytes

A,Trace shows the changes in mean open time (ms) over the course a single channel experiment, where cell attached patches were performed and the K_{ATP} channels were opened by MI in a male cardiac myocyte. Trace B shows the changes in mean closed time over the same experiment. Trace C and D show the same as traces A and B respectively, except that the experiments were performed in a female cardiac myocyte.The holding potential in both experiments was +40 mV, the patch pipette contained 140 mM K^+ and the bathing solution contained 5 mM K^+.

closed times over the course of an entire MI experiment where only one K_{ATP} channel was opened, from when the K_{ATP} channel begins to open to the end of the recording. The stability plots were calculated by averaging the open and closed times over a 500 event period, then moving the window by one event to re calculate. It can be seen from figure 5.7 that there is little variation in the mean open time distribution over the course of an MI experiment, therefore suggesting that any difference between the sexes with respect to Popen is due to differences in the mean closed times. Figure 5.8 show the changes in the mean open times for K_{ATP} channels opened by MI for both male and female rats, before and after maximal activation of the K_{ATP} channel. It can be seen that there was no difference with respect to the weighted mean open times before maximal activation of the K_{ATP} channels by MI, compared to at the end of the experiment.

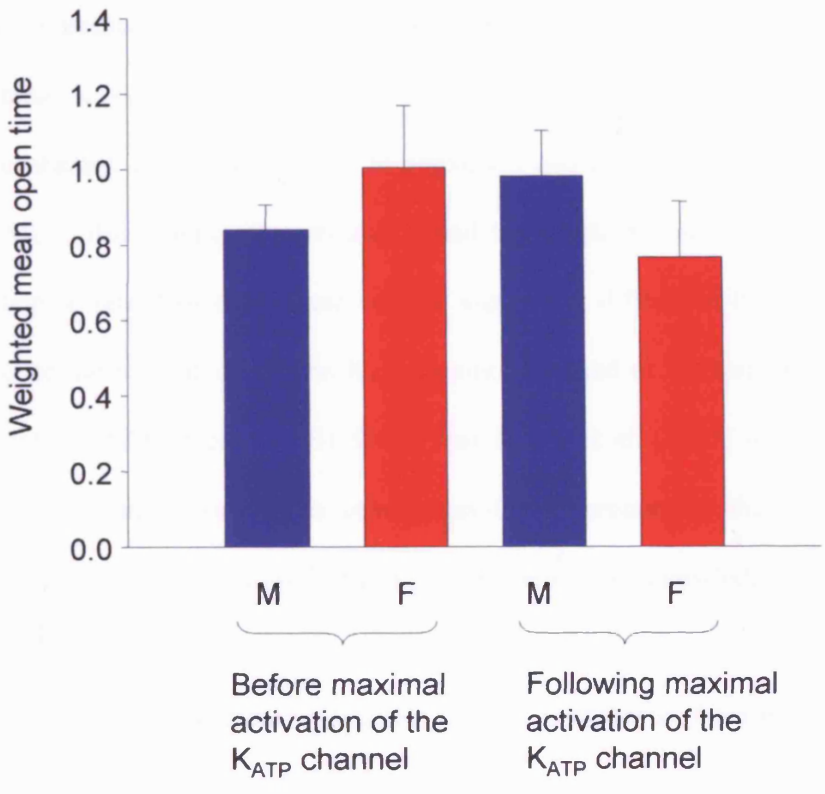

Figure 5.8 Weighted mean open times for male and female K_{ATP} channels

Times were calculated when the channel begins to open and after maximal channel activation.The mean open time was weighted with respect to the number of events measured per patch.
Male Female

5.4 Discussion

Gender specific differences in sarcolemmal K_{ATP} channel density have been linked to differences in cellular survival between the sexes (Ranki, 2001). Here I investigated whether the differences in cellular survival between the sexes could be due to differences in sarcolemmal K_{ATP} channel characteristics. I investigated differences in sarcolemmal K_{ATP} single channel conductance, time to activation and number of channels activated following MI. I also compared open and closed time distributions between cells from male and female rats. However, there was no significant difference between the sexes with respect to the time at which the K_{ATP} channels opened or the number that opened upon application of MI (figure 5.3B). Other than Ranki et al. (2001) this is the second report to suggest that there are no gender-specific differences in the single channel characteristics of the cardiac sarcolemmal K_{ATP} channels to my knowledge.

Comparison of the single channel conductance between myocytes from male and female rats

To investigate the single channel conductance between male and female sarcolemmal K_{ATP} channels, i/V curves were constructed from the current produced in response to 100 ramps in which the voltage applied to the pipette was ramped from +60 to −160 mV. The unitary conductances measured at the reversal potential and were 99.5 ± 2.6 pS (n=8, animals=3) and 93.3 ± 3.8 pS (n=7, experiments=3) for males and females respectively, characteristic of the cardiac sarcolemmal K_{ATP} channel (figure 5.2). There was no significant difference between the sexes with respect to the single channel conductance.

Further, I investigated whether there were differences between male and females with respect to the time at which the sarcolemmal K_{ATP} channels opened and the number of channels activated following MI. The time to activation of sarcolemmal K_{ATP} channels in response to metabolic inhibition was investigated in cell-attached patches. Times to single channel activation for males and females were 6.2 ± 0.2 minutes (n=17, animals=3) and 5.7 ± 0.2 minutes (n=30, animals=3) respectively. I found that there was no significant difference between male and females regarding the time at which the sarcolemmal K_{ATP} channel opened; 4.5 ± 0.4 (n=17, animals=3) and 4.3 ± 0.3 (n=30, animals=3) respectively (figure 5.3B).

Comparison of the open time distributions between male and females

Open time distributions were measured and compared between cells from male and female rats at the beginning of the effect of MI and at the end of the recording, in both cases, where only one channel was open. Figure 5.8 shows that there was no significant difference between the sexes with respect to the weighted mean open times before maximal activation of the sarcolemmal K_{ATP} channels by MI, compared to at the end of the experiment. This is in agreement with Ranki et al. (2001), who also found there to be no sex related differences in the single channel mean open times of the sarcolemmal K_{ATP} channel in guinea-pigs.

Conclusion and significance

In conclusion, this study has demonstrated that in response to MI there is no significant difference between the genders with respect to the single channel conductance, time to activation of the sarcolemmal K_{ATP} channel, number of sarcolemmal K_{ATP} channels

activated and open time distribution. Therefore the differences in cellular survival between the sexes can not be explained by differences in the behaviour of single sarcolemmal K_{ATP} channels.

CHAPTER 6

AN INVESTIGATION INTO THE SARCOLEMMAL ATP-SENSITIVE POTASSIUM CHANNEL REGULATION BY PROTEIN KINASE C

Chapter 6 An investigation into the ATP-sensitive potassium channel regulation by protein kinase C

6.1 Introduction

Adenosine 5'-triphosphate-sensitive potassium (K_{ATP}) channels are found in a variety of tissues and cell types where they couple the metabolic state of the cell to the membrane potential. First discovered by Noma (1984), the K_{ATP} channel is thought to be activated under conditions of metabolic inhibition. A suggestion is that K_{ATP} channels in the heart are thought to be protective under conditions of metabolic stress induced by ischaemia (Nichols and Lederer et al., 1991; Yamada and Inagaki, 2002). This is thought to be through a pathway initiated by ischaemia causing adenosine to increase in the cell and to diffuse into the extracellular space (Mubagwa and Flameng et al., 2001), leading to opening of the K_{ATP} channels through activation by the phosphorylation of the Kir6.2 subunit, possibly at threonine 180 by PKC (Light et al., 1996; Light et al., 2000). It is thought that the action of PKC is to decrease the Hill coefficient of ATP binding to cardiac sarcolemmal K_{ATP} channels. Therefore the open probability of the channel is increased under physiological concentrations of ATP and in addition, under conditions of ischaemia. The proposed role of the K_{ATP} channel is to stabilise the membrane potential of the cell, thereby preserving energy (Yamada et al., 2001) and reducing calcium influx (Hearse, 1995) as previously discussed in the introduction.

Since it appears the K_{ATP} channel has an important role in the electrical properties of the cell under both normal and ischaemic conditions, the question therefore is how the

number of functional K_{ATP} channels in the sarcolemmal membrane is controlled. Too many open cardiac K_{ATP} channels could have a detrimental effect on the cell and result in greater potassium efflux and consequently shortening of the action potential; both of which could contribute to arrhythmias (Wilde, 1993). Investigations into the regulation of the K_{ATP} channel under these conditions have been limited. A study by Hu et al., (2003) has suggested that a PKC-mediated downregulation of the K_{ATP} channel number is responsible for the protection against excessive activation in tissue culture, primary neuronal cells and cardiac myocytes. Their study suggests that PKC acts upon the K_{ATP} channel to control K_{ATP} activation via a dynamin-dependent endocytotic process at a dileucine motif in the Kir6.2 subunit.

This chapter describes studies designed to further investigate the role of PKC in the internalisation of the K_{ATP} channel. The effects of incubation of cardiac myocytes with both a PKC activator, phorbol-12-mystrate-13-acetate (PMA) and a PKC inhibitor (chelerythrine) were investigated using both electrophysiological and molecular biological techniques to assess the whole cell current and regulation of the δ and ε PKC isoforms via electrophysiology and western blotting respectively. Changes in the whole cell current and single channel P_{open} were also measured and compared to investigate whether the decrease in current observed after maximal activation of the K_{ATP} channel by metabolic inhibition is due to K_{ATP} channel internalisation or closing of the channel.

In my studies, electrophysiological investigations showed there to be no significant difference with respect to the K_{ATP} whole cell current between cardiac myocytes that had

been incubated with the PKC activator (100 nM PMA) or inhibitor (10 μM chelerythrine). Activation and inhibition of the δ and ε PKC isoforms was shown to occur in cardiac myocytes using Western blotting. The decrease in the K_{ATP} whole cell current observed following maximal activation of the K_{ATP} channels with MI was shown to be possibly due to closing of the channels and not due to internalisation.

6.2 Methods

6.2.1 Cell culture

Ventricular myocytes were dissociated from the animals as described in chapter 2.

6.2.3 Solutions

Isolated ventricular myocytes were continuously superperfused with normal Tyrode's solution. Where used, NaCN (2mM) and iodoacetic acid (1mM) were added to Substrate-free Tyrode's on the day of the experiment and the pH readjusted to 7.4. We refer to this solution as MI-Tyrode's. Phorbol-12-mystrate-13-acetate (PMA) was stored in the freezer at a concentration of 1 mM and diluted using normal Tyrode's to a final concentration of 100 nM on the day of the experiment. Chelerythrine was made up as a 10 mM stock solution using DMSO and stored in the freezer, and was diluted further to 10 μM using normal Tyrode's on the day of the experiment.

6.2.4 Westerns: Determination of PKC activation

The Western blotting protocol is described in chapter 2.

6.2.5 Analysis

Data are represented as mean ± SEM and values of n refer to the number of hearts examined as indicated in the text or figure legends. Mean values obtained were compared

by the paired or unpaired Student t test where appropriate. Values where $p<0.05$ were considered statistically significant. Comparison of the different densities of the protein bands of the samples on the autoradiography film was achieved using the densitometry measuring program NIH ImageJ.

6.3 Results

6.3.1 Distribution of δ and ε isoforms of PKC

PKC is thought to regulate the membrane distribution of the K_{ATP} channel (Hu et al., 2003). To assess the specific PKC isoforms that might be activated by PKC, myocytes were lysed and analyzed for the presence of δ and ε PKC isoforms by Western blotting after sodium dodecyl sulphate–10% polyacrylamide gel electrophoresis (figure 6.1). Activation of PKC isoforms is associated with their translocation from soluble to particulate fractions within the cell. Translocation was assessed after activation with 100 nM PMA, and inhibition with 10μM chelerythrine. To assess for activation of the PKC isoforms PKCδ and PKCε, 1ml of normal Tyrode's containing myocytes was stimulated with 100 nM PMA for 20 minutes, lysed with 1ml of ice-cold hypertonic buffer (composition in mM unless otherwise stated: Tris 100, EDTA 10, NaCl 150, 1% (v:v) NP40, 0.1% (w:v) SDS, 5 mg ml^{-1} deoxycholic acid, 200 μg ml^{-1} benzamidine, PMSF 1, and 10μl of protease inhibitor cocktail; pH 7.4). To assess for inhibition of the translocation of the aforementioned PKC isoforms, cells were incubated with both 100 nM PMA and 10 μM chelerythrine and were lysed using the same hypertonic buffer as previously mentioned. In both experiments, cell lysates were homogenised using a hand-held homogeniser and were then fractionated by centrifugation (30,000 rpm for 30 mins, 4°C) to create soluble and insoluble fractions for analysis by Western blotting and densitometric quantitation (figure 6.1A). The two members of the novel PKC isoform family, PKCδ and PKCε, migrated at the appropriate molecular sizes. Antisera against PKCδ recognized proteins at 76-kDa, whereas antisera against PKCε recognized proteins at 67 kDa (figure 6.1A). The data can be summarized as follows. (i) PKCδ translocated

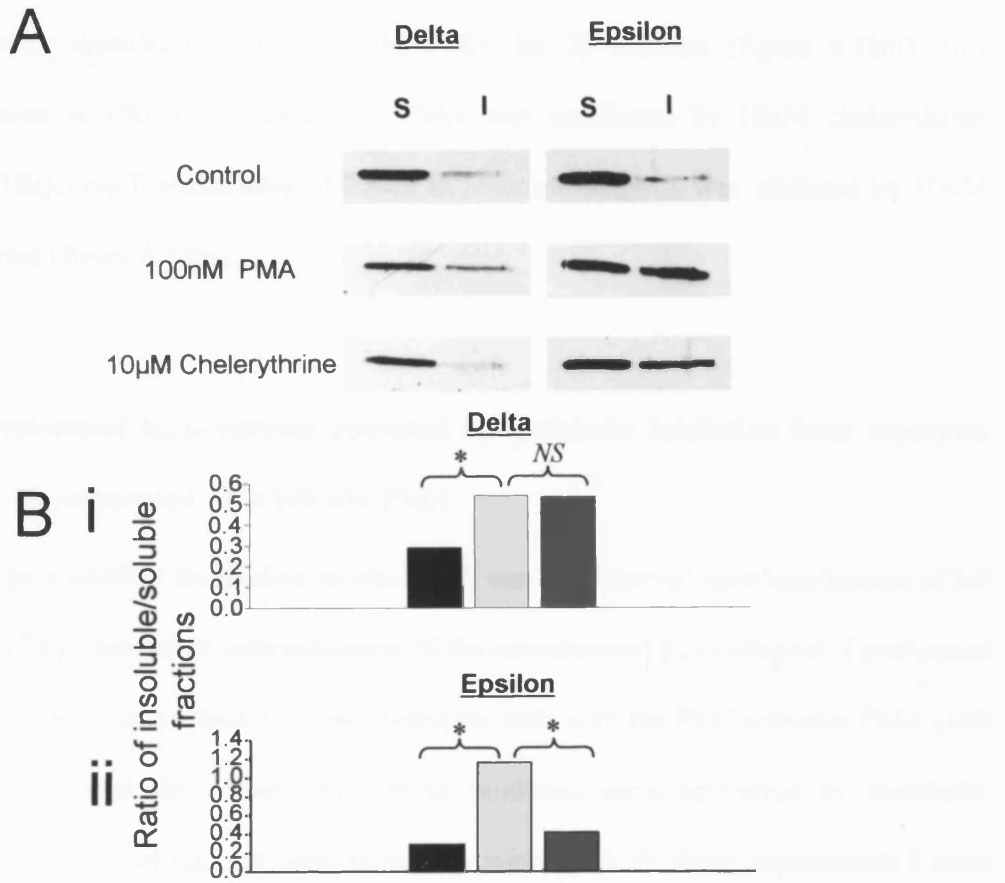

Figure 6.1 Distributions of the δ and ε isoforms of PKC between the soluble and particulate membrane fractions from cardiac myocytes upon activation by 100 nM PMA.

A, Western blot analysis shows that incubation of cardiac myocytes with 100 nM PMA results in the movement of both the δ and ε isoforms of PKC from the soluble to insoluble membrane fractions. Incubation of cardiac myocytes with 10 μM chelerythrine (PKC inhibitor) results in the inhibition of the movement of both the δ and ε isoforms of PKC. S=soluble fraction; I=particulate fraction

B, i, Histogram shows the movement in the δ isoform of PKC between the soluble and insoluble fractions upon activation by 100 nM PMA and inhibition by 10 μM chelerythrine of cardiac myocytes. The histogram shows the ratio of the insoluble to soluble fractions under the following conditions; ■ control □ PMA ▒ chelerythrine.

ii, Histogram shows the movement in the ε isoform of PKC between the soluble and insoluble fractions upon activation by 100 nM PMA and inhibition by 10 μM chelerythrine of cardiac myocytes from three rats using the same conditions as in i. Soluble fraction, n=3, Particulate fraction, n=3.$p<0.5$ □ control ■ PMA ▒ chelerythrine

from the cytosol to the particulate compartment after stimulation with 100 nM PMA for 20 minutes (figure 6.1Bi). (iii) PKCε also translocated from the cytosolic to particulate fraction after stimulation with 100 nM PMA for 20 minutes (figure 6.1Bii). (iii) Translocation of PKCδ in response to PMA was unaffected by 10μM chelerythrine (figure 6.1Bi). (iv) Translocation of PKCε in response to PMA was inhibited by 10μM chelerythrine (figure 6.1Bii).

6.3.2 Sarcolemmal K_{ATP} current activated by metabolic Inhibition from myocytes that were pre-incubated with 100 nM PMA

To investigate whether the decline in whole cell current observed upon application of MI is due to a PKC dependent internalisation of the sarcolemmal K_{ATP} channel, I performed whole cell experiments where I pre-incubated the cells with the PKC activator PMA (100 nM) and compared the whole cell current produced upon activation by metabolic inhibition to cells that had not been pretreated with PMA. In these experiments I used metabolic inhibition with 2 mM NaCN and 1 mM iodoacetic acid to elicit sarcolemmal K_{ATP} current. Sarcolemmal K_{ATP} currents were measured as shown in figure 6.2. A protocol was used where the cell was held at 0 mV throughout. It can be seen that after application of metabolic inhibition, there was an increase in current until a peak was reached for both control cells and cells pre incubated with 100 nM PMA (figure 6.2). The current then declined until the current reached the same level as that seen at the beginning of the experiment, when the cell was initially perfused with normal Tyrode's. Sarcolemmal K_{ATP} current was measured as the maximal peak current and normalised to the cell capacitance. The time to activation of the sarcolemmal K_{ATP} current was

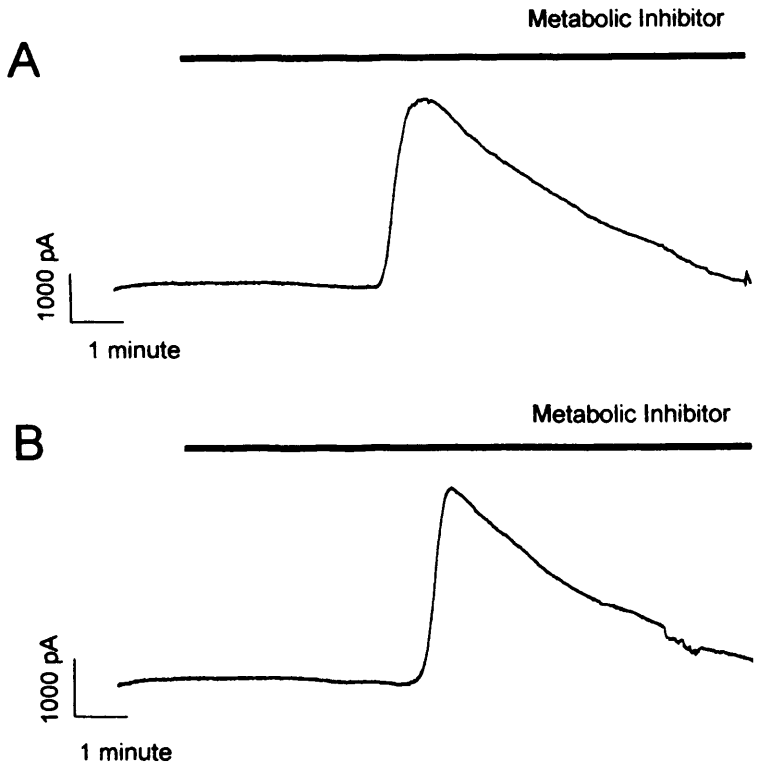

Figure 6.2 K_{ATP} current activated by metabolic inhibition in control myocytes and those pre-incubated with PMA

A, Recording of whole cell current from a male rat cardiac myocyte showing the effect of metabolic inhibition. MI Tyrode was applied as indicated and the cell was held at 0 mV throughout.

B, Recording of whole cell current from a male rat cardiac myocyte showing the effect of metabolic inhibition on cells that were pre-incubated for 15 minutes with PMA. MI Tyrode was applied as indicated and the cell was held at 0 mV throughout.

measured as the time at which the whole cell K_{ATP} current started to rise. The time to half decay of the maximal K_{ATP} current observed was also measured.

It can be seen from figure 6.3Ai that there was no significant difference between the controls and PMA pre-treated cells peak current density, 24.34 ± 0.64 pA/pF (experiments=11, n=2) and 30.07 ± 0.59 pA/pF (experiments=9, n=2) respectively (figure 6.3Aiii). There is also no significant difference between the control and PMA pre-treated cells with respect to the absolute current observed. The absolute current observed for the control cells was 2933.64 ± 79.82 pA (experiments=11, n=2) and 3680 ± 90.95 pA (experiments=9, n=2) for the PMA pre-treated cells (figure 6.3Ai). There was no significant difference between the control and PMA pre-incubated cells with respect to the time at which the K_{ATP} channels activated (figure 6.3B). Time to activation of the K_{ATP} channel was found to be 3.7 ± 0.2 (experiments=11, n=2) and 3.6 ± 0.2 minutes (experiments=9, n=2) for control and PMA pre-treated cells respectively (figure 6.3B). There was also no significant difference between male and female rats with respect to the time to half decay of the K_{ATP} current. Time to half decay was found to be 2.36 ± 0.10 (experiments=11, n=2) and 2.31 ± 0.05 minutes (experiments=9, n=2) for control and PMA pre-incubated cells respectively (figure 6.3C).

6.3.3 K_{ATP} current activated by metabolic inhibition in myocytes pre incubated with 10 μM chelerythrine

To further investigate whether the decline in whole cell current observed upon application of MI is due to a PKC dependent internalisation of the K_{ATP} channel, I also

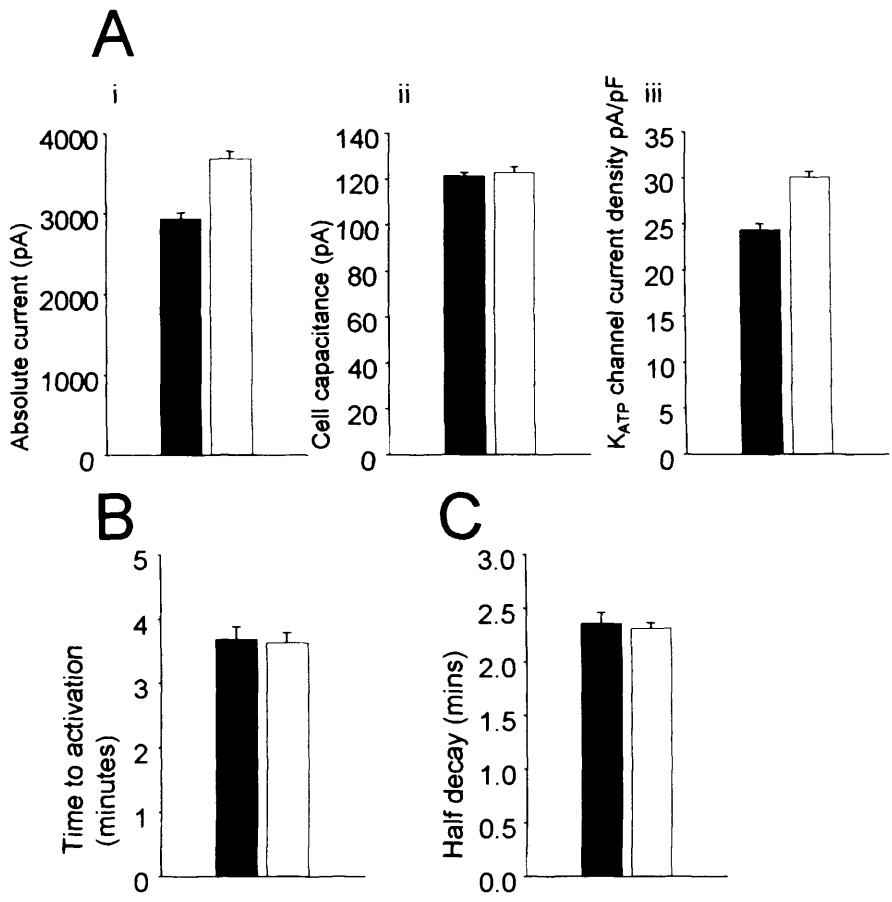

Figure 6.3 K_{ATP} current activated by metabolic inhibition and myocytes in control and those pre-incubated with PMA

A, i, Peak whole-cell K_{ATP} currents activated by metabolic inhibition in experiment like that of figure 4.2. In this figure as in B, the black bar shows mean (± s.e.m.) results for cells from control myocytes (n = 11 cells from 2 animals) and the grey bar those from myocytes incubated with 100nM PMA (n = 10 cells from 2 animals). ii, Membrane capacitance from control myocytes and those incubated with PMA. iii, K_{ATP} current density (pA/pF) for current activated by metabolic inhibition in cells from control myocytes and those incubated with PMA. ■ Control ■ PMA pre-treated

B, Shows time to activation of the whole-cell K_{ATP} currents activated by metabolic inhibition in experiment like that of figure 4.2.

C, Shows half-time to decay of the whole-cell K_{ATP} currents activated by metabolic inhibition in experiment like that of figure 4.2.

performed whole cell experiments where I pre-incubated the cells with the PKC inhibitor chelerythrine (10 μM) and compared the whole cell current produced upon activation by metabolic inhibition to cells that had not been pre incubated with chelerythrine. In these experiments I also used metabolic inhibition with 2 mM NaCN and 1 mM iodoacetic acid to elicit the K_{ATP} current (figure 6.4). The protocol used for measuring K_{ATP} currents was the same as that used for measuring the PMA currents as shown in figure 6.2.

It can be seen from figure 6.5Ai, that there was no significant difference in current density (pA/pF) between current induced by metabolic inhibition where cells had been pre incubated with 10 μM chelerythrine and the controls. Current density was found to be 29.99 ± 10.88 pA/pF (experiments=11, n=2) and 27.61 ± 1.55 pA/pF (experiments=9, n=2) (figure 6.5Aiii) for control and chelerythrine pre-incubated cells respectively. This reflects the absolute current (pA) observed for the control and chelerythrine pre-treated cells respectively. The absolute current was found to be 4409.36 ± 174.03 pA (experiments=11, n=2) and 3971 ± 219.50 pA (experiments=9, n=2). Time to activation of the K_{ATP} whole cell current was measured as being the time at which the current started to rise after application of MI. There was also no difference in the time to activation of the K_{ATP} channel between the control and chelerythrine pre-treated cells (figure 6.5B). Time to activation of the K_{ATP} channel was found to be 3.1 ± 0.1 (experiments=11, n=2) and 2.6 ± 0.1 minutes (experiments=9, n=2) for control and chelerythrine pre-treated cells respectively (figure 6.5B). There was a significant difference between control and chelerythrine pre-treated cells with respect to the time to half decay of the K_{ATP} current ($p<0.05$). Time to half decay was found to be 1.50 ± 0.05

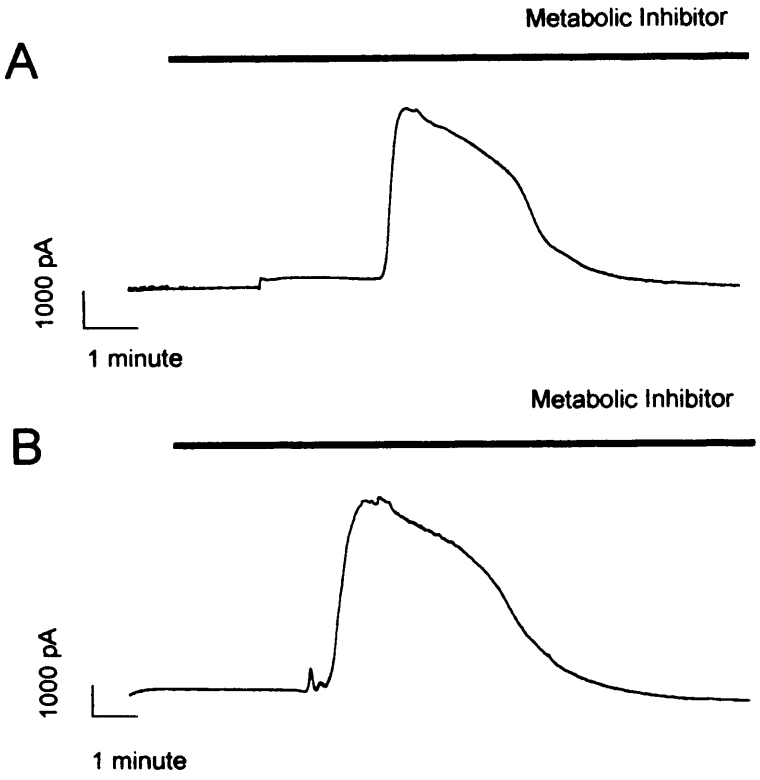

Figure 6.4 K_{ATP} current activated by metabolic inhibition in control myocytes and those pre-incubated with 10 μM chelerythyrine from male rats

A, Recording of whole cell current from a male rat cardiac myocyte showing the effect of metabolic inhibition. MI Tyrode was applied as indicated and the cell was held at 0 mV throughout.

B, Recording of whole cell current from a male rat cardiac myocyte showing the effect of metabolic inhibition on cells that were pre-incubated for 15 minutes with 10 μM chelerythyrine. MI Tyrode was applied as indicated and the cell was held at 0 mV throughout.

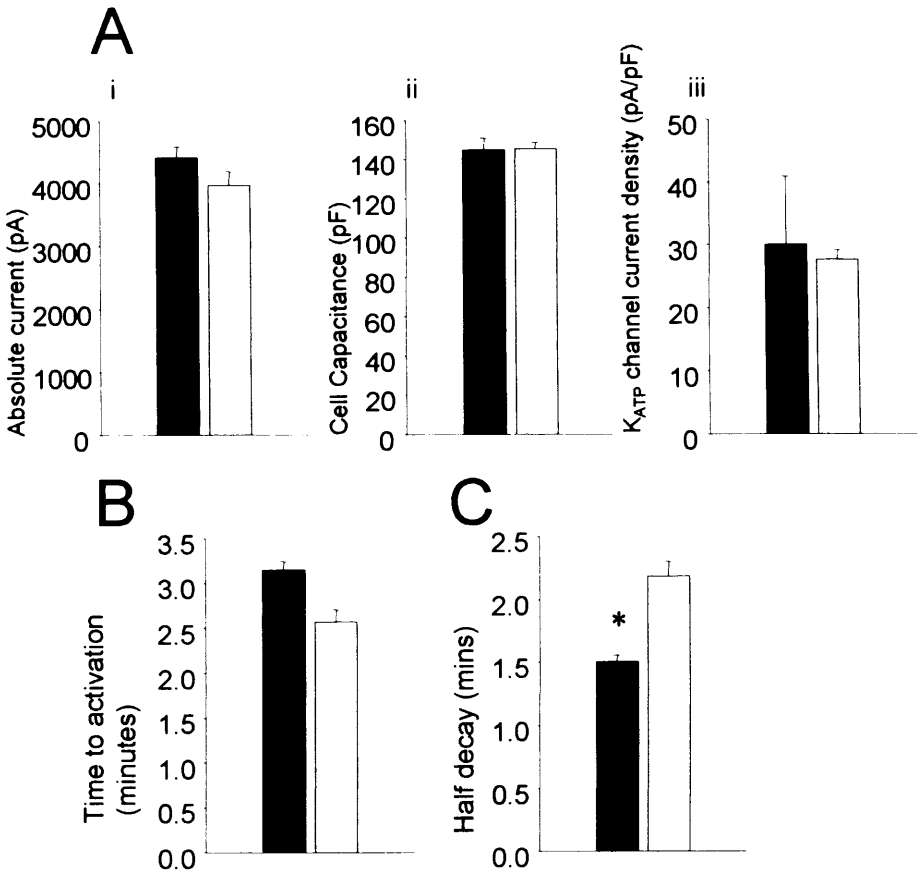

Figure 6.5 K_{ATP} current activated by metabolic inhibition and myocytes in control and those pre-incubated with chelerythrine

A, i, Peak whole-cell K_{ATP} currents activated by metabolic inhibition in experiment like that of figure 4.2. In this figure as in B, the black bar shows mean (± s.e.m.) results for cells from control myocytes (n = 11 cells from 2 animals) and the grey bar those from myocytes incubated with 10 μM chelerythrine (n = 9 cells from 2 animals). ii, Membrane capacitance from control myocytes and those incubated with 10 μM chelerythrine. iii, K_{ATP} current density (pA/pF) for current activated by metabolic inhibition in cells from control myocytes and those incubated with chelerythrine.

■ Control ■ Chelerythrine pre-treated

B, Shows time to activation of the whole-cell K_{ATP} currents activated by metabolic inhibition in experiment like that of figure 4.2

C, Shows time to half decay (ms) of the whole-cell K_{ATP} currents activated by metabolic inhibition in experiment like that of figure 4.2. * $p<0.05$

(experiments=11, n=2) and 2.18 ± 0.12 minutes (experiments=9, n=2) for control and chelerythrine pre-incubated cells respectively (figure 6.5C).

6.3.4 Measurement of NP_{open}

It was previously suggested that the decline in the K_{ATP} current observed after maximal activation of the channel is due to internalisation of the channel (Hu et al., 2003). Hu et al. (2003) suggested that the internalisation of the K_{ATP} channel acts as brake to prevent excessive activation of the channel, which could result in arrhythmias. The decline in current can be seen in figures 6.2 and 6.4 where the whole cell K_{ATP} current increased upon activation of the channels with metabolic inhibition, then declined to almost the same level of current as initially observed at the beginning of the experiment when the cell was being perfused with normal Tyrode's. Therefore, I investigated whether the decline in the sarcolemmal K_{ATP} current was due to the K_{ATP} channel being internalised. I made cell-attached patches and perfused the cell with a metabolic inhibitor to activate the K_{ATP} channels. From these recordings I measured the changes in the P_{open} of these channels over the course of an experiment as the sarcolemmal K_{ATP} channels were activated by MI. The hypothesis was that if the sarcolemmal K_{ATP} channel was being internalised to prevent excessive activation and subsequent arrhythmias in the heart then the number of channels would change but P_{open} would remain the same. Conversely, if the decline in sarcolemmal K_{ATP} current was due to the channels closing and not being internalised then the number of channels should stay the same but P_{open} would decline.

In order to investigate this, I measured the changes in P_{open} in both cell-attached single and multi K_{ATP} channel patches, over the course of an experiment where the channels were activated by perfusing cell-attached patches with an MI solution containing NaCN and iodoacetic acid. Cell-attached patches were held at +40 mV with 140mM K^+ in the pipette solution. The suggestion was that if P_{open} declined in the single channel patch then any decline in the multi channel patches was likely to be due to changes in P_{open} also and not due to internalisation of the channel.

Values for P_{open} were obtained from patches containing a single active channel. Measurement of P_{open} for multi channel patches was performed on patches containing up to eight channels by measuring the times, t_j, spent at current levels corresponding to j=0,1,2...N channels open (Davies et al., 1992). The overall P_{open} was then obtained using the following equation:

$$NP_{open} = \left(\sum_{j=1}^{N} t_j j\right) / T$$

Where the duration of the recording, T, was 15.6 seconds.

After 2 kHz filtering, the current records were used to obtain an idealized trace showing the transitions between the open and closed levels as described in the methods. Data, together with the idealized trace, were displayed in segments, and a decision made to accept or reject the idealized trace or to reset the threshold. This was to allow for and consequently compensate for any changes in the baseline due to drift, sections of the recording which contained anomalities or extraneous noise. The P_{open} values were

computed from the idealized trace and stored for analysis. Figure 6.6A and 6.7A show recordings of single and multi channel K_{ATP} openings respectively in response to the application of metabolic inhibition. Also shown is a portion of the recordings in the respective figures at an expanded time base (figure 6.6B and 6.7B). Figure 6.6C and 6.7C show the changes in P_{open} over the course of the experiment from when the K_{ATP} channel begins to open following the application of MI till the end of the experiment when the K_{ATP} current declines. It can be seen from figures 6.6C and 6.7C that the P_{open} in both the single channel and multi channel patches increase then decrease respectively.

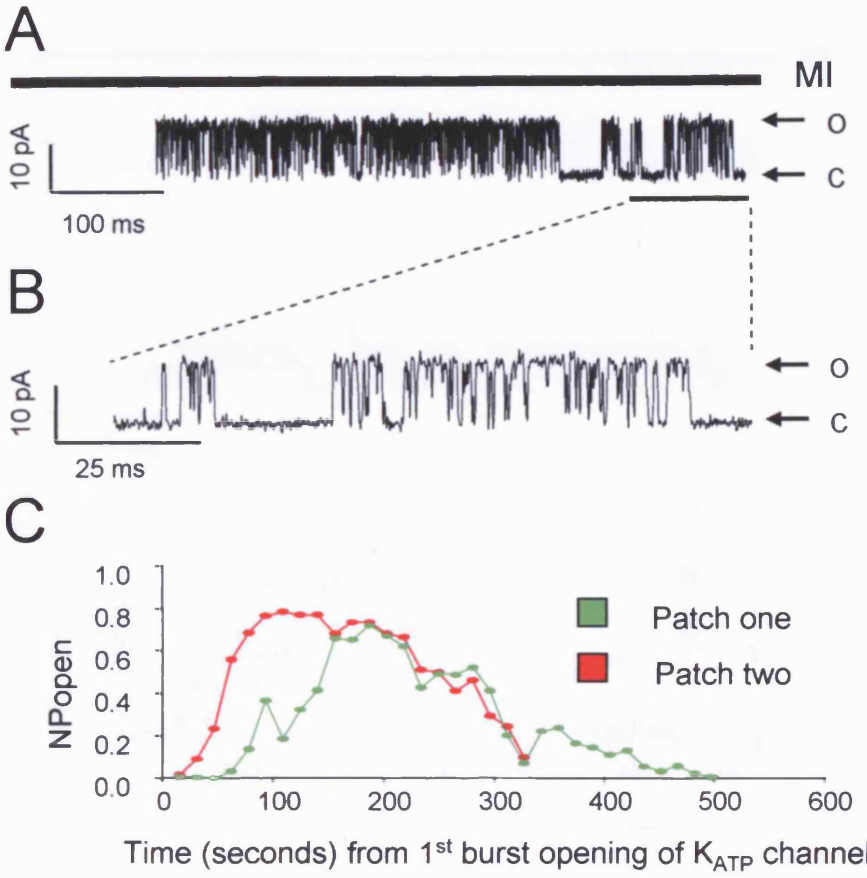

Figure 6.6 Example of K_{ATP} channel activity, recorded from a cell-attached patch of a cardiac ventricular myocyte containing a single channel.

A, The traces have been filtered at 2kHz for display and the trace below (B) show the portion of the above trace as indicated by the line at an expanded time scale. The holding potential was +40 mV, the patch pipette contained 140 mM K^+ and the bathing solution contained 5 mM K^+. O, open; C, closed.

C, Graph showing the changes in NPopen for two patches each containing a single K_{ATP} channel, over the duration of an experiment as illustrated in (A). The K_{ATP} channels were opened by superfusing the cardiac mycoytes with a metabolic inhibitor containing 2mM NaCN and 1mM IAA. Both patches contained three channels.

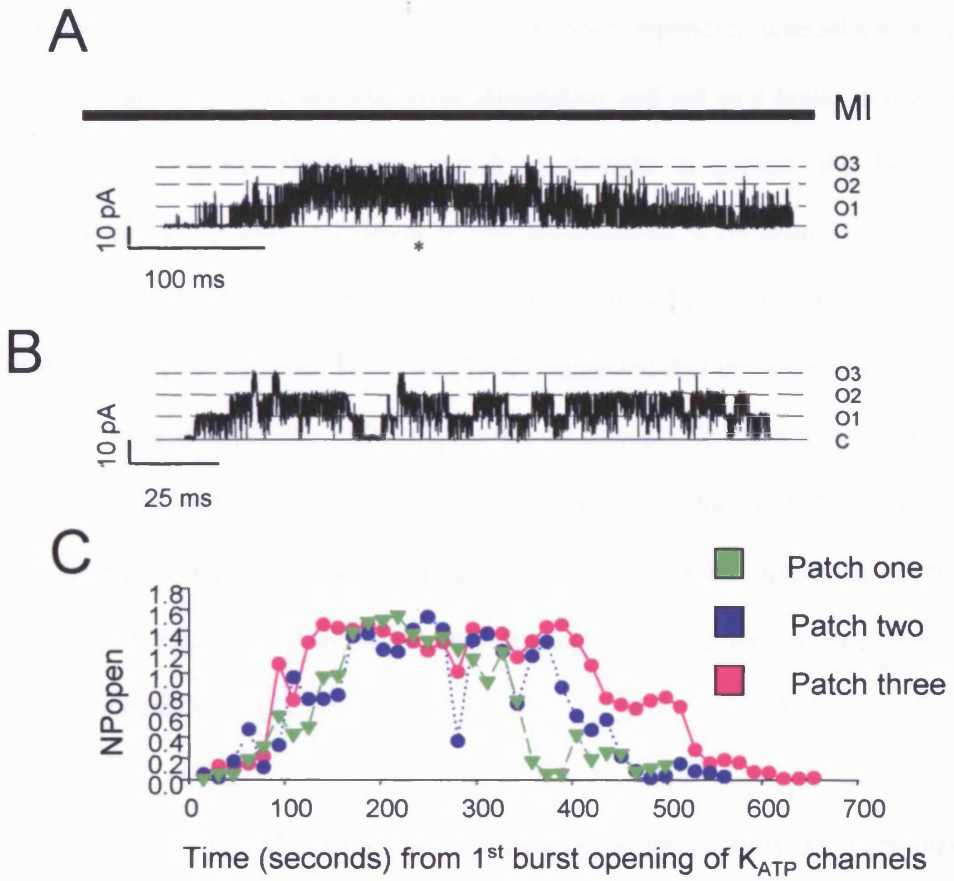

Figure 6.7 Example of K_{ATP} channel activity, recorded from a cell-attached patch of a cardiac ventricular myocyte containing multiple channels.

A, The traces have been filtered at 2kHz and the trace below (B) shows the portion of the above trace as indicated by the asterisk at an expanded time scale. The holding potential was +40 mV, the patch pipette contained 140 mM K^+ and the bathing solution contained 5 mM K^+. O, open; C, closed. The numbers (i.e O1) refer to the number of channels open.

C, Graph showing the changes in NPopen for three K_{ATP} multi-channel patches containing up to eight K_{ATP} channels, over the duration of an experiment as illustrated in (A). The K_{ATP} channels were opened by perfusing the cardiac mycytes with a metabolic inhibitor containing 2mM NaCN and 1mM IAA.

6.4 Discussion

It has previously been reported that there is a dynamin dependent internalisation of the K_{ATP} channel that might prevent excessive stimulation and act as a brake to reduce the action potential duration shortening, which is thought to protect the heart from arrhythmias caused by over activation of the sarcolemmal K_{ATP} channels (Hu et al., 2003). This is thought to protect the heart from arrhythmias caused by over activation of the sarcolemmal K_{ATP} channels. Hu et al. (2003) suggested that the internalisation of the sarcolemmal K_{ATP} channel is a PKC dependent mechanism. Robson et al. (2005) also demonstrated that sarcolemmal K_{ATP} channel rundown is due to a PKC dependent mechanism in proximal tubule cells of frog kidney, but found that activation of PKC by PMA increased sarcolemmal K_{ATP} channel rundown via a possible phosphorylation dependent mechanism.

In this chapter I investigated whether the behaviour of the sarcolemmal K_{ATP} channel was indeed consistent with internalisation by a PKC dependent mechanism, by looking at the effect of imodulating cellular PKC with PMA and chelerythrine respectively on the MI-activated K_{ATP} current. I therefore studied the effect of increasing and decreasing cellular PKC with PMA and chelerythrine respectively upon the MI-activated sarcolemmal K_{ATP} current. I then investigated whether the decline in the sarcolemmal K_{ATP} current observed after maximal activation of the channel with MI is due to either internalisation or a decrease in the P_{open} of the channel by measuring the changes in the P_{open} in both single and multi channel patches over the course of an experiment where the channels were activated by MI.

Interestingly, it can be seen from figure 6.3 that PMA had no effect upon the current density (pA/pF), time to activation of the sarcolemmal K_{ATP} channels or the time to half decay of the sarcolemmal K_{ATP} current. This suggests that there is not a PKC dependent internalisation of the channel because the decline in the sarcolemmal K_{ATP} current was unaffected with respect to the time to half decay of the sarcolemmal K_{ATP} current.

The sarcolemmal K_{ATP} channels from the cells that were pre-incubated with chelerythrine were also found to have no significant effect upon current density (pA/pF) nor time to activation of the sarcolemmal K_{ATP} channel (figure 6.5). However, chelerythrine pre-treated cells were found to have a longer half decay time compared to the control cells (figure 6.5C). This data combined with that for PMA suggests that there may a PKC dependent regulation of the sarcolemmal K_{ATP} channel. Light et al. (1996, 2000) suggested that PKC caused opening of the sarcolemmal K_{ATP} channels through activation by the phosphorylation of the Kir6.2 subunit, possibly at threonine 180 by PKC (Light et al., 1996; Light et al., 2000). Therefore under conditions of metabolic stress, such as upon application of metabolic inhibition, intracellular ATP declines and sarcolemmal K_{ATP} channels open. Consequently, if PKC is thought to open sarcolemmal K_{ATP} channels, then PMA would have no effect in the presence of metabolic inhibition, which is likely to have caused maximal opening of all sarcolemmal K_{ATP} channels (figure 4.8). By contrast, the inhibition of PKC by chelerythrine should result in a decrease in peak current density or an increase in the time to decay. As pre-incubation of the cells with chelerythrine resulted in an increase in the time to decay, this data combined with the PMA results

suggests that there is a PKC dependent reduction in the functional activity of the K_{ATP} channel due to a PKC dependent mechanism.

I also investigated the changes in the P_{open} of sarcolemmal K_{ATP} channels in both single and multi channel patches over the course of an experiment where the sarcolemmal K_{ATP} channels were activated by MI. The hypothesis was that if the sarcolemmal K_{ATP} channel was being internalised then the number of channels would change but P_{open} would remain the same. Conversely, if the decline in sarcolemmal K_{ATP} current was due to the channels closing and not being internalised then the number of channels should stay the same but P_{open} would decline. Firstly, I investigated the changes in P_{open} of the single channel patches, the suggestion was that if P_{open} declined in the single channel patch then any decline in the multi channel patches would consequently be due to changes in P_{open} also and not due to internalisation of the channel. Figures 6.6 and 6.7 show the changes in P_{open} over the course of an experiment where the sarcolemmal K_{ATP} channels were activated by MI for both single and multi channel patches. Figure 6.6 show that the P_{open} in single sarcolemmal K_{ATP} channel patches increases then declines. As the same increase and decline in P_{open} is also seen in the multi channel patches and the profile of decline is similar to that of the whole cell currents (figures 6.2 and 6.4), this data suggest that the decline in the sarcolemmal K_{ATP} current seen following maximal activation of the whole cell current by MI is not due to channel internalisation but closure of the channel instead.

Conclusion and significance

My investigations into the decline in the whole cell K_{ATP} current following maximal activation of the channel by MI suggest it is not due to channel internalisation. It has long been suggested that PKC has a role in the regulation of the sarcolemmal K_{ATP} channel, with respect to preconditioning and recently to a possible PKC dependent internalisation of the channel and in preconditioning. In this investigation, activating PKC had no effect on the peak current density, time to current activation or time to decay. However, inhibition of PKC by chelerythrine caused an increase in time to decay supporting the suggestion that there was reduced functional activity of the K_{ATP} channel due to a PKC dependent mechanism. In contrast, if PKC is thought to open sarcolemmal K_{ATP} channels, then PMA would have no effect in the presence of metabolic inhibition, as all K_{ATP} channels would be open, which indeed was observed. The P_{open} data from the single channel and multi-channel patches suggest that the sarcolemmal K_{ATP} channels are closing and not being internalised under conditions of metabolic inhibition, as clearly illustrated by the single channel patches where P_{open} declines and the number of channels stay the same. Whether a PKC dependent reduction in the functional activity of the sarcolemmal K_{ATP} channel is protective is debatable. Hu et al. (2003) suggested that a PKC dependent internalisation of the K_{ATP} channel could protect against arrhythmias that are due to excessive opening of the aforementioned channel. However, following the closing of the K_{ATP} channel there would be increased activity of the Na^{+}-Ca^{2+} exchanger acting in the reverse mode as the membrane potential would depolarise favouring this directionality of the exchanger. However, it is possible that the intrusive cell-attached

technique could affect whether the sarcolemmal K_{ATP} channel closes or is internalised in the presence of metabolic inhibition.

CHAPTER 7

MAIN DISCUSSION

Chapter 7 Main Discussion

Numerous studies have shown that males are more susceptible to cardiovascular diseases compared to women until the menopause. Recently, it has been suggested by Ranki et al., (2001) that the increased survival rate of females compared to males following metabolic inhibition and reperfusion was due to an increased sarcolemmal K_{ATP} current density. I therefore investigated whether a higher sarcolemmal K_{ATP} current density existed in female compared to male rats and whether this was responsible for the increased survival rate of the female cells compared to males following metabolic inhibition and reperfusion. It has long been suggested that the sarcolemmal K_{ATP} channel is protective and that opening of the channel results in the clamping of the membrane potential towards the potassium equilibrium potential (E_K^+) (-93 mV). This is thought to be protective because the action potential is shortened, or even prevented resulting in contractile failure, reducing Ca^{2+} entry into the cell via the L-type calcium channels. However, as demonstrated by Baczko et al. (2004) the sarcolemmal K_{ATP} channel can also be protective, as hyperpolarization towards the E_K (-93 mV) favours the calcium extrusion mode of the sarcolemmal Na^+-Ca^{2+} exchanger. Therefore limiting cellular calcium load, hypercontracture and death in contrast to conditions where the sarcolemmal K_{ATP} channel is not opened and the membrane potential may become depolarized (section 7.1). Consequently, my research focussed upon identifying which of the aforementioned hypotheses on how the sarcolemmal K_{ATP} channel is protective is the dominating mechanism affording females protection against metabolic inhibition and reperfusion.

It was clear from the data outlined in chapter 3 that females were able to maintain a lower intracellular calcium concentration compared to males following metabolic inhibition and reperfusion. Figure 3.6 showed that the average intracellular calcium concentration following metabolic inhibition and reperfusion was significantly lower in females compared to male myocytes. In my experiments and a study by Rodrigo et al. (2005) it was observed that myocytes which had an $[Ca^{2+}]_i$ >250nM following MI and reperfusion, when viewed using conventional light microscopy, were hypercontracted with membrane blebs and non-contractile. This $[Ca^{2+}]_i$ was also greater then the peak diastolic $[Ca^{2+}]_i$ determined in these cells using this techniques and was therefore taken as an indication that these cells had lost the ability to regulate their $[Ca^{2+}]_i$. Therefore I compared the numbers of male and female myocytes that had a resting calcium concentration above 250 nM at reperfusion as an indication of cellular survival. Figure 3.7 showed a significantly higher percentage of female compared to male myocytes had an intracellular calcium concentration above 250 nM at the end of reperfusion. This evidence suggests that the female cells may be protected from calcium overload and subsequent cell death.

Chapter 3 also demonstrated that differences exist between males and females with respect to the recovery of function following metabolic inhibition and reperfusion, with a higher percentage of female compared to male cells recovering contractile activity in response to electrical stimulation following metabolic inhibition and reperfusion (figure 3.3). In addition, the data show that females showed a significantly longer time to rigor compared to females. However, more importantly there was no difference between males and females with respect to the time to contractile failure (figure 3.2). If the mechanism

by which the sarcolemmal K_{ATP} channel was protective in females compared to males was by the shortening and eventual failure of the action potential, then contractile failure would be expected to occur earlier in the females. As previously mentioned, this would have the effect of a reduced calcium loading via the L-type calcium channel which is active during phase 2 of the action potential. As no difference between males and females with respect to the time to contractile failure was found then it could be suggested that the sarcolemmal K_{ATP} channel does not protect female cells against metabolic inhibition via this mechanism.

Previous studies by Ranki et al., (2001) suggested that the increased survival rate of females compared to males following reperfusion injury was due to an increased sarcolemmal K_{ATP} current density. I therefore investigated whether a higher sarcolemmal K_{ATP} current density existed in female compared to male rats, using pinacidil, P-1075 and metabolic inhibition to open the sarcolemmal K_{ATP} channels. I found that application of both pinacidil and its analogue P-1075, resulted in a higher sarcolemmal K_{ATP} current density in female compared to male myocytes (figures 4.4C and 4.7C). However, this was contradicted by the experiments using metabolic inhibition, where there was no significant difference in the K_{ATP} current density between males and females (figure 4.8Biii). Interestingly, metabolic inhibition elicited a larger current compared to when either pinacidil or P-1075 was applied to the cell (compare figures 4.4A and 4.7A to figure 4.8Bi). The difference in the sarcolemmal K_{ATP} current activated by pinacidil, P-1075 or metabolic inhibition could be attributable to the way in which these chemicals act to open the sarcolemmal K_{ATP} channel. It is thought that both pinacidil and P-1075 open

the sarcolemmal K_{ATP} channel by binding to the sulphonylurea receptor (Babenko et al., 2000). Whereas metabolic inhibition opens the sarcolemmal K_{ATP} channel by inhibiting the electron transport system and glycolysis, which leads to a decrease in intracellular ATP and opening of the K_{ATP} channel. Consequently, the observed maximal sarcolemmal K_{ATP} current for males and females may not dependent upon the number or density of the sarcolemmal K_{ATP} channels within the cell, but rather the pharmacological method used to open the channel. Investigations into whether there were differences between the sexes in the transcript abundance of the genes that constitute the sarcolemmal K_{ATP} channel, specifically SUR2A and Kir6.2, showed that there was no difference (figure 4.9). This further suggested that there was no difference in the sarcolemmal K_{ATP} channel density between males and females. However, the QPCR experiments were only examining the mRNA transcript levels of the genes that constitute the sarcolemmal K_{ATP} and not the actual protein levels of these subunits present in these cells.

The experiments investigating the whole cell K_{ATP} current between males and females were inconclusive, as they show differences between male and females in pharmacologically opened channels but failed to show any difference when the channel were opened by metabolic inhibition. which is functionally more revealing as an indicator of channel involvement in protection. However, it is possible that the differences in cellular survival between the sexes following metabolic inhibition could have resulted from early opening of single sarcolemmal K_{ATP} channels in females, resulting in earlier reduction in APD but not contractile failure. However, investigations into the time to sarcolemmal K_{ATP} single channel activation for males and females found that there was

no significant difference (figure 5.3B). I also studied whether female sarcolemmal K_{ATP} channels may have a higher single channel conductance (figure 5.2B), which could explain the increased cellular survival of female compared to male cells. The suggestion was that if females had a higher single channel K_{ATP} conductance then the tendency for the membrane potential to move towards E_K would be stronger compared to male cells. However, the unitary conductance measured at the reversal potential was found to insignificant between the sexes. The number of channels activated for male and females was also found not to be significantly different. As there was no significant difference between the sexes with respect to the time to activation of the sarcolemmal K_{ATP} channel, number of channels activated, or single channel conductance, I investigated whether there were differences in the mean open time of the sarcolemmal K_{ATP} channel between the sexes. Investigations found there was also no difference with respect to the weighted mean open times before and after maximal activation of the sarcolemmal K_{ATP} channel (figure 5.4). However, the mean open time could not be measured when the maximal numbers of channels were open, as the maximal number of channels could not easily be identified. Therefore, it could be suggested that female sarcolemmal K_{ATP} channels may stay open longer during the period of maximal activation. This would have the effect of hyperpolarising the membrane potential of the cell towards E_K for potassium (-93 mV) and therefore reducing the drive of calcium into the cell via the Na^+-Ca^{2+} exchanger.

In conclusion, my investigations have shown that clearly that females have a higher cellular survival rate following metabolic inhibition and reperfusion which could be related to an ability to maintain a lower calcium concentration under these conditions.

Recent research has shown that pre-treatment of rabbit hearts with either 17β-oestradiol or one cycle of ischaemia preconditioning prior to coronary occlusion, are equally effective in significantly reducing the infarct size. Interestingly, it was suggested that both ischaemia preconditioning and 17β-oestradiol share the same common effector, that being the mitochondrial K_{ATP} channel (Das and Sarkar, 2006). This was based on evidence which demonstrated that the beneficial effects of 17β-oestradiol or the preconditioning were prevented by pre-treatment with the mitochondrial K_{ATP} blocker, 5-HD. However, the suggestion that the sarcolemmal K_{ATP} channel density or functional characteristics are responsible for these gender differences appear unlikely, as my whole cell investigations were inconclusive and analysis of single channel characteristics and kinetics between the sexes did not show any significant differences. Further investigations would have been needed to study the precise role of the sarcolemmal K_{ATP} channel in gender specific protection, specifically the activity of the sarcolemmal K_{ATP} channel at maximal activation. Investigations into the differences in the membrane potential between males and females wild type and sarcolemmal K_{ATP} channel knock out mice during metabolic inhibition and pinacidil would be of importance to establish whether females do maintain a hyperpolarised membrane potential compared to males under stress. Investigations into the effects of acute application of oestrogen and testosterone on the membrane potential and the kinetics of the sarcolemmal K_{ATP} channel would also be paramount to defining the role of the sarcolemmal K_{ATP} in cells under metabolic stress. In addition, analysis of the single channel kinetics of the sarcolemmal K_{ATP} channel during pinacidil would be useful in comparing to those under metabolic inhibition.

Additional non-channel effects of oestrogen and testosterone

A number of cellular sites other than the sarcoplasmic K_{ATP} could be possible targets of direct oestrogen action within the cell (figure 1.8) where oestrogen may have a protective effect have also been identified. Maintenance of cellular calcium within a cell is essential, as loss of calcium homeostatis has been linked to cardiac dysfunction and cell death, consequently the majority of studies are focussed upon investigating why females can maintain a lower intracellular calcium following simulated ischaemia. Chu et al. (2006) found that oestrogen has the effect of regulating the protein abundance levels of the L-type calcium channel (Cav1.2), beta-adrenergic receptor (B_1-A and Na^+-Ca^{2+} exchanger. Therefore females may be able to control their intracellular calcium concentrations by regulating the protein level of the different entry mechanisms (L-type calcium channels, beta-adrenergic receptors) from which calcium may enter the cell. The sodium channel or the Na^+-H exchanger may be another site of oestrogen action. Supporting this, Sugishita (2001) suggested that the lower intracellular calcium found in females compared to males during metabolic inhibition was due to females having a lower intracellular sodium concentration compared to males. Sarcoplasmic reticulum release of calcium is thought to be regulated by NOS; as inhibition of NOS resulted in a higher sarcoplasmic reticulum release of calcium. It is therefore unsurprising that females were found to have more NOS than males. Consequently, it may be suggested that females maintain a lower cytosolic calcium concentration by reducing calcium release from the SR. Cross et al. (2002) also found females to have a higher expression of eNOS and NO production, which could also support the above hypothesis. Cellular survival is extremely dependent upon the maintenance of the mitochondria following simulated ischaemia. If the MPT

pore of the mitochondria is opened, the high intracellular calcium and cytochrome C are released, which can activate caspases leading to cellular apoptosis. Morkuniere et al. (2004) found that oestrogen can protect hearts against the loss of cytochrome C. Ohya et al. (2005) that oestrogen can not only enhance the activity of the BK_{Ca} channel in the mitochondria, but that the activation of the channel's associated beta subunit can couple to cytochrome C oxidase subunit I. The resulting depolarisation of the mitochondrial membrane potential would decrease the drive of intracellular calcium in the mitochondria, while secondly preventing the loss of cytochrome C through the interaction of the BK_{Ca} channel. Consequently, there are a number of additional mechanisms activated by oestrogen, which could be acting independently, or altogether to protect females from ischaemia-reperfusion injury.

By contrast, studies have suggested that testosterone may well be protective in cardiovascular cells. Activation of the $mitoK_{ATP}$ by testosterone may improve myocardial protection following ischaemia (Er et al., 2004). This conclusion was based on evidence whereby the $mitoK_{ATP}$ blocker 5-HD prevented the testosterone induced reduction in death of cardiomyocytes following ischaemia, whereas the sarcolemmal K_{ATP} blocker HMR1098 had no effect. Many other studies have also investigated the benefits of testosterone, specifically in its ability to maintain low intracellular calcium following ischaemia-reperfusion injury (Callies et al., 2003), inhibition of L-type Ca^{2+} channels (Scragg et al., 2004) and gene expression regulation of the major calcium regulatory proteins in ventricular myocytes (Golden et al., 2004). In conclusion, there is contradictory evidence as to whether oestrogen or testosterone are indeed protective and

how and where they act to produce the protection and therefore further investigation is needed.

PKC-dependent regulation of sarcK_{ATP} channel activity

The second part of my study focussed upon investigating how regulation of the sarcolemmal K_{ATP} channel by PKC, specifically whether the sarcolemmal K_{ATP} channel is internalised via a PKC dependent mechanism. A previous study by Hu et al. (2003) showed that there is a dynamin dependent internalisation of the sarcolemmal K_{ATP} channel, which is thought to prevent excessive channel stimulation and acts as a brake to reduce the action potential duration shortening. This is thought to protect cardiac myocytes from arrhythmias caused by over activation of the sarcolemmal K_{ATP} channels. Other studies have also suggested that the K_{ATP} channel is regulated by protein kinase specific mechanisms. Lin et al (2000) showed that phosphorylation of serine T224 on the Kir6.2 subunit by PKA stimulated sarcolemmal K_{ATP} channels expressed in HEK293 cells. Robson et al. (2005) demonstrated that K_{ATP} channel rundown is due to a PKC dependent mechanism in proximal tubule cells of frog kidney. They found that activation of PKC by PMA increased sarcolemmal K_{ATP} channel rundown via a possible phosphorylation dependent mechanism.

I investigated whether the behaviour of the sarcolemmal K_{ATP} channel was indeed consistent with internalisation by a PKC dependent mechanism. I studied the effect of increasing and decreasing cellular PKC with PMA and chelerythrine respectively upon the MI-activated sarcolemmal K_{ATP} current. I then investigated whether the decline in the

K_{ATP} current observed after maximal activation of the channel with MI is due to either internalisation or a decrease in the P_{open} of the channel. The suggestion was that if the K_{ATP} channel was being internalised during the decline of the K_{ATP} whole cell current (figures 6.2 and 6.4) then P_{open} would remain the same but the number of channels would rapidly decrease.

PMA was found to have no effect upon the current density (pA/pF), time to activation of the sarcolemmal K_{ATP} channels or the time to half decay of the K_{ATP} current (figure 6.3). This suggests that there is not a PKC dependent internalisation of the channel because the decline in the K_{ATP} current was unaffected with respect to the time to half decay of the K_{ATP} current. If there had been a PKC dependent internalisation of the channel, increasing PKC with the application of PMA would result in a shorter time to half decay, which was not observed.

Chelerythrine, the PKC inhibitor, was also found to have no significant effect upon current density (pA/pF) or time to activation of the sarcolemmal K_{ATP} channel (figure 6.5). However, chelerythrine pre-treated cells were found to have a longer half decay time compared to the control cells (figure 6.5C). This data suggests that there may be a PKC dependent regulation of the sarcolemmal K_{ATP} channel. In contrast, if PKC is thought to open sarcolemmal K_{ATP} channels, then PMA would have no effect in the presence of metabolic inhibition, as all K_{ATP} channels would be open, which indeed was observed. As demonstrated by Light et al. (1996, 2000) application of PKC caused opening of the sarcolemmal K_{ATP} channels through activation by the phosphorylation of

the Kir6.2 subunit, possibly at threonine 180 by PKC (Light et al., 1996; Light et al., 2000). This had the effect of increasing the Hill coefficient for the binding of ATP, meaning that the channel was more likely to be open under physiological concentrations of ATP. Under conditions of metabolic stress, such as upon application of metabolic inhibition, intracellular ATP declines and K_{ATP} channels open. By contrast, the inhibition of PKC by chelerythrine should result in a decrease in peak current density or an increase in the time to decay. As pre-incubation of the cells with chelerythrine resulted in an increase in the time to decay, this data combined with the PMA results suggests that there is a PKC dependent closing or internalisation of the sarcolemmal K_{ATP} channel.

The investigations into the changes in P_{open} of the single sarcolemmal K_{ATP} channel during the decline of the K_{ATP} whole cell current, where the sarcolemmal K_{ATP} channels were opened by MI suggested that the channel was not being internalised. The hypothesis was that if the sarcolemmal K_{ATP} channel was being internalised then the number of channels would change but P_{open} would remain the same. Conversely, if the decline in K_{ATP} current was due to the channels closing and not being internalised then the number of channels should stay the same but P_{open} would decline. Figure 6.6 show that the P_{open} in single sarcolemmal K_{ATP} channel patches increases then declines. As the same increase and decline in P_{open} is also seen in the multi channel patches (figure 6.7) and with the whole cell currents (figures 6.2 and 6.4), this data suggests that the decline in the K_{ATP} current seen following maximal activation of the whole cell current by MI is not due to channel internalisation but closure of the channel instead.

To investigate further, the suggestion that the sarcolemmal K_{ATP} channel activity is reduced in some way by PKC, Western blotting could be used to show whether PKC is mobilised during metabolic inhibition would be beneficial. In addition, studies into whether this phenomenon is observed when the sarcolemmal K_{ATP} channel is opened by other means, such as pinacidil or P-1075, would also be interesting. These studies would be able to demonstrate if closing of the sarcolemmal K_{ATP} channel following opening, is unique to metabolic inhibition or is a general phenomenon used, as suggested by Hu et al. (2003) as a mechanism to prevent excessive activation and associated arrhythmias in the heart.

In conclusion, further investigation is needed to define the role of the sarcolemmal K_{ATP} channel not only in the protection of the heart from ischaemia but also in the gender specific protection against ischaemia.

CHAPTER 8

REFERENCES

Chapter 8 References

ABI-GERGES, N., SMALL, B.G., LAWRENCE, C.L., HAMMOND, T.G., VALENTIN, J-P. & POLLARD, C.E. (2006) Gender differences in the slow delayed (I_{Ks}) but not in inward (I_{K1}) rectifier K^+ currents of canine Purkinje fibre cardiac action potential: key roles for I_{Ks}, β-adrenoceptor stimulation, pacing rate and gender. *British Journal of Pharmacology* 147, 653–660.

ADELMAN, J.P., SHEN, K-Z., KAVANAUGH, M.P., WARREN, R.A., WU, Y-N., LAGRUTTA, A., BOND, C.T., NORTH, R.A. (1992) Calcium-activated potassium channels expressed from cloned complementary DNAs. *Neuron* 9, 209-216.

AGUILAR-BRYAN, L; CLEMENT. J.P; NAMBA.; GONZALEZ, KUNJILWAR, G.K; BABENKO A. & BRYAN. J. (1998) Toward Understanding the Assembly and structure of K_{ATP} Channels. *Physiological Reviews* 78, 227-245.

AIDLEY, D.J. & STANFIELD, P.R. (1996, 2001) Ion channels: Molecules in action, Cambridge University press, Great Britain.

ALLARD, B., LAZDUNSKI, M. & ROUGIER, O. (1995) Activation of ATP-dependent K^+ channels by metabolic poisoning in adult mouse skeletal muscle: role of intracellular Mg(2+) and pH. *The Journal of Physiology* 1; 485 (Pt 2), 283-296.

ALLSHIRE, A., PIPER, H.M., CUTHBERTSON, K.S. & COBBOLD, P.H. (1987) Cytosolic free Ca^{2+} in single rat heart cells during anoxia and reoxygenation. *Biochemical journal* 1;244(2), 381-5.

ANDERSON, C.R. & STEVENS, C.F. (1973) Voltage clamp analysis of acetylcholine produced end-plate current fluctuations at frog neuromuscular junction. *The Journal of Physiology* 235, 655-91.

ARIELI, Y., GURSAHANI, H., EATON, M..M., HERNANDEZ, SCHAEFER, S. (2004) Gender modulation of $Ca^{(2+)}$ uptake in cardiac mitochondria. *Journal of Molecular and Cellular Cardiology* 37(2), 507-13.

ARMSTRONG S. & GANOTE C.E. (1994) Adenosine receptor specificity in preconditioning of isolated rabbit cardiomyocytes: evidence of A3 receptor involvement. *Cardiovascular Research* 28, 1049-56.

ARMSTRONG, S.C., LIU, G.S., DOWNEY, J.M., GANOTE, C.E. (1995) Potassium channels and preconditioning of isolated rabbit cardiomyocytes: effects of glyburide and pinacidil. *Journal of Molecular and Cellular Cardiology* 27, 1765-1774.

ASHCROFT, F.M., GRIBBLE, F.M. (2000a) Tissue-specific effects of sulphonylureas: lessons from studies of cloned K_{ATP}. *Journal of Diabetes Complications* 14 (4), 192-196.

ASHCROFT, F.M. & KAKEI, M. (1989) ATP-sensitive K^+ channels in rat pancreatic beta-cells: modulation by ATP and Mg^{2+} ions. *The Journal of Physiology* 416, 349-367.

ASHCROFT, S.J., ASHCROFT, F.M. (1990) Properties and functions of ATP-sensitive K-channels. *Cell Signalling* 2 (3), 197-214.

BABENKO, A.P., AGUILAR-BRYAN, L., BRYAN, J. (1998a) A view of SUR/KIR6.X, KATP channels. *Annual review of Physiology* 60, 667-687.

BABENKO, A.P., GONZALEZ, G. & BRYAN, J. (1999) Two regions of sulphonylurea receptor specify the spontaneous bursting and ATP inhibition of K_{ATP} channel isoforms. *Journal of Biological Chemistry* 274 (17), 11587-11592.

BAINES, C.P., SONG, C.X., ZHENG, Y.T., WANG, G.W., ZHANG, J., WANG, O.L., GUO, Y., BOLLI, R., CARDWELL, E.M. & PING, P (2003) Protein kinase Cepsilon interacts with and inhibits the permeability transition pore in cardiac mitochondria. *Circulation Research* 92: 873-80.

BAINES, C.P., KAISER, R.A., PURCELL, N.H., BLAIR, N.S., OSINSKA, H., HAMBLETON, M.A., BRUNSKILL, E.W., SAYEN, M.R., GOTTLIEB, R.A., PORN, G.W., ROBBINS, J. & MOLKEI, J.D. (2005) Loss of cyclophilin D reveals a critical role for mitochondrial permeability transition in cell death. *Nature* 31:434 (7033), 658-62.

BAINES, C.P., GOTO, M. & DOWNEY, J.M. (1997) Oxygen radicals released during ischaemia preconditioning contribute to cardioprotection in the rabbit myocardium. *Journal of Molecular and Cellular Cardiology* 29, 207-16.

BAINES, C.P., ZHANG, J., WANG, G.W., ZHENG, Y.T., XIU, J.X. CARDWELL, E.M. BOLLI, R. & PING, P. (2002) Mitochondrial PKCepsilon and MAPK form signalling modules in the murine heart: enhanced mitochondrial PKCepsilon-MAPK interactions and differential MAPK activation in PKCepsilon-induced cardioprotection. *Circulation Research* 90, 390-7.

BARRETT-CONNOR, E. & BUSH, T.L (1991) Estrogen and coronary heart disease in women. *Journal of the American Medical Association* 10;265(14):1861-7.

BAXTER, G.F., MARBER, M.S., PATEL, V.C., YELLON, D.M. (1994) Adenosine receptor involvement in a delayed phase of myocardial protection 24 hour hours after ischaemia preconditioning. *Circulation* 90, 2993-3000.

BAXTER, G.F. & YELLON, D.M. (1997) Time course of delayed myocardial protection after transient A1 receptor activation in the rabbit. *Journal of Cardiovascular Pharmacology* 29, 631-638.

BEGUIN, P., NAGASHIMA, K., NISHIMURA, M., GONOI, T., SEINO, S. (1999) PKA-mediated phosphorylation of the human K_{ATP} channel: separate roles of KIR6.2 and SUR1 subunit phosphorylation. *The EMBO Journal* 18 (17), 4722-4732.

BELL, R.M., SMITH, C.C. & YELLON, D.M. (2001) Nitric oxide as a mediator of delayed pharmacological (A1 receptor triggered) preconditioning: is eNOS masquerading as iNOS? *Cardiovascular Research* 52, 274-280.

BERS, D.M (2003) Excitation-Contraction Coupling and Cardiac force. Kluwer Academic Publishers.

BEZANILLA, F & ARMSTRONG, C.M (1972) Negative conductance caused by entry of sodium and cesium ions into the potassium channels of squid axons. *Journal of General Physiology* 60, pp.588-608.

BOLLI, R; DAWN, B; TANG, X-L, QIU, Y; PING, P; XUAN, Y-T; JONES, W.K; TAKANO, H; GUO, Y; ZHANG, J (1998) The nitric oxide hypothesis of late preconditioning. *Basic Research in Cardiology* 93, 325-338.

BRADY, P., TERZIC, A. (1998) The sulphonylurea controversy: more questions from the heart. *Journal of the American College of Cardiology* 31, 950-6.

BROWN, D.A & ADAMS, P.R. (1980) Muscarinic suppression of a novel voltage-sensitive K^+ current in a vertebrate neurone. *Nature (London)* 320, 193-218.

BROWN D.A., CHICCO A., JEW K.N., JOHNSON M.S., LYNCH J.M., WATSON P.A. & MOORE R.L. (2005) Cardioprotection afforded by chronic exercise is mediated by the sarcolemmal, and not the mitochondrial, isoform of the K_{ATP} channel in the rat. *The Journal of Physiology* 15;569(Pt 3), 913-24.

CAMPER-KIRBY, D., WEICH, S., WALKER, A., SHIRAISHI, I., SETCHELL, K.D., SCHAEFER, E., KAJSTURA, J., ANVERSA, P. & SUSSMAN, M.A. (2001) Myocardial Akt activation and gender: increased nuclear activity in females versus males. *Circulation Research* 88, 1020-1027.

CALLIES, F., STROMER, H., SCHWINGER, R.H.G., BOLCK, B., HU, K., FRANTZ, S., LEUPOLD, A., BEER, S., ALLOLIO, B. & BONZ, A.W. (2003) Administration of testosterone is associated with a reduced susceptibility to myocardial ischaemia. *Endocrinology* 144(10), 4478-4483.

CAVE A.C & HEARSE D.J. (1992) Ischaemia preconditioning and contractile function: studies with normothermic and hypothermic global ischaemia. *Journal of Molecular Cell Cardiology* 24, 1113-23.

CHAPMAN, N., MAYET, J., OZKOR, M., FOALE, R., THOM, S. & POULTER, N (2000) Ethnic and gender differences in electrocardiographic QT length and QT dispersion in hypertensive subjects. *Journal of Human Hypertension* 14(6), 403-405.

CHEN, J., PETRANKA, J., YAMAMURA, K., LONDON, R.E., STEENBERGEN, C. & MURPHY, E. (2003) Gender differences in sarcoplasmic reticulum calcium loading after isoproterenol. *American Journal of Physiology- Heart and Circulatory Physiology* 285(6), H2657-62.

CHU, S.H., SUTHERLAND, K., BECK, J., KOWALSKI, J., GOLDSPINK, P. & SCHWERTZ, D. (2005) Sex differences in expression of calcium-handling proteins and beta-adrenergic receptors in rat heart ventricle.*Life Sci*ences 22;76(23), 2735-49.

CIANI, S. & RIBALET, B. (1988) Ion Permeation and Rectification in ATP-Sensitive channels from Insulin-Secreting Cells (RINM5F): Effects of K^+, Na^+ and Mg^{2+}. *The Journal of membrane biology* 103, 171-180.

CLEMENT, J.P., KUNJILWAR, K., GONZALEZ, G., SCHWANSTECHER, M., PANTEN, U., AGULIAR-BRYAN, L. & BRYAN, J. (1997) Association and Stoichiometry of $K_{(ATP)}$ channel subunits. *Neuron* 18 (5), 827-838.

CLERK, A & SUGDEN, P.H. (1998) The p38-MAPK inhibitor, SB203580, inhibits cardia stress-activated protein kinases/c-Jun N-termincal kinases (SAPKs/JNKs). *FEBS Letters*, 426, *93-96.*

COHEN, M.V., BAINES, C.P. & DOWNEY, J.M. (2000) Ischaemia Preconditioning: From Adenosine Receptor to K_{ATP} Channel. *Annual Review of Physiology* 62, 79-109.

COHEN, M.V., LIU, G.S., & DOWNEY, J.M. (1991) Preconditioning causes improved wall motion as well as small infarcts after transient coronary occlusion in rabbits. *Circulation* 89, 341-349.

COHEN, M.V., YANG, X.M., LIU, G.S., HEUSCH, G. & DOWNEY, J.M. (2001) Acetylcholine, bradykinin, opioids, and phenylephrine, but not adenosine, trigger preconditioning by generating free radicals and opening mitochondrial $K_{(ATP)}$ channels. *Circulation Research* 89, 273-8.

COLE, W.C., MCPHERSON, C.D. & SONTAG, D. (1991) ATP-regulated K+ channels protect the myocardium against ischemia/reperfusion damage. *Circulation Research* 69, 571-581.

COLQUHOUN, D., & SIGWORTH, F.J. (1983) Fitting and statistical analysis of single-channel records. *In* Single-Channel Recording, 1st ed. B. Sakmann and E. Neher, editors. Plenum Press, New York. 191–263.

CONSTANTI, A.A. & SIM, J.A. (1987) Calcium-dependent potassium conductance in guinea-pig olfactory cortex neurones in vitro. *The Journal of Physiology* 387, 173-194.

COOK, D.L. & HALES, C.N. (1984) Intracellualr ATP directly blocks K^+ channels in pancreatic B-cells. *Nature (London)* 311, 271-273.

COOK, N.S. (1990) Potassium Channels, Ellis Horwood limited, Great Britain.

CURL, C.L., WENDT, I.R. & KOTSANAS, G. (2001) Effects of gender on intracellular [Ca^{2+}] in rat cardiac myocytes. *Pflugers Arch* 441(5), 709-16.

CROSS, H.R., LU, L., STEENBERGEN, C., PHILIPSON, K.D. & MURPHY, E. (1998) Overexpression of the cardiac Na^{+}/Ca^{2+} exchanger increases susceptibility to ischaemia/reperfusion injury in male, but not female, transgenic mice. *Circulation Research* 14-28;83(12), 1215-23.

DANA, A., BAXTER, G.F. & YELLON, D.M. (2001) Delayed or second window preconditioning induced by adenosine A1 receptor activation is independent of early generation of nitric oxide or late induction of inducible nitric oxide synthase. *Journal of Cardiovascular Pharmacology* 38, 278-287.

DANI, J.A. & LEVITT, D.G. (1990) Diffusion and Kinetic Approaches to Describe Permeation in Ionic Channels. *Journal of Theoretical Biology* 146, 289-301.

DAS, B. & SARKAR, C. (2006) Similarities between ischemic preconditioning and 17beta-estradiol mediaed cardiomyocyte K_{ATP} channel activation leading to cardioprotective and antiarrhythmic effects during ischemia/reperfusion in the intact rabbit heart. *Journal of Cardiovascular Pharmacology* 47 (2) 277-86.

DASCAL, N., LIM, N.F., SCHRIEBMAYER, W., WANG, W., DAVIDSON, N. & LESTER, H.A. (1993) Expression of an atrial G-protein-activated potassium channel in *Xenopus* oocytes. *Proceedings of the National Academy of Science USA* 90 6596-6600.

DAVIES.N.W., MCKILLEN.H-C., STANFIELD.P.R. & STANDEN.N.B. (1996) A rate theory model for Mg^{2+} block of ATP-dependent potassium channels of rat skeletal muscle. *The Journal of Physiology* 490.3, 817-826.

DAVIES, N.W., PETIT, A.I., AGARWAL, R. & STANDEN, N.B. (1991) The flickery block of ATP-dependent potassium channels of skeletal muscle by internal 4-aminopyridine. *Pflügers Archiv* 419, 25-31.

DAVIES, N.W., SPRUCE, A.E., STANDEN, N.B., & STANFIELD, P.R. (1989) Multiple blocking mechanisms of ATP-sensitive potassium channels of frog skeletal muscle by tetraethylammonium ions. *The Journal of Physiology* 413, 31-48.

DAVIES, N.W., STANDEN, N.B., & STANFIELD, P.R. (1992) The effect of intracellular pH on ATP-dependent potassium channels of frog skeletal muscle. *The Journal of Physiology* 445, 549-68.

DE JAGER, T., PELZER, T., MÜLLER-BOTZ, S., IMAM, A., MUCK, J. & NEYSES, L. (2001) Mechanisms of oestrogen receptor action in the myocardium. Rapid gene activation via the ERK1/2 pathway and serum response elements. *Journal of Biological Chemistry* 276, 27873-27880.

DEMPSEY, E.C., NEWTON, A.C., MOCHLY-ROSEN, D., FIELDS, A.P., REYLAND, M.E., INSEL, P.A. & MESSING, R.O (2000) Protein kinase C isozymes and the

regulation of diverse cell responses. *American Journal of Physiology-Lung Cellular and Molecular Physiology* 279, L429-L438.

DIAZ, M.E., EISNER, D.A. & O'NEIL, S.C (2002) Depressed ryanodine receptor activity increases variability and duration of the systolic Ca^{2+} transient in rat ventricular myocytes. *Cellular Biology* 91, 585-593.

DILLMANN, W.H., MEHTA, H.B., BARRIEUX, A., GUTH, B.D., NEELY, W.E. & ROSS, J.J. (1986) Ischaemia of the dog heart induces the appearance of a cardiac mRNA coding for a protein with migration characteristics similar to heat-shock/stress protein 71. *Circulation Research* 59 110-114.

DONG, Z; SAIKUMAR, P., WEINBERG, J.M., VENKATACHALAM, M.A. (2006) Calcium and cell injury and death. *Annual Review of Pathology: Mechanisms of Disease* 1, 405-34.

DOS SANTOS, P., KOWALTOWSKI, A.J., LACLAU, M.N., SEETHARAMAN, S., PAUCEK, P., BOUDINA, S., THAMBO, J-B., TARIOSSE, L. & GARLID, K.D (2002) Mechanisms by which opening the mitochondrial ATP-sensitive $K^{(+)}$ channel protects the ischaemic heart. *American Journal of Physiology-Heart and Circulatory Physiology* 283, H284-H295.

DOS SANTOS, P., LACLAU, M.N., BOUDINA, S. & GARLID, K.D. (2004) Alterations of the bioenergetics systems of the cell in acute and chronic myocardial ischemia. *Journal of Molecular and Cellular Biochemistry* 256-257, 157-66.

DOYLE, D.A., MORAIS CABRAL, J., PFUETZNER, R.A., KUO, A., GULBIS, J.M., COHEN, S.L., CHAIT, B.T. & MACKINNON, R. (1998) The structure of the potassium channel: Molecular basis of K^+ conductance and selectivity. *Science* 280, 69-77.

DUCHEN, M.R. (1999) Contributions of mitochondria to animal physiology: from homeostatic sensor to calcium signalling and cell death. *The Journal of Physiology* 516.1, 1-17.

EDWARDS, G. & WESTON, A.H. (1990) Structure-activity relationships of K^+ channel openers. *Trends in Pharmacological Sciences* 11 417-422.

ER, F., MICHELS, G., GASSANOV, N., RIVERO, F. & HOPPE, U.C. (2004) Testosterone induces cytoprotection by activating ATP-senstive K^+ channels in the cardiac mitochondrial inner membrane. *Circulation* 110, 3100-3107.

FINDLAY.I. (1987) ATP-sensitive K^+ channels in rat ventricular myocytes are blocked and inactivated by internal cations. *Pflügers Archiv* 410, 313-320.

FORESTIER, C. & VIVAUDOU, M. (1993) Modulation by Mg^{2+} and ADP of ATP-sensitive potassium channels in frog skeletal muscle. *Journal of Membrane Biology* 132(1), 87-94.

FRENCH, R.J. & SHOUKIMAS, J.J. (1985) An ion's view of the potassium channel. *Journal of General Physiology* 85, pp.669-698.

GABEL, S.A., WALKER, V.R., LONDON, R.E., STEENBERGER, C., KORASH, K.S., MURPHY, E. (2005) Oestrogen receptor beta mediates gender differences in ischaemia/reperfusion injury. *Journal of Molecular and Cellular Cardiology* 38(2), 289-97.

GANOTE, C.E., ARMSTRONG, S., DOWNEY, J.M (1993) Adenosine and A1 selective agonists offer minimal protection against ischaemic injury to isolated rat cardiomyocytes. *Cardiovascular Research* 27(9), 1670-1676.

GARCIA-CALVO, M., KNAUS, H.G., MCMANUS, O.B., GIANGIACOMO, K.M., KACZOROWSKI, G.J., GARCIA, M.L. & KNAUS, H.G (1994) Purification and reconstitution of the high-conductance, calcium-activated potassium channel from tracheal smooth muscle. *Journal of Biological Chemistry* 269, 676-682.

GARLID, K.D., DOS SANTOS, P., XIE, Z.J., COSTA, A.D. & PAUCEK, P. (2003) Mitochondrial potassium transport: the role of the mitochondrial ATP-sensitive K(+) channel in cardiac function and cardioprotection. *Biochimica et Biophysica Acta* 1606, 1-21.

GARLID, K.D., PAUCEK, P. & YAROV-YAROVOY, V. (1997) Cardioprotective effect of diazoxide and its interaction with mitochondrial ATP-senstive K^+ channels. Possible mechanism of cardioprotection. *Circulation Research* 81, 1072-82.

GIBLIN, J.P., LEANEY, J.L. & TINKER, A. (1999) The Molecular Assembly of ATP-sensitive Potassium Channels. *Journal of Biological Chemistry* 274 (32), 22652-22659.

GÖGELEIN, H., HARTUNG. J. & ENGLERT, H.C. (1999) Molecular Basis, Pharmacology and Physiological Role of Cardiac K_{ATP} Channels. *Cell Physiology and Biochemistry* 9, 227-241.

GOLDEN, K.L., MARSH, J.D. & JIANG, Y. (2004) Testosterone regulates mRNA levels of calcium regulatory proteins in cardiac myocytes. *Hormone and Metabolic Research (Stuttgart)* 36, 197-202.

GRIBBLE, F.M. & REIMANN, F. (2003) Sulphonylurea action revisited: the post-cloning era. *Diabetologica* 46, 875-891.

GRIFFITHS, E.J., OCAMPO, C.J., SAVAGE, J.S., RUTTER, G.A., HANSFORD, R.G., STERN, M.D. & SILVERMAN (1998) Mitochondrial calcium transporting pathways during hypoxia and reoxygenation in single rat cardiomyocytes. *Cardiovascular Research* 39(2), 423-433.

GRIFFITHS, E.J. (1999) Reversal of mitochondrial Na/Ca exchange during metabolic inhibition in rat cardiomyocytes. *FEBS Letters (Amsterdam)* 25 453 (3), 400-4.

GROHE, C., KAHLERT, S., LOBBERT, K., NEYSES, L., VAN EIKELS, M., STIMPEL, M. & VETTER, H. (1997) Cardiac myocytes and fibroblasts contain functional oestrogen receptors. *FEBS Letters (Amsterdam)* 13;416(1), 107-12.

GROSS, G.J. & AUCHAMPACH, J.A. (1992) Blockade of ATP-sensitive potassium channels prevents myocardial preconditioning in dogs. *Circulation Research* 70, 223-233.

GROVER, G.J., D'ALONZO, A.J., DZWONCZYK, S., PARHAM, C.S. & DARBENZIO, R.B. (1996) Preconditioning is not abolished by the delayed rectifier K^+ blocker dofetilide. *American Journal of Physiology- Heart and Circulatory Physiology* 271, H1207-H1214.

GROVER, G.J., D'ALONZO, A.J., PARHAM, C.S. & DARBENZIO, R.B. (1995) Cardioprotection with the K_{ATP} opener cromakalim is not correlated with ischemic myocardial action potential duration. *Journal of Cardiovascular Pharmacology* 26, 145-152.

GROVER, G.J. AND GARLID, K.D (2000) ATP-Sensitive Potassium Channels: A Review of their Cardioprotective Pharmacology. *Molecular and Cellular Cardiology Journal* 32, 677-695.

HALESTRAP, A.P., CLARKE, S.J. & JAVADOR, S.A (2003) Mitochondrial permeability ransition pore opening during myocardial reperfusion-a target for cardioprotection. *Cardiovascular Research* 61(3), 372-385.

HALESTRAP, A.P., CONNERN, C.P., GRIFFITHS, E..J & KERR, P.M (1997) Cyclosporin A binding in mitochondrial cyclophilin inhibits the permeability transition pore and protects hearts from ischaemia/reperfusion injury. *Molecular and Cellular Biochemistry* 174, 167-172.

HAMILL, O.P., MARTY, A., NEHER, E., SAKMANN, B. & SIGWORTH, F.J. (1981) Improved patch-clamp techniques for high-resolution current recording from cells and cell-free membrane patches.*Pflugers Arch* 391(2), 85-100.

HANLEY, P.J. & DAUT, J. (2005) K_{ATP} channels and preconditioning: A re-examination of the role of mitochondrial K_{ATP} channels and an overview of alternative mechanisms. *Journal of Molecular and Cellular Cardiology* 39, 17-50.

HANLEY, P.J., DROSSE, S., BRANDT, U., LAREAU, R.A., BANERJEE, A.L. SRIVASTAVA, D.K., BANASZAK, L.J., BARYCKI, J.J., VAN VELDHOVEN, P.P & DAUT, J. (2005) 5-Hydroxydecanoate is metabolised in mitochondria and creates a rate-limiting bottleneck for beta-oxidation of fatty acids. *The Journal of Physiology* 562: 307-18.

HANLEY, P.J., MICKEL, M., LOFFLER, M., BRANDT, U. & DAUT, J.K. (2002) K(ATP) channel-independent targets of diazoxide and 5-hydroxydecanoate in the heart. *The Journal of Physiology* 542, 735-741.

HARUNA, T., HORIE, M., KOUCHI, I., NAWADA, R., TSUCHIYA, K., AKAO, M., OTANI, H., MURAKAMI, T. & SASAYAMA, S. (1998) Coordinate interaction between ATP-sensitive K^+ channel and Na^+, K^+-ATPase modulates ischaemia preconditioning. *Circulation* 98, 2905-10.

HAUSENLOY, D., WYNNE, A., DUCHEN, M. & YELLON, D (2004) Transient mitochondrial permeability transition pore opening mediates preconditioning-induced protection. *Circulation* 109, 1714-7.

HAWORTH, R.A., HUNTER, D.R. & BERKOFF, H.A. (1981) Contracture in isolated adult rat heart cells. Role of Ca^{2+}, ATP, and compartmentation. *Circulation Research.* 49(5) 1119-28.

HEARSE, D.J. (1995) Activation of ATP-sensitive potassium channels: a novel pharmacological approach to myocardial protection? *Cardiovascular Research* 30(1), 1-17.

HEGINBOTHAM, L., ABRAMSON, T. & MACKINNON, R. (1992) A functional connection between the pores of distantly related ion channels as revealed by mutant K^+ channels. *Science* 258, 1152-1155.

HILLE, B (1992, 2000) Ionic Channels of Excitable Membranes. Second and third editions. Sinauer Associates Inc. Sunderland, Massachusetts.

HILLE, B. & SCHWARZ, W. (1978) Potassium channels as multi-ion single-file pores. *Journal of General Physiology*. 72, 409-442.

HIGGINS, C.F. (1995) The ABC of Channel regulation. *Cell*. 82, 693-696.

HO, K., NICHOLS, C.G., LEDERER, W.J., LYTON, J., VASSILEV, P.M., KANAZIRSKA, M.V. & HEBERT, S.C (1993) Cloning and expression of an inwardly rectifying ATP-regulated potassium channel. *Nature* 362, 31-38.

HORIE, M., IRISAWA, H. & NOMA, A. (1987) Voltage-Dependent Magnesium Block of Adenosine-Triphosphate-Sensitive Potassium channel in Guinea-Pig Ventricular Cells. *The Journal of Physiology* 387, 251-272.

HU, K., HUANG, C.S., JAN, Y.N. & JAN, L.Y. (2003) ATP-sensitive potassium channel traffic regulation by adenosine and protein kinase C. *Neuron* 38, 417-432.

IKONOMIDIS, J.S., TUMIATI, L.C., WEISEL, R.D., MICKLE, D.A & LI, R.K. (1994) Preconditioning human ventricular cardiovascular with brief periods of stimulated ischaemia. *Cardiovascular Research* 28, 1285-91.

IMAGAWA, J., BAXTER, G.F. & YELLON, D.M. (1997) Genistein, a tyrosine kinase inhibitor, blocks the "second window of protection" 48 h after ischaemia preconditioning in the rabbit. *Journal of Molecular and Cellular Cardiology* 29, 1885-1893.

INAGAKI N., GONOI, T., CLEMENT, J.P., IV, WANG C-Z, AGUILAR-BRYAN L, BRYAN J, SEINO S (1996) A family of sulphonylurea receptors determines the pharmacological properties of ATP-sensitive K^+ channels. *Neuron*, 16, 1017.

INOUE, I., NAGASE, H., KISHI, K. & HIGUTI, T. (1991) ATP-sensitive K^+ channel in the mitochondrial inner membrane. *Nature* 352:244-247.

ISOMOTO, S., KONDO, C., YAMADA, M., MATSUMOTO, S., HIGASHIGUCHI, O., HORIO, Y., MATSUZAWA, Y.& KURACHI, Y. (1996) A Novel Sulphonylurea Receptor forms with BIR (Kir6.2) a Smooth Muscle Type ATP-sensitive K^+ Channel. *The Journal of Biological Chemistry* 271; 40, 24321-24324.

JUHASZOVA, M., ZOROV, D.B., KIM, S.H., PEPE, S., FU, Q., FISHBEIN, K.W., ZIMAN, B.D., WANG, S., YTREHUS, K., ANTOS, C.L., OLSON, E.N. & SOLLOTT, S.J. (2004) Glycogen synthase kinase-3beta mediates convergence of protein signalling to inhibit the mitochondrial permeability transition pore. *Journal of Clinical Investigation* 113, 1535-49.

JOHN, S.A., MONCK, J.R., WEISS, J. & RIBALET, B. (1998) The sulphonylurea receptor SUR1 regulates ATP-sensitive mouse KIR6.2 K^+ channels linked to the green fluorescent protein in human embryonic kidney cells (HEK 293). *The Journal of Physiology* 510 (Pt 2), 333-345.

JOHNSON, M.S., MOORE, R.L. & BROWN, D.A. (2006) Sex differences in myocardial infarct size are abolished by sarcolemmal K_{ATP} channel blockade in rat. *American Journal of Physiology: Heart and Circulatory Physiology* 290(6), H2644-36.

JOHNSON, B.D., ZHENG, W., KORACH, K.S., SCHEUER, T., CATTTERALL, W.A. & RUBANYI, G.M. (1997) Increased expression of the cardiac L-type calcium channel in oestrogen receptor-deficient mice. *Journal of General Physiol*ogy 110(2), 135-40.

JOVANOVIC, A., JOVANOVIC, S., LORENZ, E. & TERZIC, A. (1998) Recombinant cardiac ATP-sensitive K^+ channel subunits confer resistance to chemical hypoxia-reoxygenation injury. *Circulation* 98, 1548-1555.

KEATING, M.T. & SANGUINETTI, M.C (2001) molecular and cellular mechanisms of cardiac arrhythmias. *CELL* 104(4), 569-580.

KOH, D.S., JONAS, P. & VOGEL, W. (1994) Na^{2+}-activated K^+ channels localized in the nodal region of myelinated axons of *Xenopus. The Journal of Physiology (London)* 479, 183-197.

KONG, X., TWEDDELL, JS., GROSS, G.J., BAKER, J.E. (2001) Sarcolemmal and mitochondrial K(ATP) channels mediate cardioprotection in chronically hypoxic hearts. *Journal of Molecular and Cellular Cardiology* 33(5), 1041-1045.

KOSTER, J.C., SHA, Q. & NICHOLS, C.G. (1999) Sulphonylurea and K^+ channel opener sensitivity of K_{ATP} channels. Functional coupling induces profound neonatal diabetes. *Cell* 100 (6), 645-654.

KUBO, Y., BALDWIN, T., JAN, Y.N. & JAN, L.Y. (1993) Primary structure and functional expression of a mouse inward rectifier potassium channel. *Nature* 362, 127-133.

KUZUYA, T., HOSHIDA, S., YAMASHITA, N., FUJI, H, OE, H., HORI, M., KAMADA, T., & TATA, M. (1993) Delayed effects of sublethal ischemia on the acquisition of tolerance to ischemia. *Circulation Research,* 72, 1293-1299.

LALLI M.J., JOHNS D.C., JANECKI M., LIU Y., O'ROURKE B. & MARBAN E. (1998) Suppression of K_{ATP} currents by gene transfer of a dominant negative Kir6.2 construct. *Pflugers Arch* 436(6), 957-61.

LANCASTER, B. & ADAMS, P.R. (1986) Calcium-dependent current generating the afterhyperpolarization of hippocampal neurons. *Journal of Neurophysiology* 55, 1268-1282.

LATORRE, R., OBERHAUSER, A., LABARCA, P. & ALVAREZ, O. (1989) Varieties of calcium-activated potassium channels. *Annual Review of Physiology* 51, 385-399.

LAWRENCE C.L., BILLUPS, B., RODRIGO, G.C. & STANDEN, N.B. (2001) The K_{ATP} channel opener diazoxide protects cardiac myocytes during metabolic inhibition without causing mitochondrial depolarization or flavoprotein oxidation. *British Journal of Pharmacology* 134(3), 535-42.

LAWRENCE, C.L., PROKS, P., RODRIGO, G.C., JONES, P., HAYABUCHI, Y., STANDEN, N.B. & ASHCROFT, F.M. (2001) Gliclazide produces high-affinity block of KATP channels in mouse isolated pancreatic beta cells but not rat heart or arterial smooth muscle cells. *Diabetologia* 44(8),1019-25.

LAWRENCE, C.L & RODRIGO, G.C. (1999) A Na^+-activated K^+ current ($I_{K,Na}$) is present in guinea-pig but not rat ventricular myocytes. *Pflügers Archiv* 437, 831-838.

LEE, T.M., SU, S.F., LEE, Y.T & TSAI, C.H (1999) Effect of oestrogen n ventricular repolarization in menopausal patients with syndrome X and effects of nicorandil. *American Journal of Cardiology* 84, 6569.

LEE, T.M., SU, S.F., TSAI, C.C., LEE, Y.T. & TSAI, C.H. (2000) Cardioprotective effects of 17 beta-estradiol produced by activation of mitochondrial ATP-sensitive $K^{(+)}$Channels in canine hearts. *Journal of Molecular and Cellular Cardiology* 32(7)1147-58.

LESAGE, F. & LAZDUNSKI, M. (2000) Molecular and functional properties of two-pore-domain potassium channels. *American journal of physiology-Renal Physiology* 279, F793-F801.

LI, G.C., VASQUEZ, J.A., GALLAGHER, K.P. & LUCCHESI, B.R. (1990) Myocardial protection with preconditioning. *Circulation* 82, 609-19.

LIGHT, P.E., BLADEN, C., WINKFEIN, R.J., WALSH, M.P., FRENCH, R.J. (2000) Molecular basis of protein kinase C-induced activation of ATP-sensitive potassium channels. *Proceedings of the National Academy of Sciences* 97 (16), 9058-9063.

LIGHT, P.E., KANJI, H.D., MANNING FOX, J.E. & FRENCH, R.J. (2001) Distinct myoprotective roles of cardiac sarcolemmal and mitochondrial K_{ATP} channels during metabolic inhibition and recovery. *FASEB* 15, 2586-2594

LIGHT P.E., SABIR A.A., ALLEN B.G., WALSH M.P. & FRENCH R.J.(1996) Protein kinase C-induced changes in the stoichiometry of ATP binding activate cardiac ATP-sensitive K^+ channels. A possible mechanistic link to ischaemia preconditioning. *Circulation Research* 79(3), 399-406.

LIN, Y.F., JAN, Y.N. & JAN, L.Y. (2000) Regulation of ATP-sensitive potassium channel function by protein kinase A-mediated phosphorylation in transfected HEK293 cells. *The Journal of Physiology* 19, 942-955.

LIU, X-K., LIU, A., KATCHMAN, M.-D., DRICI ET AL., EBERT, S.N., DUCIC, I., MORAD, M. & WOOSLEY, R.L. (1998) Gender difference in the cycle length-dependent QT and potassium currents in rabbits. *Journal of Pharmacology and Experimental Therapeutics* 285, 672–679.

LIU, G.S., RICHARDS, S.C., OLSSON, R.A., MULLANE, K., WALSH, R.S., & DOWNEY, J.M. (1994) Evidence that the adenosine A_3 receptor may mediate the protection afforded by preconditioning in the isolated rabbit heart. *Cardiovascular Research.* 28, 1057-1061.

LIU, G.S., THORNTON, J., VAN WINKLE, D.M., STANLEY, W.H., OLSSON, R.A., & DOWNEY J.M. (1991) Protection against infarction afforded by preconditioning is mediated by A_1 adenosine receptors in rabbit heart. *Circulation* 84, 350-356.

LIU, Y., SATO, T., O'ROURKE, B. & MARBAN, E. (1998) Mitochondrial ATP-dependent potassium channels: novel effectors of cardioprotection? *Circulation* 97, 2463-9.

LOUSSOUARN, G., MAKHINA, E.N., ROSE, T. & NICHOLS, C.G. (2000) Structure and Dynamics of the Pore of Inwardly Rectifying K_{ATP} Channels. *The Journal of Biological Chemistry*. 275 (2), 1137-1144.

LU, Z. & MACKINNON, R. (1994) Electrostatic tuning of Mg^{2+} affinity in an inward rectifier K^+ channel. *Nature* 371, 243-246.

MACKINNON, R. (1991) Determination of the subunit stoichiometry of a voltage-activated potassium channel. *Nature* 350, 232-235.

MANNHOLD, R. (2004) K_{ATP} channel openers: structure-activity relationships and therapeutic potential. *Medicinal Research Reviews* 24, 213-266.

MARTIN, A.R. & DRYER, S.E. (1989) Potassium channels activated by sodium. *Quarterly Journal of Experimental Physiology* 74, 1033-1041.

MATSUO, M., TRAPP, S., TANIZAWA, Y., KIOKA, N., AMACHI, T., OKA, Y., ASHCROFT, F.M. & UEDA, K. (2000) Functional analysis of a mutant sulphonylurea receptor, SUR1-R1420C, that is responsible for persistant hyperinsulinemic hypoglycemia of infancy. *Journal of Biological Chemistry*. 275 (52), 41184-41191.

MAULIK, N., YOSHIDA, T., ZU, Y-L., SATO, M., MANERJEE, A., & DAS, D.K. (1998) Ischemic preconditioning triggers tyrosine kinase signalling: a potential role for

MAPKAP kinase 2. *American Journal of Physiology-Heart and Circulatory Physiology,* 275, H1857-H1864.

MENDELSOHN, M.E. (2002) Genomic and nongenomic effects of oestrogen in the vasculature. *American Journal of Cardiology* 90, 3F-6F.

MEYER, R., LINZ, K.W., SURGES, R., MEINARDUS, S., VEES, J., HOFFMAN, A., WINDHOLZ, O. & GROHE, C. (1998) Rapid modulation of L-type calcium current by acutely applied oestrogens in isolated cardiac myocytes from human, guinea-pig and rat. *Experimental Physiol*ogy 83(3), 305-21.

MICHEL, M.C., LI, Y., & HEUSCH, G. (2001) Mitogen-activated protein kinases in the heart. *Naunyn-Schmiedebergs Archives of Pharmacology,* 363, 245-266.

MIKHAILOV, M.V., PROKS, P., ASHCROFT, F.M. & ASHCROFT, S.J. (1998) Expression of functionally active ATP-senstive K-channels in insect cells using baculovirus. *FEBS Letters* 429 (3), 390-394.

MILNER, C (2000) An overview of the potassium channel family. *Genome Biology* 1 (4), 0004.1-0004.5.

MITCHESON, J.C., HANCOX, J.L & LEVI, A.J (1996) Action potentials, ion channel currents and transverse tubule density in adult in adult rabbit ventricular myocytes maintained for 6 days in cell culture. *Plugers Arch* 431: 814-827.

MORKUNIENE, R., ARANDARCIKAITE, O. & BORUTAITE, V. (2006) Estradiol prevents release of cytochrome c from mitochondria and inhibits ischaemia-induced apoptosis in perfused heart. *Experimental Gerontology* 41(7):704-8.

MORKUNIENE, R., JEKABSONE, A. & BORUTAITE, V. (2002) Oestrogens prevent calcium-induced release of cytochrome *c* from heart mitochondria. *FEBS letters* 521, 53-56.

MUBAGWA, K & FLAMENG, W (2001) Adenosine, adenosine receptors and myocardial protection: an updated overview. *Cardiovascular Research* 52, 25-39.

MURRY, C.E., JENNINGS, R.B. & REIMER, K.A. (1986) Preconditioning with ischaemia: a delay of lethal cell injury in ischaemia myocardium. *Circulation*, 74 (5), 1124-36.

NEHER, E. & SAKMANN, B. (1976) Noise analysis of drug induced voltage clamp currents in denervated frog muscle fibres. *The Journal of Physiology* 258(3) 705-29.

NICHOLS, C.G., HO, K. & HERBERT, S. (1994) Mg^{2+}-dependent inward rectification of ROMK1 potassium channels expressed in *Xenopus* oocytes. *The Journal of Physiology,* 476 (3), 399-409.

NICHOLS, C.G & LEDERER, W.A. (1991) Adenosine triphosphate-sensitive potassium channels in the cardiovascular system. *The Journal of Physiology* 261(6 Pt 2):H1675-86.

NICHOLS, C.G. & LOPATIN, A.N. (1997) Inward Rectifier potassium Channels. *Annual Review of Physiology* 59, 171-191.

NISHIOKA, K., NAKANISHI, T. & JARMAKANI, J.M. (1984) Effect of ischaemia on calcium exchange in the rabbit myocardium. *The Journal of Physiology* 247(2 Pt 2):H177-84.

NOMA, A. (1983) ATP-regulated K^+ channels in cardiac muscle. *Nature* 305, 147-148.

NORTH, R.A. (1995) Ligand and voltage-gated ion channels, CRC Press.

NUEDLING, S., KARAS, R.H., MENDLSOHN, M.E., KATZENELLENBOGEN, J.A., KATZENELLENBOGEN, B.S., MEYER, R., VETTER, H. & GROHE, C. (2001)

Activation of ostrogen receptor β is a prerequisite for oestrogen-dependent upregulation of nitric oxide synthases in neonatal rat cardiac myocytes. *FEBS Letters* 502, 103-108.

ORCHARD, C.H. & KENTISH, J.C. (1990) Effects of changes of pH on the contractile function of cardiac muscle. *American Journal of Phyiology*. Jun; 258(6 pt 1):C967-81.

PEI, J.M., KRAVTSOV, G.M., WU, S., DAS, R., FUNG, M.L. & WONG, T.M. (2003) Calcium homeostasis in rat cardiomyocytes during chronic hypoxia: a time course study. *American journal of Physiology-Cell Physiology* 20-8.

PENNEFATHER, P., LANCASTER, B., ADAMS, P.R. & NICOLL, R.A (1985) Two distinct Ca-dependent K currents in bullfrog sympathetic ganglion cells. *Proceedings of the National Academy of Sciences of the United States of America* 82, 3040-3044

PHAM, T. & ROSEN, M. (2002). Sex, hormones, and repolarization. *Cardiovascular research* 53, 538-549.

PING, P. & MURPHY, E. (2000) Role of p38 mitogen-activated protein kinases in preconditioning. *Circulation Research*, 86, 921.

QUAYLE, J.M., NELSON, M.T. & STANDEN, N.B. (1997) ATP-sensitive and inwardly rectifying potassium channels in smooth muscle. *Physiological Reviews* 77(4), 1165-232.

RADONIC, A., THULKE, S., MACKAY, I.M., LANDT, O., SIEGERT, W. & NITSCHE, A. (2004) Guideline to reference gene selection for quantitative real-time PCR. *Biochemical and Biophysical Research Communications* 23, 313 (4): 836-62.

RAINBOW, R.D., LODWICK, D., HUDMAN, D., DAVIES, N.W., NORMAN, R.I. & STANDEN, N.B. (2004) SUR2A C-terminal fragments reduce K_{ATP} currents and ischaemic tolerance of rat cardiac myocytes. *The Journal of Physiology* 557, 785-794.

RANKI H.J., BUDAS G.R,, CRAWFORD R.M., DAVIES A.M., JOVANOVIC A. (2002) 17Beta-estradiol regulates expression of $K_{(ATP)}$ channels in heart-derived H9c2 cells. *Journal of the American College of Cardiology* 17;40(2), 367-74.

RANKI, H.J., BUDAS G.R., CRAWFORD RM., JOVANOVIC, A. (2001) Gender-specific difference in cardiac ATP-sensitive K^+ channels. *Journal of the American College of Cardiology* 38, 906-915.

REGITZ-ZAGROSEK, V. (2006) Therapeutic implications of the gender-specific aspects of cardiovascular disease. *Nature* 5, 425-438.

ROBITAILLE, R., GARCIA, M.L., KACZOROWSKI, G.J., CHARLTON, M.P. (1993) Functional colocalizaion of calcium and calcium-gated potassium channels in control of transmitter release. *Neuron* 11, 645-655.

ROBSON, L. & HUNTER, M. (2005) Phosphorylation regulates an inwardly rectifying ATP-sensitive K^+-conductance in proximal tubule cells of frog kidney. *Journal of Membrane Biology* 207, 161-167.

RODRIGO, G.C & STANDEN, N.B (2005) Role of mitochondrial re-energization and Ca^{2+} influx in reperfusion injury of metabolically inhibited cardiac myocytes. *Cardiovascular Research* 67(2), 291-300.

RODRIGO, G.C. & STANDEN, N.B. (2005) ATP-sensitive potassium channels. *Current Pharmaceutical Design* 11 (15), 1915-40.

ROSSOUW, J.E. (2002) Hormones, genetic factors, and gender differences in cardiovascular disease. *Cardiovascular Research*. 15;53(3):550-7.

SAH, P. (1995) Properties of channels mediating the apamin-insensitive afterhyperpolarization in vagal motoneurons. *Journal of Neurophysiology* 74, 1772-1776.

SAH, P (1996) Ca^{2+}-activated K^+ currents in neurones: types, physiological roles and modulation. *Trends in Neuroscience* 19, 150-154.

SAH, P. & MCLACHLAN, E.M. (1991) Ca^{2+}-activated K^+ currents underlying the afterhyperpolarization in guinea pig vagal neurons: a role for Ca^{2+}-activated Ca^{2+} release. *Neuron* 7: 257-264.

SAKURA, H., TRAPP, S., LISS, B. & ASHCROFT, F.M. (1999) Altered functional properties of K_{ATP} channel conferred by a novel splice variant of SUR1. *The Journal of Physiology* 521 (Pt 2), 337-350.

SANADA, S., ASANUMA, H., TSUKAMOTO, O., MINAMINO, T., NODE, K., TAKASHIMA, S., FUKUSHIMA, T., OGAI, A., SHINOZAKI, Y., FUJITA, M., HIRATA, A., OKUDA, H., SHIMOKAWA, H., TOMOIKE, H., HORI, M & KITAKAZE, M. (2004) Protein kinase A as another mediator of ischaemic preconditioning independent of protein kinase C. *Circulation* 110, 51-7.

SANADA, S., KITAKAZE, M., ASANUMA, H., HARADA, K., OGITA, H., NODE, K., TAKASHIMA, S., SAKATA, Y., ASAKURA, M., SHINOZAKI, Y., MORI, H., KUZUYA, T. & HORI, M. (2001) Role of mitochondrial and sarcolemmal K_{ATP} channels in ischaemia preconditioning of the canine heart. *American Journal-Heart and Circulatory Physiology* 280, H256-263.

SANCHEZ, J.A., GONOI, T., INAGAKI, N., KATADA, T. & SEINO, S. (1998) Modulation of reconstituted ATP-sensitive K^+-channels by GTP-binding proteins in a mammalian cell line. *The Journal of Physiology* 507 (Pt 2), 315-324.

SASAKI, N., MURATA, M., GUO, Y., JO, S.H., OHLER, A., AKAO, M., O'ROURKE, B., XIAO, R.P., BOLLI, R. & MARBAN, E. (2003) MCC-134, a single pharmacophore, opens surface ATP-sensitive potassium channels, blocks mitochondrial ATP-sensitive potassium channels, and suppresses preconditioning. *Circulation* 107, 1183-1188.

SATO, T., O'ROURKE, B. & MARBAN, E. (1998) Modulation of mitochondrial ATP-dependent K^+ channels by protein kinase C. *Circulation Research.* 83, 110-4.

SCRAGG, J.L., JONES, R.D., CHANNER, K.S., JONES, T.H. & PEERS, C (2004) Testosterone is a potent inhibitor of L-type $Ca(^{2+})$ channels. *Biochemical and Biophysical Research Communications* 28; 318 (2): 503-6.

SEINO, S. (1999) ATP-SENSITIVE POTASSIUM CHANNELS: A model of Heteromultimeric Potassium Channel/Receptor Assemblies. *Annual review of Physiology.* 61, 337-62.

SEINO, S. (2003) Physiological and pathophysiological roles of ATP-sensitive K+ channels. *Progress in Biophysics and Molecular Biology,* 81, 133-176.

SHARMA, N., CRANE, A., CLEMENT, J.P.T., GONZALEZ, G., BABENKO, A.P., BRYAN, J. & AGUILAR-BRYAN, L., (1999) The C terminus of SUR1 is required for trafficking of K_{ATP} channels. *Journal of Biological Chemistry*. 274 (29), 20628-20632.

SHIMONI, Y. & LIU, X. (2003) Sex differences in the modulation of K^+ currents in diabetic rat cardiac myocytes. *The Journal of Physiology* 550;2, 401-412.

SHIKI K. & HEARSE D.J. (1987) Preconditioning of ischaemia myocardium: reperfusion-induced arrhythmias. *The Journal of Physiology* 253, H1470-6

SHINDO, T., YAMADA, M., ISOMOTO, S., HORIO, Y. & KURACHI, Y. (1998) SUR2 subtype (A and B)-dependent differential activation of the cloned ATP-sensitive K^+ channels by pinacidil and nicorandil. *British Journal of Pharmacy* 124, 985-991.

SHYNG, S-L. & NICHOLS, C.G. (1997) Octameric Stoichiometry of the K_{ATP} Channel Complex. *Journal of General Physiology* 110, 655-664.

SIEMEN, D., LOUPATATZIS, C., BORECKY, J., GULBINS, E. & LANG, F (1999) Ca^{2+}-activated K channel of the BK-type in the inner mitochondrial membrane of a human glioma cell line. *Biochemical and Biophysical Research Communications* 257, 549-54.

SILVERMAN, H.S. & STERN, M.D. (1994) Ionic basis of ischaemia cardiac injury: insights from cellular studies. *Cardiovascular Research*. 28(5), 581-97.

SPRUCE, A.E., STANDEN, N.B. & STANFIELD, P.R. (1987b) The action of external tetraethylammonium ions on unitary delayed rectifier potassium channels of frog skeletal muscle. *The Journal of Physiology* 393, 467-478.

STANFIELD, P.R., DAVIES, N.W., SHELTON, P.A., SUTCLIFFE, M.L., KHAN, I.A., BRAMMAR, W.J. & CONLEY, E.C. (1994) A single aspartate residue is involved in both intrinsic gating and blockade by Mg^{2+} of the inward rectifier, IRK1. *The Journal of Physiology* 478, 1-6.

STERN, M.D., CAPOGROSSI, M.C. & LAKATTA, E.G (1988) Anoxic contractile failure in rat heart myocytes is caused by failure of intracellular calcium elease due to alteration of the action potential. *Proceedings of the National Academy of Sciences of the United States of America* 85(18), 6954-6958.

STERN, M.D., CHIEN, A.M., CAPOGROSSI, M.C., PELTO, D.J. & LAKATTA, E.G. (1985) Direct observation of the "oxygen paradox" in single rat ventricular myocytes. *Circulation Research* 56(6), 899-903.

STUMPF, W.E. & SAR, M. (1977) Steroid hormone target cells in the periventricular brain: relationship to peptide hormone producing cells. *Federation Proceedings* 36(7), 1973-7.

SUGISHITA, K., SU, Z., LI, F., PHILIPSON, K.D., BARRY, W.H. (2001) Gender influences $Ca^{2+}i$ during metabolic inhibition in myocytes overexpressing the $Na^{(+)}$-$Ca^{(2+)}$ exchanger.*Circulation* 23;104(17), 2101-6.

SUN, J-Z., TANG, X-L., PARK, S-W., QIU, Y., TURRENS, J.F., & BOLLI, R. (1996) Evidence for an essential role of reactive oxygen species in the genesis of late preconditioning against myocardial stunning in conscious pigs. *Journal of Clinical Investigation*, 97, 562-576.

SUZUKI, M., LI, R.A., MIKI, T., UEMURA, H., SAKAMOTO, N., OHMOTO-SEKINE, Y., TAMAGAWA, M., OGURA, T., SEINO, S., MARBAN, E. & NAKAYA, H. (2001) Functional roles of cardiac and vascular ATP-sensitive potassium channels clarified by Kir6.2-knockout mice. *Circulation Research* 88, 570-577.

SUZUKI, M., SAITO, T., SATO, T., TAMAGAWA, M., MIKI, T., SEINO, S. & NAKAYA, H. (2003) Cardioprotective effect of diazoxide is mediated by activation of sarcolemmal but not mitochondrial ATP-sensitive potassium channels in mice. *Circulation* 107, 682-685.

SUZUKI, M., SASAKI, N., MIKI, T., SAKAMOTO, N., OHMOTO-SEKINE, Y., TAMAGAWA, M., SEINO, S., MARBAN, E. & NAKAYA, H. (2002) Role of the sarcolemmal $K_{(ATP)}$ channels in cardioprotection against ischaemia/reperfusion injury in mice. *Journal of Clinical Investigation* 109, 509-516.

SZABO, I., BOCK, J., JEKLE, A., SODDERMANN, M., ADAMS, C., LANG, F., ZORATTI, M. & GULBINS, E (2005) A novel potassium channel in lymphocyte mitochondria. *Journal of Biological Chemistry.* 1; 280(13): 12790-12798.

TAGLIALATELA, M., WIBLE, B.A., CAPORASO, R. & BROWN, A.M. (1994) Specification of pore properties by the carboxyl-terminus of inwardly rectifying K^+ channels. *Science* 264, 844-867.

TAKASHI, E., WANG, Y. & ASHRAF, M. (1999) Activation of mitochondrial K_{ATP} channel elicits late preconditioning against myocardial infarction via protein kinase C signalling pathway. *Circulation Research* 85, 1146-1153.

TAN, H.L., MAZON, P., VERBERNE, H.J., SLEESWIJK, M.E., CORONEL, R., OPTHOF, T. & JANSE, M.J. (1993) Ischemic preconditioning delays ischaemia induced

cellular electrical uncoupling in rabbit myocardium by activation of ATP sensitive potassium channels. *Cardiovascular Research* 27, 644-651.

TANABE, K., TUCKER, S.J., ASHCROFT, F.M., PROKS, P., KIOKA, N., AMACHI., T. & UEDA, K. (2000) Direct photoaffinity labelling of Kir6.2 by [gamma-(32)P]ATP-[gamma]4-azidoanilide. *Biochemical and Biophysical Research Communications* 272 (2), 316-319.

TANNO, M., MIURA, T., TSUCHIDA, A., MIKI, T., NISHINO, Y., OHNUMA, Y. & SHIMAMOTO, K. (2001) Contribution of both the sarcolemmal K_{ATP} and mitochondrial K_{ATP} channels to infarct size limitation by K_{ATP} channel openers: differences from preconditioning in the role of sarcolemmal K_{ATP} channels. *Naunyn-Schmiedeberg's Archives of Pharmacology* 364, 226-232.

TONG, H., CHEN, W., STEENBERGEN, C. & MURPHY, E. (2000) Ischaemia preconditioning activates phosphatidylinositol-3-kinase upstream of protein kinase C. *Circulation Research* 87, 309-315.

TORO, L., WALLNER, M., MEERA, P., TANAKA, Y. (1998) Maxi K_{ca} a unique member of the voltage-gated K channel superfamily. *News in Physiological Sciences,* 13, 112-117.

TOSAKI, A., MAULIK, N., CORDIS, G.,TRIFAN, O.C., POPESCU, L.M., DAS, D.K (1997) Ischemic preconditioning triggers phospholipase D signalling in rat heart. *American Journal of Physiology-Heart and Circulatory Physiology* 273, H1860-H1866.

TOYODA, Y., FRIEHS, I., PARKER, R.A., LEVITSKY, S. & MCCULLY, J.D. (2000) Differential role of sarcolemmal and mitochondrial K_{ATP} channels in adenosine-enhanced ischaemia preconditioning. *American Journal of Physiology-Heart and Circulatory Physiology* 279, H2694-H2703.

TREPANIER-BOULAY, V., ST-MICHEL, C., TREMBLAY, A. & FISCET, C. (2001) Gender-based differences in cardiac repolarization in mouse ventricle. *Circulation Research* 31;89(5), 437-44.

TSAI, C.H., SU, S.F., CHOU, T.F. & LEE, T.M. (2002) Differential effects of sarcolemmal and mitochondrial $K_{(ATP)}$ channels activated by 17 beta-estradiol on reperfusion arrhythmias and infarct sizes in canine hearts. *Journal of Pharmacology and and Experimental Therapeutics* 301, 234–240.

TSENG, G.N. & HOFFMAN, B.F. (1989) Two components of transient outward current in canine ventricular myocytes. *Circulation Research* 64(4), 633-47.

TSENG-CRANK, J., FOSTER, C.D., JRAUSE, J.D., MERTZ, R., GODINOT, R., DICHIARA, T.J., REINHART, P.H. (1994) Cloning, expression, and distribution of functionally distict Ca^{2+}-activated K^+ channel isoforms from human brain. *Neuron* 13, 1315-1330.

TSUJIMOTO, Y., NAKAGAWA, T. & SHIMIZU, S. (2006) Mitochondrial membrane permeability transition and cell death. *Biochimica et Biophysica Acta* 19 (Ahead of print)

TUCKER, S.J., GRIBBLE, F.M., ZHAO, C., TRAPP, S. & ASHCROFT, F.M. (1997) Truncation of Kir6.2 produces ATP-sensitive K^+ channels in the absence of the sulphonylurea receptor. *Nature* 387 (6629), 179-183.

UEDA, K., INAGAKI, N. & SEINO, S. (1997) MgADP antagonism to Mg^{2+} - independent ATP binding of the sulphonylurea receptor SUR1. *Journal of Biological Chemistry* 272 (37), 22983-22986.

UEDA, K., MATSUO, M., TANABE, K., MORITA, K., KIOKA, N. & AMACHI, T. (1999b) Comparative aspects of the function and mechanism of SUR1 and MDR1 proteins. *Biochimica et Biophysica Acta* 1461 (2), 305-313.

VEGH, A., PAPP, J.G, & PARRATT, J.R. (1994) Prevention by dexamethasone of the marked antiarrhythmic effects of preconditioning induced 20 h after rapid cardiac pacing. *British Journal of Pharmacology*, 113, 1081-1082.

VERGARA, C., LATORRE, R., MARRION, N.V & ADELMAN, J.P. (1998) Calcium-activated potassium channels. *Current opinion in Neurobiology* 8, 321-329.

WADA, Y., YAMASHITA, T., IMAI, K., MIURA, R., TAKAO, K., NISHI, M., TAKESHIMA, H., ASANO, T., MORISHITA, R., NISHIZAWA, K., KOKUBUN, S. & NUKADA, T. (2000) A region of the sulphonylurea receptor critical for a modulation of ATP-sensitive K^+ channels by G-protein betagamma-subunits. *The EMBO Journal* 19 (18), 4915-4925.

WAHLER, G.M. (1997) Cardiac action potentials. *Cell Physiology Source Book*. Ed. N. Sperelakis San Diego: Academic Press.

WILDE, A.A. (1993) Role of ATP-sensitive K^+ channel current in ischaemia arrhythmias. *Cardiovascular drugs and therapy* 7 Suppl 3, 521-6.

XIE, L.H., TAKANO, M., KAKEI, M., OKAMURA, M. & NOMA, A. (1999) Wortmannin, an inhibitor of phosphatidylinositol kinases, blocks the MgATP-dependent recovery of Kir6.2/SUR2A channels. *The Journal of Physiology* 514 (Pt 3), 655-665.

YAKHIN, S. & XIU-FANG, L. (2003) Sex differences in the modulation of K^+ currents in diabetic rat cardiac myocytes. The Journal of Physiology 550.2, 401-412.

YAMADA, K. & INAGAKI, N. (2002) ATP-sensitive K(+) channels in the brain: sensors of hypoxic conditions. *News in Physiological Sciences* 17, 127-30.

YAMADA, K., JI, J.J., YUAN, H., MIKI, T., SATO, S., HORIMOTO, N., SHIMIZU, T., SEINO, S. & INAGAKI, N. (2001) Protective role of ATP-sensitive potassium channels in hypoxia-induced generalized seizure. Science 25; 292(5521),1543-6.

YANG, S., CHOUNDRY, M.A., HSIEH, Y.C., HU, S., RUE, L.W. 3^{RD}., BLAND, K.I. AND CHAUDRY, I.H. (2006) *American Journal of Physiology- Heart and Circulatory Physiology.* Dec; 291(6): H2807-15.

YANG, J., JAN, Y.N. & JAN, L.Y. (1995) Control of rectification and permeation by residues in two distinct domains in an inward rectifier K^+ channel. *Neuron* 15, 1441-1447.

YAO, Z. & GROSS, G.J. (1994) Effects of the K_{ATP} channel opener bimakalim on coronary blood flow, monophasic action potential duration, and infarct size in dogs. *Circulation* 89,769-1775.

YAZEJIAN, B., DIGREGORIO, D.A., VERGARA, J., POAGE, R.E., MERINEY, S.D. & GRINNEL, A.D. (1997) Direct measurement of presynaptic calcium ana calcium-activated potassium currents regulating neurotransmitter release at cultured Xenopus nerve-muscle synapses. *Journal of Neuroscience*, 17, 2990-3001.

YELLON, D.M. & BAXTER, G.F. (1995) A "second window of protection" or delayed preconditioning phenomenon: future horizons for myocardial protection? *Journal of Molecular and Cellular Cardiology*, 27, 1023-1034.

YELLON, D.M. & DOWNEY, J.M. (2003) Preconditioning the myocardium: from cellular physiology to clinical cardiology. *Physiological Reviews*, 83, 1113-1151.

YOKOSHIKI, H., SUNAGAWA, M., SEKI, T. & SPERELAKIS, N. (1998) ATP-sensitive K^+ channels in pancreatic, cardiac, and vascular smooth muscle cells. *American journal of Physiology*, 274, C25–C37.

Theses

MCKILLEN, H.C (1994) A study of the ATP-dependent potassium channel of rat skeletal muscle. University of Leicester.

PASSMORE, G.M (2003) Structure-function studies of inwardly rectifying potassium channels. University of Leicester.

RAINBOW, R (2003) A study of cloned and native K_{ATP} channels in HEK293 cells and rat ventricular myocytes. University of Leicester.

Websites

http://heartdisease.about.com/cs/coronarydisease/a/CSX.htm-fogoros

http://www.americanheart.org/presenter.jhtml?identifier=4637